Physiol Rev 92: 1005–1060, 2012
doi:10.1152/physrev.00037.2011

INTERSTITIAL FLUID AND LYMPH FORMATION AND TRANSPORT: PHYSIOLOGICAL REGULATION AND ROLES IN INFLAMMATION AND CANCER

Helge Wiig and Melody A. Swartz

Department of Biomedicine, University of Bergen, Bergen, Norway; and Laboratory of Lymphatic and Cancer Bioengineering, Institute of Bioengineering and Swiss Institute for Experimental Cancer Research, Ecole Polytechnique Fédérale de Lausanne, Lausanne, Switzerland

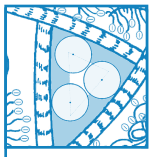

Wiig H, Swartz MA. Interstitial Fluid and Lymph Formation and Transport: Physiological Regulation and Roles in Inflammation and Cancer. *Physiol Rev* 92: 1005–1060, 2012; doi:10.1152/physrev.00037.2011.—The interstitium describes the fluid, proteins, solutes, and the extracellular matrix (ECM) that comprise the cellular microenvironment in tissues. Its alterations are fundamental to changes in cell function in inflammation, pathogenesis, and cancer. Interstitial fluid (IF) is created by transcapillary filtration and cleared by lymphatic vessels. Herein we discuss the biophysical, biomechanical, and functional implications of IF in normal and pathological tissue states from both fluid balance and cell function perspectives. We also discuss analysis methods to access IF, which enables quantification of the cellular microenvironment; such methods have demonstrated, for example, that there can be dramatic gradients from tissue to plasma during inflammation and that tumor IF is hypoxic and acidic compared with subcutaneous IF and plasma. Accumulated recent data show that IF and its convection through the interstitium and delivery to the lymph nodes have many and diverse biological effects, including in ECM reorganization, cell migration, and capillary morphogenesis as well as in immunity and peripheral tolerance. This review integrates the biophysical, biomechanical, and biological aspects of interstitial and lymph fluid and its transport in tissue physiology, pathophysiology, and immune regulation.

I. INTRODUCTION

The interstitial space, or interstitium, is a general term pertaining to the connective and supporting tissues of the body that are localized outside the blood and lymphatic vessels and parenchymal cells. It is comprised of two phases: the interstitial fluid (IF), consisting of interstitial water and its solutes, and the structural molecules of the interstitial or the extracellular matrix (ECM). The IF transports nutrients and waste products between cells and blood capillaries, signaling molecules between cells, and antigens and cytokines to local draining lymph nodes for immune regulation. Its composition and biophysical properties vary between organs and in tissue development, pathogenesis, inflammation, and remodeling as well as over normal functional cycles. Whereas there has been a rapidly growing interest in the tissue microenvironment over the last decade, the IF in general and especially that of tumors is largely overlooked.

The IF volume (V_i) is kept fairly constant under normal conditions at ~20% of body weight by several interstitial buffering mechanisms (25) including structural changes, adjustment of forces acting across the capillary wall, and lymph flow. This traditional concept of the interstitium does not include a role for cells (24, 25). These cells are, however, an integral part of this space, since they participate in continuous bidirectional cell-matrix interactions that ultimately bring about microenvironmental changes. Moreover, cells in the interstitium have important roles in initiating immune responses (375). Due to their potential roles in fluid volume regulation in inflammation (381) and since the "deranged" IF phase of inflamed tissue and of solid tumors are central elements in this review, we will here need to include cells in the term *interstitium*. The typical connective tissue cells in this context are those that are not organ-specific, but an integral part of the ECM, e.g., fibroblasts or dendritic cells.

IF flow and lymph formation have been addressed in previous extensive reviews in this journal (24, 25, 414). In sev-

eral areas, our work is an update of the review by Aukland and Reed (25) almost two decades ago. During this period, IF research has shifted focus away from IF volume regulation and buffering ("autoregulation"), and instead made new advances in elucidating the roles of IF in physiology, inflammation, cancer, and immune regulation. One notable example is the role of mechanical forces, namely, IF flow through the interstitium and into the lymphatic capillaries, in modulating important biological events that contribute to morphogenesis, ECM remodeling, cell migration, and cell-cell signaling that we will cover here.

During the last 15 years, lymphatic vascular biology has advanced rapidly through the discovery of lymphangiogenic factors, identification of lymphatic vascular markers that can be used to distinguish lymphatic from blood vessels, isolation and culture of lymphatic endothelial cells and the development of animal models to study lymphangiogenesis. These discoveries have bearings on the formation and transport of IF and will be discussed in that light when pertinent. The topic of lymphangiogenesis, however, has been addressed in several recent reviews (e.g., Refs. 11, 12, 305, 459, 501) and will not be covered in this review.

II. STRUCTURE AND BIOPHYSICAL PROPERTIES OF THE INTERSTITIUM

The interstitium, located between the capillary wall and cells (25), consists of a predominantly collagen fiber framework, a gel phase of glycosaminoglycans (GAGs), a salt solution, and plasma proteins. The relative composition of these components varies considerably between tissues **(TABLE 1)**. Furthermore, the amount of IF varies from ~50% of wet tissue weight in skin to ~10% in skeletal muscle. The composition and structure of the normal interstitium (50, 91, 147, 216, 246, 374) and that of tumors (93, 230, 231, 273, 282, 303, 444) have been covered in several extensive reviews and are thus only briefly described here. GAGs and the major fibrous structural elements (collagen) are the central mediators of V_i regulation, volume exclusion, and hydraulic conductivity (497), and they are discussed summarily here. Other components of the ECM include elastin as well as the cell adhesion proteins, fibronectin, vitronectin, thrombospondins, and laminins (216, 296). We will first address the structure of the normal interstitium in this perspective and then turn to that of tumors.

Additionally, the IF phase contains plasma proteins and electrolytes in addition to other substances either produced locally or originating from plasma. The protein composition of IF along with techniques for its isolation are addressed in section VI.

A. The Interstitial Matrix

1. Collagen

The collagens are a family of ECM proteins with a multitude of functions that include a dominant role in scaffolding of various tissues, and their structures and functions have been extensively reviewed (e.g., Refs. 19, 227, 309, 429). All collagens consist of three polypeptide chains (α chains) with characteristic triple-helical collagenous as well as noncollagenous domains. There are 28 types of collagen reported to date in vertebrates, that based on supramolecular assemblies and other features can be grouped into nine distinct families (227, 309).

As will be seen in sections IIC and IV*D*, when discussing fluid pressure and volume regulation, the fibrillar collagens I, II, III, V, and XI (227) that assemble into long, highly ordered polymers needed to withstand high tensile forces are of particular interest. They have a characteristic 67-nm axial periodicity, are millimeters in length, and have diameters that range from a few nanometers to ~500 nm depending on the tissue and stage of development (76).

Most abundant are collagen types I, II, and III, while V and XI are quantitatively less important. In the body, types I, III, and V are widely distributed, whereas types II and XI are mainly restricted to cartilage, vitreous body, and the tectorial membrane of the inner ear (19). In tissues, fibrils are most often assembled into higher-order structures (76). Tendon, bone, and skin have type I collagen as their major component, whereas in cartilage, fibrils mainly comprise type II collagen. Usually fibrils are heterotypic in that they can contain more than one type of fibrillar collagen, exemplified by skin made up of both types I and type III collagen.

Table 1. *Volume and composition of interstitium*

Tissue	V_i, ml/g wet wt	Collagen, mg/g wet wt	GAG, mg/g wet wt	Hyaluronan, mg/g wet wt
Skin	0.40–0.45 (496, 509)	170–190 (379, 509)	3.7–4.2 (379, 509)*	0.5–1.6 (379, 380, 509)
Muscle	0.07–0.12 (173, 496)	10–13 (233, 509)	2.2 (509)*	0.09–0.13 (380, 509)
Lung	0.24 (321)	5–35 (462, 475)	6.1 (475)	0.07–0.13 (13, 475)

Reference numbers are given in parentheses. *Based on a conversion factor GAG:uronic acid of 2.61 (28). V_i, interstitial fluid volume; GAG, glycosaminoglycans. Amount collagen was calculated as 6.94 μg collagen/μg hydroxyproline (214).

In tendons, fibrils vary in diameter from 30 to 300 nm, depending on the stage of development (135). In skin, collagen fibril diameter ranges from 50 to 100 nm (407, 446), and collagen accounts for almost 20% of tissue wet weight (e.g., Ref. 379 and **TABLE 1**). Collagen is the dominant component of connective tissue in skeletal muscle, accounting for 1–10% of the mass (246) **(TABLE 1)**. In intramuscular connective tissue, several collagen types have been found, whereas the fibrillar type I and III and to some extent type V and VI are the dominating ones in epi-, peri-, and endomysium. Of these, collagen I dominates as being the major intramuscular collagen (246).

Another aspect of interest in relation to collagen structure here is whether the fibril is charged at physiological pH, since this factor may affect fluid volume exchange as discussed in section IIC. Collagen is a protein polyampholyte with both positively and negatively charged groups that self-compensate at pH 7.4. Although charge may vary with the microenvironment (161), collagen I fibrils generally possess a slightly positive charge (pI ~8.0) at physiological pH (267, 384), estimated to +14 mol/mol in reconstituted collagen (236), while collagen II has a zero net charge density in cartilage (485), leaving a slight net positive charge on the molecule (160, 267). Accordingly, since collagen has almost no net charge, it behaves as a tissue element with effectively no areas with high local charge (i.e., it does not support an electron cloud and has no Debye length) (502).

2. GAGs

GAGs are polyanionic polysaccharide chains of variable length consisting of repeating disaccharide units of hexosamine and uronic acid or galactose (91). The disaccharide groups are fully charged at physiological pH and thereby contribute strongly to the negative charge of the interstitium in vivo. There are four main classes of GAGs (374): heparin/heparan sulfate, chondroitin/dermatan sulfate, keratin sulfate, and hyaluronan. All are bound covalently to a protein backbone with the exception of hyaluronan, and the combined macromolecule is called a proteoglycan (PG) (25). They are immobilized in the interstitium with the exception of hyaluronan that has been found in lymph in substantial amounts (464). Recently, an important role for GAGs has been suggested in maintaining a concentration gradient of growth factors or morphogens because of the graded affinities between different GAG sequences with the given protein (374).

The high net negative charge density of GAGs attracts counterions and establishes a Donnan distribution of diffusible species that is mostly responsible for the osmotic pressure and thereby the hydration of the interstitium (24). Hyaluronan, a major constituent of GAGs in skin (25), is particularly important in this context. Hyaluronan has a quarternary structure of a random coil, which implies that the molecules will occupy a domain with radius 100–1,000 times larger than that of the organic material (91) and has a molecular mass of several thousand kilodaltons. As determined by Reed et al. in rats (380), the largest pool of hyaluronan in the body (>50% of total) is found in skin, whereas <10% is located in skeletal muscle (173, 379). The composition of the ECM in absolute terms is of relevance for, e.g., interstitial exclusion of macromolecules (see sect. IIC). Examples of data on collagen, GAG, and hyaluronan in skin, muscle, and lung have been summarized in **TABLE 1**.

3. Elastin

Elastin fibers are composed of an elastin core and a surrounding microfibrillar network (19) and provide elasticity and resilience to flexible tissues like skin (347). The amount of elastin in most tissues (except arteries and ligamentum nuchae) is, however, small (e.g., amounting to 2–5% of the dry weight in skin; Ref. 50), so the quantitative importance of elastin for fluid exchange in most organs is limited and can be neglected in the present context.

4. Interstitial composition of solid tumors

The tumor interstitium has a different composition and features than normal tissue (**TABLES 2** and **3**). Properties of the tumor ECM or "reactive" stroma, which are covered in several extensive recent reviews (e.g., Refs. 74, 110, 122, 231, 242, 282, 303, 444, 469) are mostly outside of the

Table 2. *Interstitial fluid volume in tumors*

Tumor Type	Host	Plasma Volume, ml/g wet wt	Interstitial Fluid Volume, ml/g wet wt	Reference Nos.
Thyroid carcinoma (KAT-4)*	Mouse	0.02 ± 0.02	0.34 ± 0.09	338
Ovarian carcinoma (OVCAR-3)	Mouse	0.01 ± 0.001	0.60 ± 0.03	137
Ovarian carcinoma (SKOV-3)	Mouse	0.01 ± 0.003	0.53 ± 0.11	137
Fibrosarcoma (chemically induced)	Rat	0.007 ± 0.003	0.60 ± 0.05	332
Mammary carcinoma (DMBA induced)	Rat	0.014 ± 0.001	0.39 ± 0.02	494
Fibrosarcoma	Rat		0.50 ± 0.11	251

*Assuming wet/dry weight of 4.88 as for mammary carcinoma (494).

Table 3. *Composition of the extracellular matrix in tumors*

Tumor Type	Host	Collagen, mg/g wet wt	Hyaluronan,* mg/g wet wt	Proteoglycans,† mg/g wet wt	Reference Nos.
Mammary carcinoma (murine) MCa1V	Mouse	1.7 ± 0.4	0.22 ± 0.02	0.16 ± 0.04	323
Colon adenocarcinoma (human) (LS174T)	Mouse	1.8 ± 0.7	0.10 ± 0.04	0.18 ± 0.04	323
Glioblastoma (human) (U87)	Mouse	9 ± 4	0.10 ± 0.04	0.18 ± 0.05	323
Soft tissue sarcoma (human) (HSTS)	Mouse	6 ± 1	0.22 ± 0.03	0.16 ± 0.04	323
Osteosarcoma (human) (orthotopic- OHS cell line)	Mouse	2.0 ± 0.2	0.78 ± 0.09	1.9 ± 0.1	105
Mammary carcinoma (DMBA induced)	Rat	4.6 ± 0.7	1.9 ± 0.3	1.6 ± 0.9	494
Ovarian carcinoma (OVCAR-3)‡	Mouse	7.7 ± 0.5	0.08 ± 0.04		85
Ovarian carcinoma (SKOV-3) ‡	Mouse	9 ± 3	0.20 ± 0.02		85
Rhabdomyosarcoma (BAHAN) (average of 3 clones)	Mouse	5.9 ± 0.3	1.4 ± 0.09	1.1 ± 0.04	104

*Hyaluronan/uronic acid coversion factor 2.28. †Proteoglycan/uronic acid conversion factor 2.61 (28). ‡Assuming wet/dry weight of 4.88 as for mammary carcinoma (494). Amount collagen calculated as 6.94 μg collagen/μg hydroxyproline (214).

scope of the present review except for issues related to fluid exchange (231). Briefly, a reactive tumor ECM often contains myofibroblasts, vascular endothelial growth factor (VEGF), and enhanced capillary density (71). VEGF increases microvascular permeability and promotes extravasation of plasma proteins such as fibrinogen, leading to extravascular fibrin that is invaded by fibroblasts, inflammatory cells, and endothelial cells (121, 422). Additionally, the tumor ECM contains increased amounts of collagens, PGs, and GAGs, especially hyaluronan and chrondroitin sulfate (122, 280, 391, 458, 525).

Early pioneering work on collagen content in tumors was performed by Gullino and co-workers (163, 165), both studies summarized in an earlier review by Jain (219). Gullino et al. studied collagen in various tumor types, mainly focusing on hepatomas, and found that tumors contained more collagen than the original tissues from which the tumors arose (219). Furthermore, there was a significant variation in collagen content depending on tumor type. They also showed that collagen in tumors is produced by the host stromal cells, although its synthesis is regulated by the tumor cells, and that during growth of a given tumor type, the collagen content per unit tumor weight is constant at all tumor transplant generations independent of age and site (163). Collagen content can vary depending on the tumor type; measured values include ~2 mg/g tissue in xenografted adenocarcinoma (323), osteosarcoma (105), and ovarial carcinoma (85) and 4.6 mg/g tissue (85) in chemically induced mammary carcinoma (494).

In addition to providing structural features to the interstitium, GAGs together with collagen offer a significant resistance to interstitial fluid flow (see sect. III*D*), in turn influencing the uptake of therapeutic agents (104, 323, 365). Both hyaluronan as well as PGs play important roles in tumor growth and progression (54, 134, 408, 466). Many of their functions depend on the ability to bind and affect the activity of various ECM components, and the fine structure of the GAG chains determines the ability of PGs to interact with other molecules, such as growth factors and chemokines. PGs can serve both tumor-promoting as well as tumor-suppressing roles depending on the protein core, the GAG attached, molecules they associate with, localization, tumor subtype, and tumor stage (134). Interestingly, PGs may also influence the structure and organization of collagens that in turn influence transvascular exchange in experimental tumors. In KAT-4 tumors grown in mice deficient in fibromodulin, a PG with a known role in collagen assembly and maintenance (14), collagen fibrils were thinner and less abundant compared with wild-type mice (338). These changes in the tumor matrix structure resulted in a reduced IF pressure (P_{if}) and an increased V_i, in turn affecting fluid convection out of the stroma.

As for collagen, PG content varies with tumor type, but not to the same extent as for collagen (see above). For two tumor types, one neuroblastoma and one sarcoma, the PG content was 0.06–0.07 mg/g tissue (323), whereas somewhat lower values were found for osteosarcomas (1.0–1.2 μg/g) (105) and rhabdomyosarcomas (0.3–0.4 μg/g) (104).

Another important GAG-structural component of the tumor interstitium is hyaluronan. The role of hyaluronan in tumor growth and development has been realized for many years (219) and has been the topic of several extensive recent reviews (156, 473, 474). Hyaluronan is overproduced by many tumors, and hyaluronan is known to promote cell invasiveness and epithelial-mesenchymal transition.

Elastin is not a common component of tumors. In "scirrhous" breast carcinomas, however, elastoid material has been observed in breast carcinomas in significant amounts (up to 3% of dry tissue weight) (226) and, furthermore, in malignant salivary gland tumors and some intestinal tumors (226).

B. Charge of the Interstitium

The various components of the interstitium may carry charges that can affect the composition of the IF and affect fluid balance. This may particularly apply to GAGs that carry one to three negatively charged side groups on each disaccharide unit at physiological pH (91), but the charge of collagen, although small (see sect. II*B*), may also influence the composition of the IF. Such charge effects have been particularly well-studied in cartilage by Maroudas and coworkers, who showed that the intra- and extrafillbillar distribution of extracellular fluid, and thereby molecular packing of collagen, is dependent on electrostatic repulsion (485) and the amount of osmotically active components in the extrafibrillar fluid (236). Furthermore, these polyanionic GAGs will draw monovalent cations into the gel, resulting in a very high Na^+ concentration that may exceed 250 mM (299). The fluid within the collagen fiber may influence the structural organization of the collagen fibril and thereby the interstitial distribution of macromolecules as discussed in the following section.

Whether charged components affect the composition of the IF in other compartments has been debated. In rabbit skin, Haljamäe et al. (177) compared IF sampled by micropipettes with fluid from implanted capsules and plasma. They found a higher K^+ and Na^+ and a lower Cl^- content in tissue and capsular fluid than in plasma and ascribed this to a higher content of GAGs in both extravascular fluids. Differences in electrolyte concentration and protein concentrations between capsular and tissue fluid were interpreted in light of differences in types of GAG species and thereby charges in the two compartments from where the fluid derived. Such differences in ionic composition were not found by Gilanyi and Kovach (150), who concluded that the ions distributed according to the Gibbs-Donnan equilibrium, where the negatively charged plasma proteins attracts cations to increase Na^+ and K^+, and decrease Cl^- concentrations in plasma compared with the interstitium. Interestingly, whereas Haljamäe et al. (177) found a higher protein concentration in capsular fluid than in IF, the opposite was observed by Gilanyi and Kovach (150). These discrepancies may be due to methodological approaches used; Haljamäe et al. (177) isolated up to 50 nl by careful aspiration, whereas Gilyanyi and Kovach (150) collected 20–60 μl without aspiration but after exposure of subcutaneous tissue surfaces by electrocoagulation. Clearly, the latter procedure is more traumatic and may have resulted in an inflammatory reaction, plasma protein leakage, and a higher protein concentration in interstitial than in capsule fluid less exposed to inflammation. Their experiments might therefore not be used as evidence of a Gibbs-Donnan distribution of ions between plasma and interstitium.

Later Gilyani and Kovach (151) modified tissue charge by local generation of H^+ and OH^- in a classical Guyton capsule to show significant effects on P_{if} of generated positive as well as negative charge, supposedly resulting from increased charge repulsion in the interstitial gel. Since the most positive P_{if} was observed upon generation of a low amount of negative charge (151), it was concluded that subcutaneous tissue has a positive charge. This might seem surprising considering the negative charge of the GAGs present in the interstitium. The explanation might be that collagen has a weak net positive charge at physiological pH (236) (see sect. II*A1*) and that the larger amount of collagen may contribute to cancel out the negative charges of GAGs in rat skin. Even if Gilanyi and Kovach's conclusion that the subcutaneous tissue has a positive charge is correct, negatively charged GAGs still influence fluid volume distribution in skin and muscle as discussed below and in section II*C*.

A series of recent experiments by Titze and collaborators have suggested a new and more active role of skin GAGs in total body Na^+ and thus fluid volume regulation. They first showed that Na^+ retention during high salt feeding was associated with increasing GAG content in cartilage and skin (468). Then, they measured osmotically active and inactive Na^+ (i.e., Na^+ accumulation without corresponding accumulation of water) during growth of rats on a low- (0.1%) vs. high-salt (8%) diet (412) and found that while salt was lost from the body during growth, there was additionally a dietary-induced salt loss of osmotically inactive Na^+ that originated mostly from skin. Long-term salt deprivation resulted in a shift of PG composition with reduced sulfated PGs and increased hyaluronan, which lowered the charge density and water-free Na^+ binding to the ECM. These important findings suggest that GAGs may provide an actively regulated interstitial cation exchange mechanism for regulating fluid volume and blood pressure. Later experiments have suggested that the response to high salt is orchestrated by activation of tonicity-responsive enhancer binding protein (TonEBP) in infiltrating macrophages, that in addition to change in GAG charge density and amount results in VEGF-C secretion and hyperplasia of the lymph capillary network (279) **(FIGURE 1)**. Although the function of the newly formed lymphatics was not tested, i.e., whether the skin lymph flow was actually increased, they concluded that TonEBP-VEGF-C signaling in macrophages were major determinants of extracellular fluid volume and blood pressure. In this context, it would be of interest to assess the concentration of Na^+ in IF proper, i.e., whether the tissue GAGs create a gradient in Na^+ different from what is predicted by the Gibbs-Donnan effect discussed above for the capsule and IF (151).

C. Interstitial Volume Exclusion

1. Definition

Structural interstitial macromolecules, particularly GAGs and collagen, will restrict the space available to macromolecules in the interstitial space simply because the molecules

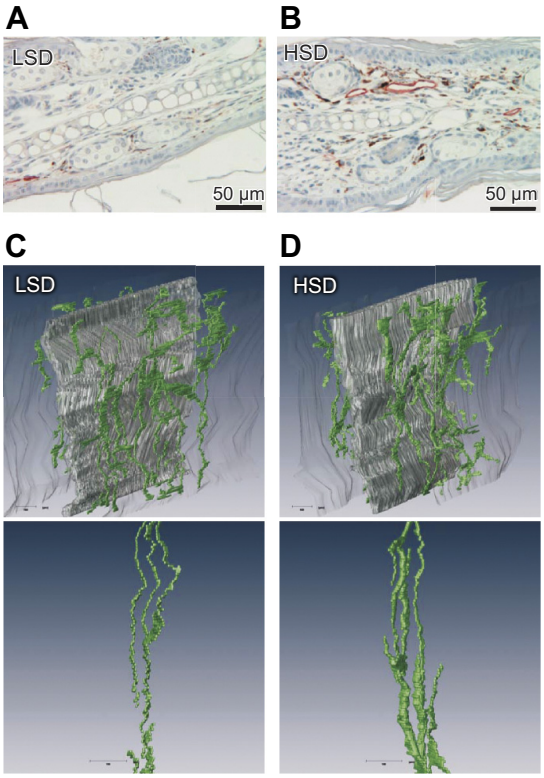

FIGURE 1. Lymphatic hyperplasia induced by high salt. *A* and *B*: representative images of ear lymphatic capillaries in mice fed a low-salt diet (LSD) (*A*) or a high-salt diet (HSD) (*B*) for 2 wk visualized by LYVE-1 immunostaining (red). *C* and *D*: representative images of the lymphatic capillary network in proximity to cartilage within the ear of rats fed a LSD (*C*) or HSD (*D*) for 2 wk. Reconstructions of three-dimensional lymphatic capillary networks (green) using 143 individually stained 7-μm serial sections of rat ear specimens in a rat with LSD and in a rat with HSD. *Bottom panels* show reconstructions of 3 selected lymph capillaries. [Modified from Machnik et al. (279), with permission from Nature Publishing Group.]

cannot occupy the same space **(FIGURE 2*A*)**. This phenomenon is called geometrical or steric interstitial exclusion and was first described by Ogston and co-workers (333, 334). ECM GAGs that are negatively charged at physiological pH values may add to this steric effect by exerting an electrostatic exclusion effect on negatively charged macromolecules, notably plasma proteins, and as evident from several recent studies discussed below, both effects contribute in determining the distribution volume of macromolecules **(FIGURE 2*B*)**. To quantify available and excluded volume, which may be expressed either as a fraction of the total IF volume or as an absolute volume, it is essential to have a reliable method to estimate the concentration of the macromolecular probe in the IF. Methods for IF isolation are evaluated in section VI*A*.

Interstitial exclusion phenomena with focus on in vitro data have been reviewed extensively in this journal (24, 25, 91), and more recently by Wiig et al. (497). A significant amount of new data originates from skin and muscle, and central questions have been how charged tissue elements and hydration affect the excluded volume effect.

2. Excluding structures

The structures responsible for interstitial exclusion are the major components of the ECM, i.e., collagen and GAGs. By combining in vitro and in vivo data it is possible to assign excluded volumes to specific tissue components and thereby to provide information on the structural organization of tissues. The importance of the structural organization of macromolecules was illustrated using collagen from human dermis by Bert et al. (49), who compared albumin exclusion in collagen fiber preparations versus intact dermis and found that disorganized fibrils excluded albumin from twice the volume of 1.57 g fluid/g collagen found in the intact dermis. It is likely that the excluded volume ascribed to collagen may be modified by hyaluronan as shown for the rat tail (26). Hyaluronan in the IF will furthermore have an additional exclusion effect, estimated at 50 g fluid/g hyaluronan in vitro (257). Although hyaluronan has a ~30-fold higher exclusion effect than collagen in vitro, the fact that the collagen content in dermis is >600 times that of total hyaluronan (502) makes hyaluronan quantitatively less important in that tissue. The remaining GAGs, however, may contribute significantly to the excluded volume effect. On the basis of the value 1.57 g fluid/g collagen (49), it was estimated that collagen and GAGs contributed to 56 and 44% of the exclusion effect, respectively (502), and that >90% of the GAG effect was due to PGs. In the same experiments, the specific excluded volume for PGs was estimated at 44 g fluid/g, i.e., close to that of hyaluronan discussed above.

The origin of the excluded volume effect is strongly dependent on the ECM composition, as shown in rat mammary tumors where the excluded volume that could be ascribed to hyaluronan was 10 times that of collagen (498). Furthermore, in the rat mesentery, a change in ECM structure caused an 80% increase in albumin excluded volume with increasing age (352).

3. Physiological influence of exclusion

Mathematical modeling has provided much insight into the importance of the exclusion phenomenon with respect to interstitial volume regulation (158, 378). These studies indicated that the extent of exclusion has little effect on the steady-state IF protein concentration and thereby colloid osmotic pressure. A higher excluded volume will, however, shorten the tissue response time to perturbations in IF volume and decrease the transfer of interstitial protein to plasma for a given capillary hyperfiltration. The amount of exclusion will accordingly influence plasma volume regulation (25).

Although not commonly thought of in a fluid balance perspective, the volume exclusion effect may also be important in shaping the structure of the ECM as suggested by recent experiments in vitro. Increased macromolecular crowding

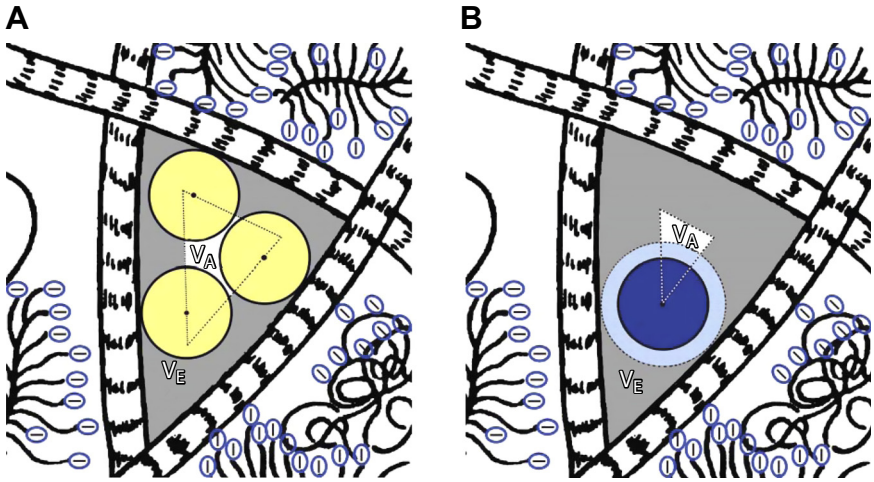

FIGURE 2. Schematic models of the interstitium and the exclusion phenomenon. *A*: sterical exclusion. The presence of structural molecules, e.g., neutral collagen (cross-striped bars) and negatively charged hyaluronan and proteoglycans, results in macromolecular crowding of the interstitial space. Consequently, the fluid space available for other species diffusing through the interstitial media is less than the total interstitial fluid volume V_i. The center of the spherical molecule (yellow) can only access the area inside the dotted line, the available volume V_A, and is excluded from the area outside the dotted line, V_E. *B*: sterical and charge exclusion. GAGs are negatively charged at physiological pH values that may add to its steric exclusion effect. Electrostatic factors are involved in selectively excluding negatively charged macromolecules that are distributed in and transported through the interstitium. A negatively charged probe will accordingly have a higher apparent radius (light blue) than an uncharged one. The case illustrated shows that, when the combined effect of steric and electrostatic factors are considered, V_E is higher than in the case where only steric factors were accounted for (*A*). [From Wiig et al. (497).]

(and thereby volume exclusion) was shown to have dramatic consequences for reaction kinetics and molecular assembly resulting in strongly accelerated collagen deposition, reactions that were affected by hydrodynamic radius of macromolecules as well as charge (256).

4. Interstitial volume exclusion in skin and muscle

The question whether ECM charge can affect the macromolecular distribution in the IF has been addressed in several recent studies in vitro and in vivo by Wiig and collaborators. By titration of albumin charge from an isoelectric point (pI) of 4.8 (native albumin) in gradual steps to a value of pI = 8.0 and equilibrating the tracer in fully swollen dermis (502) or in an equilibration cell where swelling was restricted (513) in vitro, they demonstrated that there is a significant and graded effect of the probe charge (**FIGURE 3*A***). This effect was shown as a distribution volume of native albumin of 49% of the corresponding V_i, increasing to 72% for positively charged albumin (pI 8.0). From other experiments they estimated that the steric and the charge effects accounted for 61 and 39% of the exclusion effect in fully swollen dermis, respectively (502), and accordingly that the charge effect was significant.

Interestingly, this effect of charge was dependent on hydration (513) (**FIGURE 3*B***). As the interstitial fluid volume V_i was reduced, the absolute difference in available volume between the neutral and the negative albumin decreased. Calculations showed that whereas charge contributed significantly to the exclusion effect at high hydration, this effect was gradually reduced and abolished when albumin was excluded from the entire extracellular fluid phase. The authors explained the findings by a gradual loss of hydration domains for negatively charged macromolecules in conditions of increased electrostatic interactions resulting in a change in matrix geometry at low hydration. Then a situation may occur where polyelectrolyte chains merge and the network tends to collapse (59), resulting in reduced contribution of charge to volume exclusion at reduced hydration. Another conclusion from the same study was that hyaluronan associated with collagen might influence the intrafibrillar volume of collagen and thereby available and excluded volume fraction.

The question of distribution volumes of macromolecules has also been addressed in more recent in vivo studies. By applying a continuous infusion method to establish steady-state levels of radiolabeled tracers, available and excluded volumes have been measured in several organs (496), showing that albumin was excluded from 41 and 26% of the rat hindlimb skin and muscle, respectively. With the use of the same approach, similar excluded volumes were found for albumin and the larger IgG (Stokes radius 3.53 vs. 5.61 nm, respectively; Refs. 50, 372) and suggested that electrostatic differences due to a more positively charged IgG might compensate for the larger size of this molecule compared with albumin (500). That there is a significant charge effect on

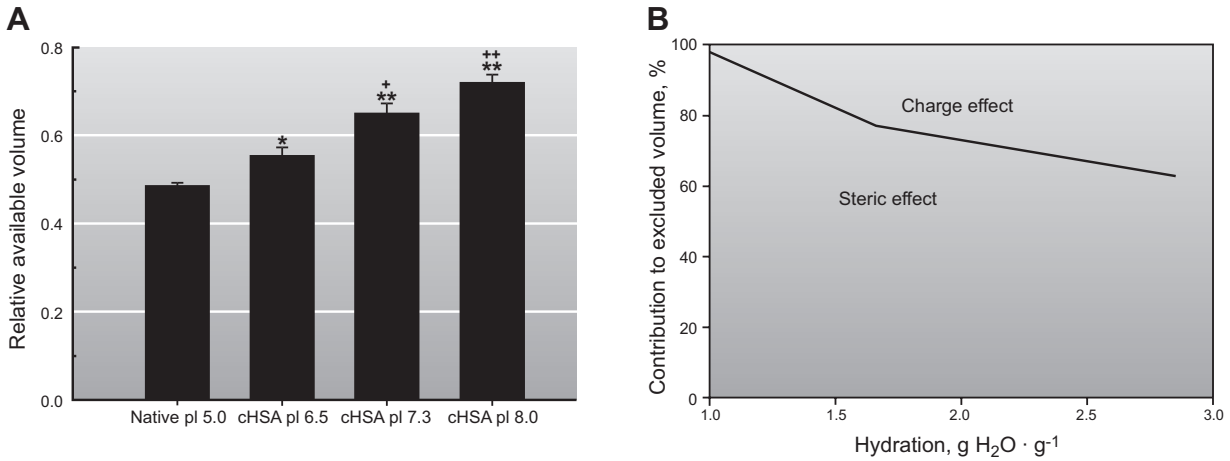

FIGURE 3. *A*: available volume fraction for native and charge-modified human serum albumin (cHSA) relative to that of the extracellular tracer ^{51}Cr-EDTA. A gradual change in pI was achieved by varying the reaction time. $*P < 0.05$ and $**P < 0.01$ compared with native albumin; $+P < 0.05$ and $++P < 0.01$ when compared with cHSA-pI 6.5. Error bars indicate ±SE. [Modified from Wiig et al. (502).] *B*: relative contribution of steric and charge effects to excluded volume of native human serum albumin (pI = 4.9) related to hydration of dermis. Area below division line represents steric whereas area above line represents charge effect. There is an increased importance of steric and a reduced importance of charge for exclusion of HSA with reduced hydration. [From Wiig et al. (513).]

plasma protein distribution volume in rat skin and skeletal muscle was shown using native albumin (pI = 5.0) and cationized neutral albumin (pI = 7.6) (173), as well as using subclasses of human IgG, namely, IgG 1 (pI = 8.7) and IgG 4 (pI = 6.6), where the negative IgG 4 was excluded from a volume of about twice that of the positive IgG 1 (512). From the former study it was estimated that the fixed negative charges of the interstitium were responsible for 40% of the total albumin exclusion in skeletal muscle and 25% in full skin and, moreover, that the similar exclusion of homologous IgG and albumin was due to a more negative charge of the latter (173).

A controversial issue has been if and how variation in hydration during perturbations in fluid balance affects excluded volume. Reed et al. (379) found that absolute available and excluded volume for albumin varied with hydration in rat skin. Suspecting that hydration status might be the explanation for deviation in reported available and excluded volume, Wiig et al. (513) compiled available data related to hydration from dermis **(FIGURE 4)**. From these data it is evident that there is a linear relationship between hydration in the range of 1.0–3.0 and available volume, strongly suggesting that the initial hydration is an important determinant of available and excluded volume, a fact that may also explain some of the diversion in published control values.

5. *Interstitial volume exclusion in tail tendon and rabbit lung*

Aukland and co-workers have used the tail tendon as a model for a well-organized tissue with high collagen content (40% of wet weight, Ref. 20), a model well-suited to study the effect of tissue structure on excluded volume. They applied a centrifugation technique to isolate interstitial fluid and assayed the distribution volumes for a range of endogenous proteins as well as radioactive probes (20, 26, 28). In this specialized tissue only 39% of the V_i was available to albumin, in agreement with previous data from another collagen-rich tissue, namely, dermis (51). These experiments also suggested that the intrafibrillar water con-

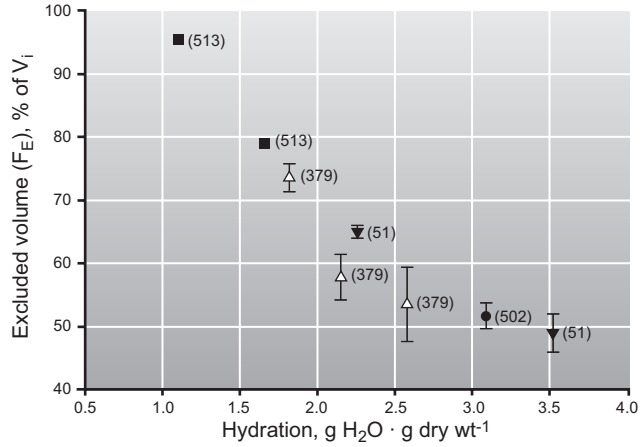

FIGURE 4. Excluded volumes relative to hydration. Compiled relative excluded volumes (F_E) in dermis expressed as percent of interstitial fluid volume (V_i) relative to hydration. Symbols represent data from the following studies: ▼, Ref. 51; ●, Ref. 502; △, Ref. 379; ■, Ref. 513. Values are ±SE. Results for Ref. 513 are derived from regression equations and SE not shown. A linear relationship between hydration and excluded volume is demonstrated [Excluded volume (F_E) (%) = 109–19 * Hydration, $r = 0.93$]. [Modified from Wiig et al. (497).]

tained in collagen fibers was variable, a phenomenon that may affect fibril volume and organization and thus the overall exclusion value provided by such fibers (26). Such variation was ascribed to hyaluronan that was intrafibrillar and elutable (26) and may thus contribute to variation of the absolute excluded volume of collagen dependent on hydration.

In the rabbit lung, albumin distribution volumes have also been estimated in recent studies using the tracer equilibration technique described above and sampling of interstitial fluid by implanted wicks. Negrini et al. (321) found a high excluded volume fraction of 0.66 in control situation compared with previous values of ~0.38 in dog lung (353, 354), a finding that led them to conclude that the lung interstitium must have a tight fibrous structure that is highly restrictive with respect to plasma protein distribution. In another study they found that the albumin distribution volume was highly sensitive to hydration, since an increase in V_i of 39% reduced the excluded volume fraction to 33% of the control value (320). It is likely that the discrepancy in excluded volumes in control situations is due to tissue hydration as discussed for skin in section II*C4*.

6. Interstitial volume exclusion in tumors

Apart from its physiological importance in normal tissues, exclusion phenomena in tumors are of additional interest in the context of drug delivery. The tumor interstitium is considered a major barrier to drug delivery (136, 217, 221, 251), and excluded volume fraction is thereby one of the factors that may affect uptake and distribution of protein and antibody therapeutics. The question of distribution volume of macromolecules has therefore also been addressed in tumors. Krol et al. (251) determined available volumes for various dextrans (mol mass 10^4 to 2×10^6 Da) and bovine serum albumin and related these volumes to extracellular volume measured using inulin as an extravascular tracer in tissue slices of fibrosarcomas. They found low available volumes of ~5% of the total tissue volume for albumin using low tracer concentrations (0.1 and 1.0 mg/ml), thus corresponding to ~10% of the extracellular volume since this was estimated at 50% of tumor weight. The albumin volume increased to 18% of total and thereby 36% of the extracellular volume when tracer albumin concentration was increased to 10 mg/ml. It is likely that they underestimated the available volume fraction, thereby overestimating the excluded volumes significantly, even with the highest tracer concentration since albumin is >10 mg/ml in tumor interstitial fluid (439, 494). In a later study they found no effect of hyaluronidase treatment (250), thought to reduce excluding GAGs, but hyaluronan fragments resulting from degradation might be as effective excluding agents as intact hyaluronan because the total charge density is maintained.

In a recent study of chemically induced mammary tumors in rats, the effects of macromolecular size and charge on distribution volume were assessed using native (pI = 4.8) and cationized albumin (pI = 7.6), IgG (pI = 7.6), and the monoclonal antibody trastuzumab (pI = 9.2) (498). Neutralizing albumin resulted in a reduction of excluded volume by 50%. Trastuzumab, the most positively charged probe, had the largest distribution volume (71%), compared with 64% for IgG. The available volumes in tumors were higher for all probes than in back skin, suggesting a lower restriction of macromolecular uptake in tumors, thus contrasting the ex vivo studies discussed above. Later, with the use of similar approaches in ovarian carcinoma models, somewhat lower IgG available volumes of ~50% have been found (85), but it is likely that these volumes were affected by variation in ECM structure as well as hydration as discussed above.

Clearly, the increased density of charged matrix components in tumors, notably hyaluronan (391, 474), influences volume exclusion and thus the distribution of charged macromolecular species and therapeutic agents. In light of the studies discussed above, it has been proposed that either the extracellular GAGs or the net charge of therapeutic molecules can be modulated to increase the available volume, thus enhancing drug distribution and thereby the likelihood of therapeutic effect (497). This hypothesis needs to be further tested experimentally.

D. Structural Properties of Lymphatic Capillaries

IF is formed continuously by filtration, and lymph vessels are required for carrying fluid, interstitial proteins and peptides, and cells to the lymph nodes and back to the blood circulation. We will briefly discuss the structure of the initial part of the lymph system based on several more extensive reviews (336, 414), adhering to the terminology of Schmid-Schönbein (414).

Prelymphatic channels, whose existence has been debated (78), are characterized as well-defined tissue channels that conduct fluid from the capillaries to the initial lymphatic vessels, also described as a "low-resistance pathway" in skin and muscle as opposed to the "high-resistance pathway" exerted by the ground substance (ECM) (185). Such structures have also been described in liver (335), lymphoid tissue (29), and lung (418). In the brain, nonendothelialized spaces between the internal vascular and the external glial basal laminae act as a prelymphatic drainage system (283).

Lymph vessels are present in almost all tissues. Exceptions are avascular tissues such as epidermis, cartilage, the eye lens, and cornea as well as some vascularized organs like brain, retina, and bone marrow, and lymphatic architecture can vary depending on the organ and tissue (414). The

lymphatic system originates in the interstitium as initial lymphatic vessels (also referred to as lymphatic capillaries or terminal lymphatics). With the exception of bat wing, these vessels are noncontractile, considerably larger (10–60 μm; Ref. 448) than surrounding blood capillaries, consist of a single layer of endothelial cells without pericytes or smooth muscle media, and have little or discontinuous basement membrane (30). Of note, the fact that bat wing initial lymphatics are contractile is important when interpreting data on lymph formation discussed in section V*A*. The abluminal part of the initial lymphatics is connected to the elastic fibers in the surrounding ECM via so-called anchoring filaments (258, 260) consisting of collagen VII (238, 404), a connection made via the transmembrane integrin and focal adhesion kinase (148). The single layer of endothelial cells are overlapping and interdigitated, as first demonstrated in elegant microscopy studies of Leak and Burke (258–260). More recently, these overlapping endothelial cells were found to be joined together by the junctional protein VE-cadherin in "buttonlike" patterns (32, 307) that may serve as flaps that allow one-way absorption of cells, fluid, and proteins. These structures may also be considered as the "primary" valves proposed to exist based on functional analysis (476) **(FIGURE 5*A*)**.

Lymph forming in the initial lymphatics drains to larger collecting lymphatics that are generally not tethered to the ECM but often surrounded by adipose tissue. Collecting lymphatics are endowed with smooth muscle cells, continuous endothelium, basement membrane, and regular valves

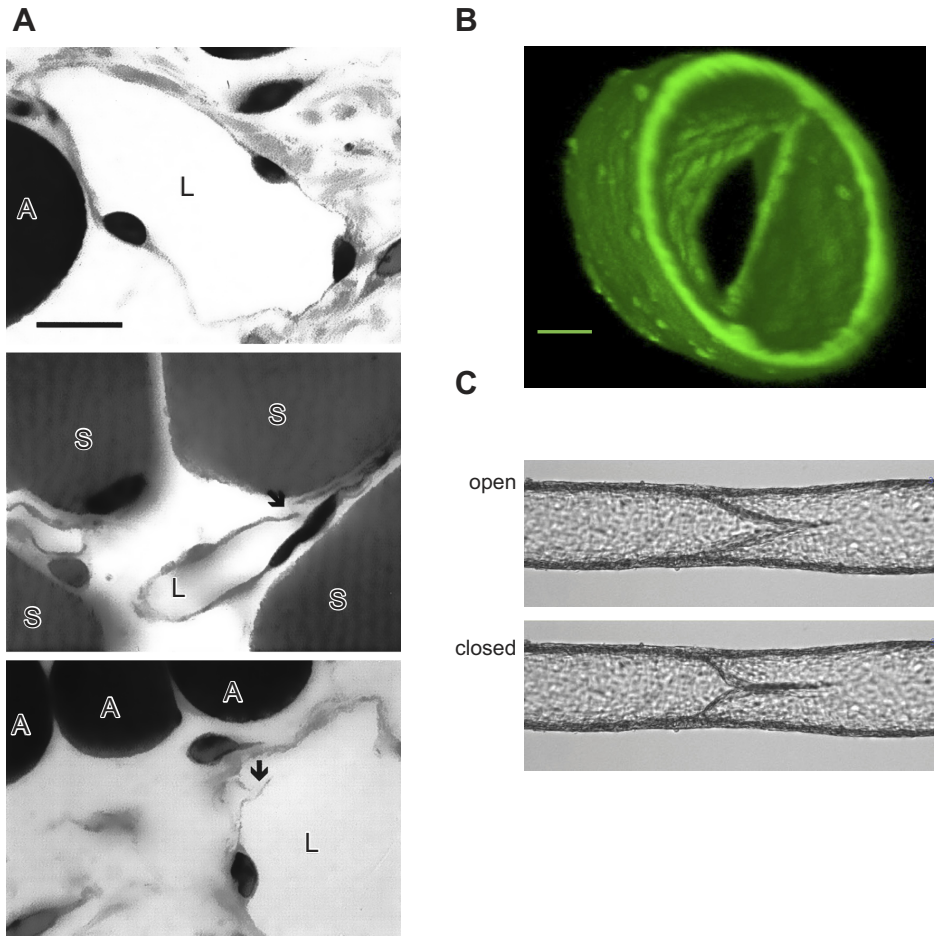

FIGURE 5. *A*: lymphatic endothelial flap junctions ("primary valves") in skeletal muscle. Typical cross sections of initial lymphatic channels (L) in muscle fixed without muscle compression (*top panel*) and during periodic muscle contraction to enhance lymph flow (*middle* and *bottom panels*). The lymphatics are located adjacent to skeletal muscle fibers (S) and some adipose cells (A). Note the presence of open flaps along the lymphatic endothelium (arrows), which are absent in resting lymphatics. These open flaps were encountered in small initial lymphatics (*middle panel*) and in a larger one (*bottom panel*) irrespective of size or location inside the muscle, and were denoted primary valves (476). No open endothelial flaps were encountered in muscles fixed in the resting state. [From Trzewik et al. (476).] *B*: confocal reconstruction of a secondary valve in a rat mesenteric lymphatic obtained in Ca^{2+}-free solution to prevent contractions. View is taken from downstream, looking back (against normal flow) into the valve. Structures at 1 o'clock and 7 o'clock at the inner edge of the lumen are the valve insertion points, or buttresses. Calibration bar = 40 μm. *C*: images of a representative vessel with the valve in the open (*top*) and closed (*bottom*) positions. Calibration bar = 120 μm. [Images kindly provided by Dr. Michal J. Davis and modified from Davis et al. (106).]

[i.e., "secondary" valves using the notation by Trzewik et al. (476)] that aid lymph propulsion and prevent retrograde flow, elegantly visualized in rat mesentery in a recent paper by Davis et al. (106) **(FIGURE 5, *B* AND *C*)**. In the human skin, there are nonmuscular precollectors that connect the subpapillary initial lymphatics with collecting vessels deeper in dermis (252). Precollectors have been difficult to differentiate from initial as well as collecting lymph vessels (403), but recent studies show that precollectors express lower levels of the membrane mucoprotein podoplanin ($LEC^{podo\text{-}low}$) compared with initial lymphatics (denoted as $LEC^{podo\text{-}high}$) (489). The authors could thus show that precollector vessels branch out of $LEC^{podo\text{-}high}$ initial lymphatic capillaries as well as differerential expression of chemokines in the two segments, implicating that the expression pattern might have functional consequences with respect to dendritic cell and T-cell trafficking in skin inflammation.

Collecting lymphatic segments between valves are called lymphangions, which serve as contractile compartments that propel lymph to the next compartment. Lymph in collecting vessels passes through lymph nodes, and vessels are accordingly classified as pre- or postnodal (or afferent or efferent) to specify whether lymph is carried to or from the lymph node, respectively. This distinction is functionally important since lymph composition is altered during passage through the nodes (7, 414) and important immune cell modifications occur in lymph nodes (375), as will be discussed in section IX. Lymph nodes are organized in clusters throughout the lymphatic system and are compartmentalized with narrow fluid crevices where the vascular compartment opposes each lymph compartment for fluid exchange and cell transport (375, 448).

Significant knowledge in lymphatic biology has accumulated during the last ~15 years due to the discovery of lymphangiogenic factors and identification of lymphatic vascular markers, isolation of lymphatic endothelial cells, and the development of animal models to study lymphangiogenesis. Since our focus is lymph formation and transport, we will not cover the molecular regulation of lymphangiogenesis and lymphatic function but rather refer to excellent recent reviews addressing these topics (11, 12, 222, 305, 459), along with a review of how the interstitial microenvironment can influence lymphangiogenesis (501).

III. MECHANICAL PROPERTIES OF THE INTERSTITIUM

The mechanical properties of the interstitium have critically important consequences for normal cell function, and changes in these mechanical properties that are seen in many pathological situations often drive cell behaviors that govern tissue remodeling, cell migration, stem cell differentiation, and even malignant transformation. The IF composition, P_{if}, and flow depends on the biomechanical properties of the matrix, and thus we first define and differentiate mechanical stress, strain, and material properties like stiffness, since these three terms are often misused.

A. Definitions of Stress, Strain, and Mechanical Properties

Mechanical stress is an applied force per unit area. Both fluid and solid stresses exist in the interstitium, and because the interstitial space is a poroelastic medium, they are intrinsically coupled. For example, a tissue perfusion causes local increases in P_{if}, which in turn exerts tensile forces on the ECM. The heightened pressure gradients also cause interstitial flow, which brings both tangential (shear) stresses as well as normal (drag) stresses on cells and ECM components in the interstitium. In addition to extrinsic forces, biomechanical stress in the interstitium can also arise from intrinsic forces due to fibroblast contraction or tissue growth (as in solid tumors).

Mechanical strain, in contrast, is the relative deformation of a material under applied mechanical stress. The degree of strain for a given stress is determined by the mechanical properties; the stiffer the matrix, the lower the strain for a given applied stress. Mechanical stress is often transmitted to cells by strain (e.g., by the degree to which interstitial matrix fibers pull on integrins, or the extent to which glycocalyx molecules or primary cilia deform).

The mechanical properties of the interstitium thus relate stress and strain. Cells can apply mechanical stresses on the ECM by contraction, and measure stiffness based on how easily they can deform the matrix. Other than this intrinsic contraction, cells cannot control extrinsic stresses or strains; however, they can actively regulate mechanical properties to alter stresses or strains locally. For example, an interstitial fibroblast may maintain homeostasis according to "normal" levels of shear stress and matrix strain imposed by physiological interstitial flow. However, if interstitial flow increases, the cell then experiences heightened shear stress and matrix strain due to shear stresses on the ECM fibers (358). In response, the cell can align the ECM fibers locally to shield itself from stress (325–327, 359), thereby changing the local interstitial mechanical properties to modulate its mechanical stress environment.

The matrix stiffness is a material property that describes resistance to deformation under mechanical stress. For a linearly elastic material, the stiffness is defined by the Young's modulus E, the slope of the stress versus strain relationship (i.e., stress = E·strain). For nonlinearly elastic or viscoelastic materials, as most tissues, we can either define the Young's modulus for a small linear range of stress/strain or describe it more accurately with different types of models and multiple moduli.

Most often used in interstitial physiology is the inverse of stiffness, the compliance, because it can be directly measured experimentally. The interstitial compliance (C_i) is defined as the change in interstitial fluid volume (V_i) divided by the corresponding change in P_{if} measured with fluid equilibration techniques (discussed in sect. IIIC) during perturbations of in fluid volume; i.e., $C_i = \Delta V_i/\Delta P_{if}$. C_i will determine how much the tissue will swell under a given fluid pressure, or conversely, how much P_{if} will change under a given change in V_i. C_i is governed by the composition, organization, architecture, degree of crosslinking, and charge of the interstitium and can be modulated by proteolysis, matrix synthesis, cell infiltration, and other events that occur in inflammation, injury, fibrosis, remodeling, and cancer.

Another important mechanical property of the interstitial space is the hydraulic conductivity or permeability. Analogous to compliance, which describes the inverse resistance to matrix strain, the hydraulic conductivity represents the inverse resistance to fluid flow (451). It can be modeled as the entire fluid-solid composite, or as a porous solid medium through which a fluid of viscosity (μ) flows. It depends on the extent of hydration of the interstitium, and thus indirectly depends on P_{if} and tissue compliance. These are described below.

B. Interstitial Fluid Pressure

P_{if} is the normal, isotropic force exerted on the interstitium by hydrostatic forces. It is balanced by the elastic properties of the structural components; in steady-state conditions without tissue deformation, solid tensile stresses are balanced with P_{if} according to the bulk elastic modulus (452). P_{if} relates V_i, transendothelial flow, interstitial flow, and lymph flow, and thus its importance in drug delivery, immunity, and potentially a host of pathological conditions related to defects in transport or aggregation cannot be overstated.

1. Definitions

Pioneering work by Guyton and co-workers about five decades ago, using implanted perforated capsules showing that P_{if} in subcutis was subatmospheric (169, 171), is still central in our conceptual understanding of this area. They defined "total tissue pressure" as the sum of the pressure in the interstitial fluid, i.e., P_{if}, and "solid tissue pressure" suggested to result from local compression exerted by the interstitial gel and fibers. Moreover, they introduced the concept of "fluid equilibration techniques" defined as pressure in a saline column brought in contact with the interstitium through various approaches allowing sufficient time for equilibration with the fluid in the tissue spaces.

As pointed out by Aukland and Reed (25), a prerequisite for negative pressures in vivo is that the interstitium is kept in a state of relative dehydration by removal of fluid by lymph vessels combined with a small net capillary filtration pressure. An ex vivo parallel to the negative interstitial pressure is the tendency of an excised tissue to swell or imbibe fluid when soaked in a saline solution (66, 291). A central question that remains unresolved is what generates this swelling pressure, i.e., whether it is of hydrostatic or osmotic origin. The energy of dehydration may be "stored" in the interstitial gel either as an osmotic pressure of immobilized substances or as a negative intragel hydrostatic pressure balanced by elastic forces of tissue elements (24, 25, 158). Here we will understand P_{if} as the pressure measured with fluid equilibration techniques irrespective of its origin. This pressure will be the sum of immobilized GAG osmotic pressure and intragel hydrostatic pressure and thus equal to the hydrostatic pressure in any free fluid in the tissue. Other pressures introduced by Guyton (171) to explain differences between subcutaneous capsule and needle pressures, the solid tissue pressure; a stress exerted by solid elements, and total tissue pressure; the sum of P_{if} and solid tissue pressure, might be considered obsolete in light of more recent data showing similar steady-state pressures with all fluid equilibration techniques (493). As pointed out previously (25, 493), P_{if} is of interest for several reasons, since it is one of the determinants of capillary fluid filtration, is a likely determinant of initial lymph formation, and is a necessary parameter for estimating interstitial compliance.

2. Measurement of P_{if}

The conclusions reached in previous summaries on techniques for P_{if} measurement about two decades ago (25, 493) are still valid and may be used when choosing a method. Although there has been some methodological development during the recent years, a few of the basic techniques are still applied and may be considered as "gold standards," notably the micropipette and wick-in-needle techniques. Common for all the established techniques is that they measure the hydrostatic pressure in the free interstitial fluid surrounding the probe, and whereas all techniques have previously been named "fluid equilibration techniques" because of a saline-filled column connecting the interstitium and the transducer, this may still be the case even if the transducer is moved to the interstitium itself.

The established methods may be classified as "acute" and "chronic." With acute methods, measurements are made within minutes to a few hours after insertion of the device, whereas the chronic devices are implanted into the tissue 4–6 wk before a measurement can be made. Chronic devices are the classical implanted perforated Guyton capsule (169), and variants thereof like the implanted porous capsule (346) and skin cup method (4). Although the chronic techniques were important for the development of this field, they seem to not have been used during the last decades.

Acute methods are the needle method (73), the wick catheter technique (416), the wick-in-needle technique (129), and the micropipette technique developed by Wiederhielm et al. (491) to determine microvascular pressure and later used for P_{if} measurements (508). As previously summarized (25, 493), the acute and chronic techniques give similar P_{if} when used in steady-state conditions. When assembling data from skin/subcutis and muscle in rat, cat, and dog, pressures ranged from −2 to 0 mmHg with no difference between techniques except for cat skin, where the wick-in-needle was more positive than the micropipette pressure, assumed to result from the insertion trauma (493). During acute transcapillary fluid perturbations, however, the chronic methods will overestimate the changes in pressure due to changes in vascular volume and low protein permeability in the capsular wall (507). The micropipette method is practically atraumatic, reproducible, requires a low displacement volume, and should be used whenever applicable, but is restricted to immobilized tissue and few millimeters of depth. Wick techniques are clearly more traumatic, but are more versatile, and recorded pressures in skin and muscle have been found to agree well with the micropipette when compared directly, although that has not been tested in other tissues. Still, the wick-in-needle is a generally accepted standard method and is frequently used in experimentally induced tumors in animals as well as in patients.

Recently, transducer-tipped catheters (349) and fiberoptic pressure transducers (348) were introduced for measurement of P_{if}. The transducers are introduced into tumor or subcutis using a fairly large (18 gauge) introduction needle, and because of their fragility, fiberoptic transducers need to be located in a perforated tube when in the tissue to prevent breakage (348), adding to the needle insertion trauma. Since these devices are not connected to the pressure transducer via a saline-filled column but rather the transducers are directly in contact with the interstitial fluid, they cannot be classified as fluid equilibration techniques in a traditional sense. Moreover, since the sensor is introduced into the tissue, the pressure-sensitive area may be directly in contact with tissue elements and thereby susceptible to solid tissue pressure artifacts, as also realized by the authors (349). Still, the good correspondence between P_{if} measured with miniature transducers introduced into mouse skin with the wick-in-needle technique, all giving a pressure in subcutis of ~−3 mmHg, suggests that this effect is minimal and that miniature tissue-implanted transducers may be used for P_{if} recording.

C. Interstitial Compliance

Interstitial compliance (C_i) is as discussed in section III*A* above defined as the change in interstitial fluid volume (V_i) divided by the corresponding change in interstitial fluid pressure (P_{if}) measured with fluid equilibration techniques during perturbations of in fluid volume, i.e., $C_i = \Delta V_i/\Delta P_{if}$. C_i will determine the hydrostatic counterpressure to a given change in V_i. Accordingly, in a tissue with low C_i, an increased net filtration will be counteracted by a marked increase in P_{if} even at a low increase in V_i, whereas in a tissue with low C_i a considerable amount of volume will be allowed to accumulate before P_{if} rises. The importance of C_i in fluid volume regulation has been suggested by mathematical models describing whole body fluid and macromolecule exchange, having shown that volume-pressure relationship of the interstitium as a sensitive parameter with significant effects on predictions of distribution and transport of fluid and plasma proteins (e.g., Refs. 82, 378, 521).

In pioneering studies by Guyton (170), a C_i of 0.2 ml·100 g^{-1}·$mmHg^{-1}$ was found in subcutis using implanted capsules and by estimating interstitial volume changes by plethysmography. Later studies, where local changes in V_i and P_{if} were measured with extracellular tracers and micropipettes, respectively, showed severalfold higher C_i of 3.4 ml·100 g^{-1}·$mmHg^{-1}$ (corresponding to 7.6% of V_i per mmHg decrease in P_i) in dog skin (506), similar to measurements in skin and muscle in other species (493). The underestimation of C_i due to overestimation of the change in P_{if} (25, 493) notwithstanding, the more recent studies verified the overall shape of the initial volume-pressure curve **(FIGURE 6)** observed by Guyton (170) as being *1*) linear in dehydration and in the initial phase of overhydration; *2*) showing practically no rise in P_{if} at >50–100% increase in V_i, indicating an almost infinite C_i; and *3*) showing an increased P_{if} at extreme overhydration because of tissue volume restriction most likely by collagen-rich fascias. The $\Delta P_{if,max}$ **(FIGURE 6)**

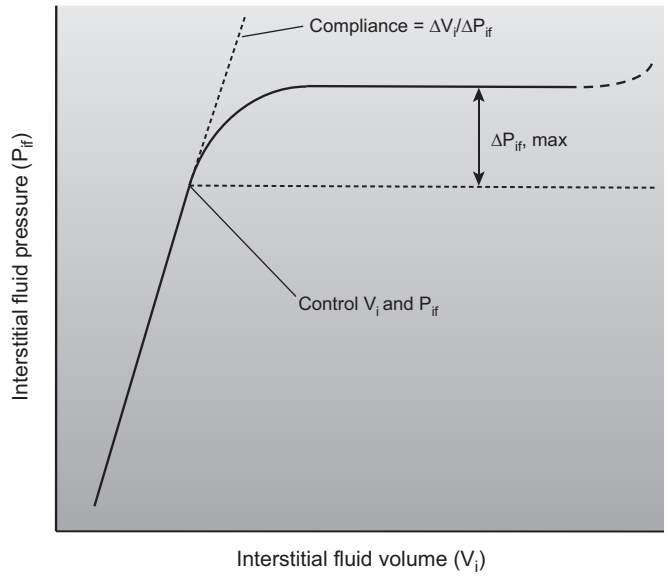

FIGURE 6. General shape of the interstitial volume-pressure relationship. The following features should be noted: *1*) interstitial compliance ($C_i = \Delta V_i/\Delta P_{if}$) is constant in dehydration and the initial part of overhydration; *2*) at further overhydration, compliance increases to infinity but decreases at excessive increase in V_i; and *3*) maximal rise in P_{if} that can be obtained as counterpressure toward filtration ($\Delta P_{if,max}$). [Modified from Aukland and Reed (25).]

represents the maximal counterpressure against increased fluid filtration discussed in more detail in section VII*A*.

1. Compliance of normal tissues

Bert and Reed (53) determined the volume-pressure relationship in vitro by compression of excised rat dermis. Using hydration as a surrogate for V_i, they found a volume change of 6.6%/mmHg around normal hydration, ~50% of C_i in rat skin measured in vivo (504). Although it has not been established how different interstitial components affect the shape of the volume-pressure curve, collagen and hyaluronan were shown to influence C_i in skeletal muscle and back skin of hypothyroid rats (503). In hindlimb muscle, V_i changed by 12.2 and 19.9%/mmHg in hypothyroid and euthyroid rats, respectively, and was suggested to result from a 56% higher muscle hyaluronan (509). This structural change was suggested to result in an increased gel osmotic pressure and thereby a more negative P_{if} for the same change in V_i in the hypothyroid rats. If so, we would expect the opposite effect on C_i upon removal of hyaluronan, which was actually observed in abdominal wall muscle (530). During increased hydration, C_i increased severalfold from control levels corresponding to 4%/mmHg that was associated with a 50% reduction in hyaluronan. The collagen content and fiber distribution may also influence C_i (503), but this has not been shown experimentally.

Evidently, the state of hydration and condition of the tissue may also influence C_i. In rats, P_i rose by 2 mmHg to approximately +1 mmHg, and the compliance in hindlimb skin was almost infinite at a hydration 2–3 times control (504). In freeze injury, however, the volume-pressure relationship in rat paw skin was linear up to an overhydration of 140% with a corresponding C_i of 6%/mmHg (46). A C_i more than 50% lower than in dehydration in normal rats (504) suggests that the matrix is stiffer in this injury model, an assumption supported by the dramatic increase in P_{if} that rose to 22 mmHg 60 min postfreeze (46). Interestingly, this study also indicated that C_i may change with time due to stress relaxation as suggested by Guyton (170), since P_{if} fell by 15 mmHg at constant tissue volume during the 60 min following placement of a tourniquet. Relaxation of tissue elements in longstanding overhydration may also be the explanation for the relatively high compliance of 21%/mmHg in upper arm skin in secondary lymphedema (37).

The volume-pressure relationship is of particular importance in the lung. Miserocchi et al. (297) measured P_{if} by micropipettes and volume by weight to estimate lung compliance at 0.47 ml·100 g^{-1}·$mmHg^{-1}$, which is in the same range as abdominal wall muscle (530). Interestingly, disruption of the lung ECM causes dramatic increases in C_i (318, 319, 364). C_i has also been estimated as 8% in trachea (520) and 6% in rat submandibular gland (47), showing that these organs will counteract fluid filtration more efficiently than rat skin, where C_i is 14%/mmHg (504).

2. Interstitial compliance of tumors

Since C_i determines the counterpressure against fluid filtration and thereby affects tissue distribution of therapeutic agents, tumor C_i is important for cancer therapy. We are not aware of any C_i data based on local V_i measurements in tumors, but this parameter has been estimated from the pressure generated during constant inflow of fluid by Boucher et al. (64). In human colon adenocarcinoma tumors implanted in mice, they found a C_i of 35 μl/mmHg. This value translates to ~100% of the tissue volume per mmHg if we assume that the infused substance distributes in a sphere with radius 2 mm surrounding the infusion point that corresponds to the outer limit used for P_{if} recording. As pointed out by the authors, however, the values were first-order approximations only and difficult to compare with values discussed above because the data were highly dependent on assumptions used in the calculations. Of note, in this study, compliance increased approximately threefold after cardiac arrest, suggesting that vascular distension strongly affected the estimated value.

D. Hydraulic Conductivity of the Interstitium

Just as the interstitial compliance determines how much a tissue will deform under stress, the hydraulic conductivity is another mechanical property of the interstitium that determines how fast fluid will move through the tissue under a given fluid stress (pressure gradient). It can also be considered as an inverse resistance to fluid flow. It is a bulk property of the interstitium, and like compliance, it is determined by the interstitial composition, organization, and charge, although these contribute differently to conductivity versus compliance. In particular, while the overall strength of fibrous components like collagen and its degree of cross-linking largely determine compliance, the free water volume fraction, resulting from the balance between swelling forces (hydrostatic and osmotic pressure and electrostatic forces from highly charged macromolecules like GAGs) and counteracting forces like cell contraction and matrix tension, largely determines the hydraulic conductivity (25, 382).

1. Darcy's law

The civil engineer Henry Darcy first described a linear relationship between pressure gradients and flow rate through a sand bed (97); his empirically determined relationship was later theoretically confirmed by considering the resistance due to shear stress on the fluid-solid interface in a fluid-filled porous matrix. Darcy's law is most commonly written as follows:

$$v_{if} = -K' \nabla P = -(K/\mu) \nabla P \quad (1)$$

where v_{if} is the bulk interstitial fluid velocity (or flow rate divided by cross-sectional area), K' is the hydraulic conductivity (with units of $cm^2 \cdot s^{-1} \cdot mmHg^{-1}$), ∇P is the pressure gradient (i.e., the pressure drop ΔP divided by the distance L, or $\nabla P = \Delta P/L$), K is the hydraulic permeability or specific permeability (with units of cm^2), and μ is the viscosity of the fluid phase. Note the difference between K' and K; the first (K') is an effective property of the combination of fluid and porous solid matrix, while the second (K) is a property of the porous matrix alone, independent of the fluid viscosity. The latter is also often referred to as the Darcy permeability coefficient. These relationships emphasize the fact that the fluid viscosity is directly proportional to the effective resistance to flow through porous media.

This simple relationship has been widely used in interstitial physiology. Measurements of hydraulic conductivity can reveal important functional information about changes in tissue hydration (e.g., during acute phases of inflammation) and matrix remodeling (e.g., in fibrosis). For example, in three-dimensional perfused culture systems, an increase in the resistance to flow (i.e., decreased K) was correlated with matrix alignment and synthesis (326, 327). **TABLE 4** shows measurements of hydraulic conductivity and permeability in a variety of tissues and biomaterials (451).

2. *Relationship between shear stress and hydraulic conductivity*

While Darcy's law is an excellent approximation for relating pressure and flow through a bulk material, it is a first-order equation and as such does not permit one to account for nonporous boundaries, because it does not permit no-slip boundary conditions. In the case of interstitial tissues, an example of the type of problem this poses is when attempting to calculate shear stresses on the surface of a cell embedded in a porous (interstitial) matrix. To address this, Brinkman modified Darcy's law in 1947 (70) by including a second-order viscous term and is most often written as the following:

$$\nabla P = -(\mu/K) v_{if} + \mu \nabla^2 v_{if} \quad (2)$$

Table 4. *Selected permeabilities measured in tissues*

	Tissue/Material	*K*, cm^2	*K'*, cm^2/mmHg-s	Method*
Biopolymers	Fibrin (3 mg/ml)	10^{-8} to 10^{-11} (111)		3
	Type I collagen (1.5–3.5 mg/ml)	10^{-9} to 10^{-10} (15, 326)		3
Tumors	MCaIV tumor		248 (323)	2
	LS174T tumor		45 (323)	2
	U87 tumor		65 (323) to 7,000 (288)‡	2,1
	HSTS26T tumor		9.2 (323)	2
	Rat fibrosarcoma		1.36 to 1360 (533)‡	2
	B16F10 murine tumor		4100 to 11000 (288)‡	1
	4T1 murine tumor		950 to 2300 (288)‡	1
	Hepatoma		0.8 to 4.1 (531)†, 28 (265)†	2,1
Normal tissues	Rat abdominal muscle		15 to 78 (531)	1
	Rat dermis		5.33 (52)	2
	Mouse tail skin		70 to 150 (452)	1
	Subcutaneous plane		0.6 to 0.85 (531)	1,2
	Subcutaneous slice		6 (265)†	2
	Vitreous body		280 to 560 (265)	2
	Blood clot, unretracted/retracted	10^{-8} to 10^{-10} (111)		4
	Corneal stroma		0.7 to 1.6 (265)	2
	Mesentery		41 to 253 (265)†	2
	Cartilage (femoral condyle)		0.3 to 0.7 (265)†	2
	Cartilage (femoral head)		0.1 (265)†	2
	Aortic media and intima		0.4 to 2.0 (265)†	2
	Sclera		1.7 (265)†	2
	Wharton's jelly		26.7 (265)†	2
	Synovial intima		0.5 to 1.3 (265)†	1

Values are listed as either specific permeability (*K*) or hydraulic conductivity (*K'*). *Method key refers to how the measurement was made: *1*) in vivo, *2*) ex vivo, *3*) in vitro, and *4*) unknown. †References contained within cited work. ‡Values found to be pressure dependent. [From Swartz and Fleury (451), with permission.]

Using the Brinkman equation, Wang and Tarbell (486, 487) estimated that the average shear stress τ on spherical cells embedded in three-dimensional matrices undergoing flow can be estimated by

$$\tau_{avg} \cong \frac{\mu v_{if}}{\sqrt{K'}} \quad (3)$$

Pedersen et al. (358) further showed using computational fluid dynamics simulations of cells embedded in three-dimensional fibrous matrices that shear stresses on such cells were extremely heterogeneous, with peak stresses up to an order of magnitude above average. Furthermore, even small changes in fiber alignment or reorientation locally around the cell may have drastic effects on the local permeability and thus shear stress on the cell (359). Thus, while such approximations are useful for estimating average shear stresses and how these may be affected by interstitial flow velocity or hydraulic conductivity, they cannot estimate the peak shear stresses and shear stress gradients that may be imposed by interstitial flow.

3. *Effects of tissue swelling and compaction on hydraulic conductivity*

As mentioned, fluid volume fraction is the most important determinant of the hydraulic conductivity K (52), and the relationship between fluid volume fraction and K is nonlinear (172). As a tissue undergoes deformation, its microarchitecture and fluid volume fraction changes, leading to changes in K. For example, in acute stages of inflammation or after tissue injury, increased blood vessel permeability leads to increased P_{if}, which induces tissue swelling and increased fluid volume fraction. In such cases, K is rapidly increased (52).

Guyton (172) was the first to demonstrate that hydraulic conductivity varies nonlinearly with P_{if}, and when tissue pressure exceeded atmospheric pressure, hydraulic conductivity increased by orders of magnitude. He also reproduced this result in a nonbiological system using collapsible tubes with fibrous filling, confirming the physical basis for the pressure and swelling dependence of K. More recently, it was shown that K was drastically increased in secondary lymphedema (402, 452) and after overhydration in the cornea (126). In mouse tumor perfusion models, Yuan and collaborators (288, 533) demonstrated drastically nonlinear increases in hydraulic conductivity with increasing perfusion pressures.

On the other hand, tissue compaction leads to decreases in K. A classic example is the articular cartilage during walking (240), when water is exuded from the tissue as if from a sponge being squeezed. In fact, most ex vivo methods for measuring K rely on compression tests. Removing PGs and GAGs, which imbibe water due to their high electrostatic charge density, also leads to decreased hydraulic conductivity (48).

Thus, to summarize, the hydraulic conductivity K is an important property of the interstitial matrix that determines how fast fluid will flow through the matrix for a given pressure gradient driving force. It is strongly and nonlinearly dependent on hydration, whereby small increases in tissue hydration lead to large increases in K; conversely, small amounts of compression greatly increase the resistance to flow.

IV. INTERSTITIAL FLUID FORMATION AND FLOW

A. Transcapillary Transport of Water

The transcapillary exchange and formation of interstitial fluid is determined by properties of the capillary wall, hydrostatic pressure, and protein concentrations in the blood and interstitium. Although the basic principles for such transport originating from fundamental work by Starling more than a century ago (436) still applies, important modifications have been introduced (266), leading to the following conventional expression for transmembrane flux J_v (representing the volume of fluid crossing the membrane per unit time), known as the Starling Equation

$$J_v = L_p S\left[(P_c - P_{if}) - \sigma(COP_c - COP_{if})\right] \quad (4)$$

where J_v is the volume filtration rate (cm^3/s), L_p is the hydraulic permeability of the capillaries ($cm \cdot mmHg^{-1} \cdot s^{-1}$); S is the surface area available for filtration (cm^2); σ is the capillary reflection coefficient (dimensionless, with values between 0 and 1); P_c and P_{if} are the hydrostatic pressures (mmHg) in the blood capillary and interstitial compartments, respectively; and COP_c and COP_{if} are the colloid osmotic pressures (mmHg) in the capillary and interstitial compartments, respectively. The colloid osmotic pressure difference is due to the relative impermeability of the vessel wall to macromolecules and proteins (of which albumin is the most abundant), and σ corrects for the overall effective permeability to these proteins. For example, $\sigma = 1$ represents a completely impermeable barrier, while $\sigma = 0$ refers to a freely permeable barrier (and thus no effective oncotic pressure difference). These hydrostatic and colloid osmotic pressure differences are commonly referred to as Starling forces, and due to our focus on IF we will mainly address the interstitial fluid or the "inaccessible tissue factors" in fluid volume regulation (24) and not transcapillary transport in general. We will, however, briefly discuss two factors pertaining to filtration: transcapillary protein transfer and the quantitative importance of interstitial proteins and thereby COP_{if} in the Starling equation. Others have provided detailed, comprehensive reviews on transcapillary fluid exchange and V_i regulation (25, 96, 290, 292, 294, 387, 410, 460).

B. Transcapillary Transport of Proteins

Proteins may be transported across the capillaries by diffusion and convection, and we assume that the same amount filtered is removed by the lymphatics in a steady-state situation (25). The flux of proteins (or other solutes) across the capillary wall (J_s) is generally considered as the sum of convective and diffusive fluxes (460)

$$J_s = J_v(1 - \sigma)C_p + PS(C_p - C_{if}) \quad (5)$$

where C_p and C_{if} are concentrations in plasma and interstitium, respectively, and *PS* is the permeability-surface area product, i.e., a measure of the diffusive capacity of the capillary membrane. *Equation 5* describes convection and diffusion as separate processes, whereas these processes occur simultaneously in the same pathway and influence each other. This fact is reflected in the Patlak equation (357) used extensively by Taylor et al. (460) to describe transcapillary transport:

$$J_s = \underset{\text{(convection)}}{J_v(1 - \sigma)C_p} + \underset{\text{(diffusion)}}{PS(C_p - C_{if})[x/(e^x - 1)]} \quad (6)$$

where x is the Peclet number describing the convective flux relative to the diffusive capacity of the membrane. With increasing J_v, the modifying term $x/(e^x - 1)$ for the *PS* product decreases and *Equation 6* will approach a constant value

$$J_s = J_v(1 - \sigma)C_p = J_vC_l \text{ or } C_l = (1 - \sigma)C_p \quad (7)$$

predicting that the protein concentration in lymph (C_l) will approach a constant value at high J_v. This will occur at Peclet numbers >3–5, resulting in a more dilute capillary filtrate and washdown of interstitial proteins with a limiting concentration in the filtrate of $C_p(1 - \sigma)$.

C. Interstitial Proteins as Determinants of Filtration

Equation 4 is the "classical" Starling equation where C_{if} and thereby COP_{if} are determinants of fluid filtration, but recently the importance of COP_{if} in filtration has been questioned. Rather, it has been suggested that the pressure relevant for fluid exchange is that immediately distal to the filtration barrier or glycocalyx, denoted as COP_g, which is significantly lower because of continuous fluid filtration and dilution of proteins. That there might be gradients in interstitial albumin (and thereby protein) concentration was initially proposed for fenestrated capillaries by Levick (264) based on data from rabbit synovium (287). In these experiments they found that changes in bulk COP_{if} had approximately one-third the effect on fluid exchange as COP_c, a result that could be explained by local gradients of albumin.

In continuous capillaries there are clefts (pores) (8, 9) that in the endothelial lumen are covered with fiber matrix glycocalyx (recently reviewed in Refs. 40, 385) proposed to represent the ultrafiltration pore (95). This led Michel (293) to suggest that because of high fluid flow resulting in protein dilution in the cleft, the COP to be used in the Starling equation is that immediately below the glycocalyx rather than the global COP_{if}. This model was further developed by Hu and Weinbaum (203) and predicts substantial gradients in subglycocalyx and global (COP_{if}) colloid osmotic pressure depending on velocity in the filtration cleft and thereby filtration rate. These model predictions have been substantiated by experiments performed by Curry and co-workers in mesenteric capillaries of frogs (202) and rats (8).

In the rat experiments they measured filtration in venular capillaries (25–40 μm) at capillary pressures of 15–60 cmH_2O with no or 50 mg/ml albumin in the perfusate, and could assess tissue concentration by confocal microscopy within 5 μm of a microvessel wall. Their experiments indicated that the effect of interstitial protein on filtration was substantially less than predicted from the Starling equation. These observations were in keeping with the model predictions that the colloid osmotic pressure in the global interstitial fluid does not directly determine microvascular fluid balance. Their results were summarized in a model **(FIGURE 7)**, predicting the COP gradients in the immediate vicinity of the capillary at variable filtration, suggesting that the transcapillary oncotic pressure gradient is highly filtration dependent. At low filtration rates, the difference between glycocalyx and tissue COP is reduced, and the model suggests that the effective COP (i.e., relevant for filtration) is ~80% of the global COP_{if} at normal filtration pressures (8). That this gradient effect is modest during control conditions is also suggested by experiments by Smaje et al. in rat cremaster muscle (434), where a direct correlation was found between COP_{if} and filtration. Although these recent developments suggest less importance in high filtration states, COP_{if} as determined in global IF is still a major determinant of normal fluid filtration.

D. Interstitial Fluid Forces and Flow in Inflammation and Tumors

Whereas in section III*B* above we have considered P_{if} as a concept, we will in this section discuss P_{if} as determinant of interstitial fluid formation. Up to three decades after the introduction of the chronically implanted Guyton capsule in 1963 (169), much of the discussion was related to the level of P_{if} in various tissues and to the role of P_{if} to counteract an increased filtration in situations with fluid perturbations (safety factor against edema formation) and interstitial compliance (see sect. III*C*). Much of the debate originated in the question of appropriate methods for P_{if} measurement and were to a large extent resolved when direct comparison showed similar steady-state pressures

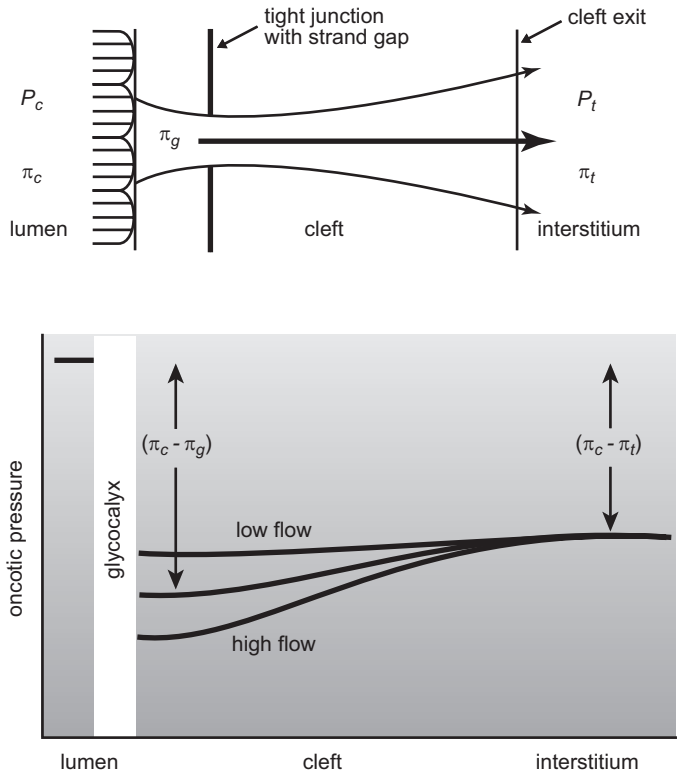

FIGURE 7. Proposed model for the effective oncotic pressure in a filtering microvessel. P_c and P_t represent hydrostatic pressure in capillary and interstitial fluid, respectively; π_c is the colloid osmotic (oncotic) pressure in the capillary; and π_g and π_t are the oncotic pressure in the subglycocalyx space and the "global" interstitium, respectively. The effective oncotic pressure difference determining fluid balance in filtering microvessels is greater when calculated using the oncotic pressure in the subglycocalyx region ($\pi_c - \pi_g$) rather than the mixed interstitial fluid ($\pi_c - \pi_t$). The model predicts that it is the oncotic pressure in the subglycocalyx region (π_g) that offsets the π_c in the Starling equation, and that the difference between π_g and π_t is highest at high transcapillary filtration (high flow). [From Adamson et al. (8), with permission from John Wiley and Sons.]

with all methods as reviewed (25, 493). During the last two decades, this has not been an area of active research. In this period, however, data have been emerging suggesting that P_{if} plays an active role during edema formation in inflammation and in tumor fluid exchange and biology, and these topics will be considered below.

1. *Interstitial pressure and flow in inflammation and injury*

During the last two decades it has been established that a reduction in (more subatmospheric) P_{if} generated during tissue injury and inflammation is a major factor responsible for the acute edema generation. The data emerging during this period to show such an edema-promoting effect of P_{if} under these conditions were recently reviewed by Reed and Rubin (381). This topic has also been addressed in a previous review (510) and will therefore not be discussed in detail here. The initial observations showing that P_{if} could contribute to acute edema formation came from rats, where full skin burn injuries resulted in a precipitous reduction in P_{if} (277). Whereas edema in rat skin is usually associated with a positive P_{if} (e.g., Ref. 504), they found strongly negative pressures during injury. This effect was most pronounced when transcapillary fluid transport into skin was blocked by circulatory arrest and prevention of fluid transport from muscle, when pressure fell from −1 mmHg in control situation to −150 mmHg after injury. Later experiments suggested that the P_{if} reduction was associated with denaturation of collagen (276) and introduced the concept that the interstitium can "actively" contribute in P_{if} regulation and thus enhance rather than prevent filtration. Such a mechanism of edema generation has later been confirmed in other burn injury models (245, 428) and in frostbite injury (46). Although less pronounced, inflammation induced by a multitude of agents without simultaneous denaturation of collagen also resulted in P_{if} reduction (for references, see Ref. 381), suggesting that this is a general mechanism for inflammatory edema generation. Later, Reed and collaborators have worked to establish the molecular mechanisms involved and found that the collagen-binding $\beta1$ integrins (382), more specifically $\alpha2\beta1$ (389) and recently $\alpha11\beta1$ (445) integrins, have a role in control of P_{if} in inflammation. Interestingly, the inflammatory reduction in P_{if} can be attenuated by the BB-isoform of platelet-derived growth factor BB (PDGF-BB) (389) mediated by the PDGF-β receptor. This effect is dependent on phosphatidylinositol 3′-kinase (192), and is exerted via the $\alpha v\beta3$ integrin (269). Taken together, these experiments suggest that during control conditions, tension from fibroblasts on dermal collagen fibers is maintained via $\beta1$ integrin mediated contraction. Proinflammatory mediators will release this tension resulting in negative P_{if} and edema formation, an effect that can be counteracted by PDGF-BB stimulation via $\alpha v\beta3$ integrin (381). Later experiments have suggested that a reduction in P_{if} not only contributes to inflammatory edema but also to the normal formation of saliva from the submandibular gland (47).

Although most of these mechanistic experiments were done on skin, other data indicate that reduced P_{if} may also be important for inflammatory edema formation in trachea (519) and oral mucosa (57). It may, however, not be a general mechanism for edema formation, since there was no effect on P_{if} in the rabbit synovium after disrupting the cytoskeleton by cytochalasin D treatment, although resulting in hyperfiltration into the joint mimicking an inflammatory reaction (368).

In the sustained phase of skin edema, P_{if} has generally been around 0 to +2 mmHg (e.g., Ref. 504), suggesting that the counterpressure against filtration (edema safety factor) is modest. Recent experiments in mice lacking initial lymphatics, however, suggest that P_{if} can increase by 6–8 mmHg

and thus have a quantitatively more important role in edema prevention and at the same time showing the role of lymphatics to determine the level of P_{if} (232, 401).

2. Interstitial fluid pressure and flow in solid tumors

Since the early studies showing a high P_{if} in rabbit testicular (528) and rat mammary cancer (515), it is now well established that P_{if} is elevated compared with normal tissues in all solid tumors, which in turn affects uptake of therapeutic agents and thus treatment outcome (e.g., Refs. 142, 187, 218, 221, 278). Whereas P_{if} in skin and muscle ranges from −2 to 0 (see sect. III*B*), the corresponding pressure in tumors is positive in experimental animals as well as humans, with reported values in humans in the range of 10–40 mmHg (142, 187). On the basis of one study in tissue-isolated and subcutaneous tumors (63), it has been claimed that there are no pressure gradients within tumors (142), whereas previous (515) and more recent studies (136) have suggested that such gradients exist. The reason for such discrepancy is not evident, but there may be variation between various models. This question is not a semantic one since existing gradients will determine whether there is fluid and substance flow within the tumor.

As recently summarized (142, 187, 221), there are several factors that contribute to the high P_{if} in tumors. One important contributor is the tumor vasculature that due to the effect of VEGF and other factors is irregular, convoluted and highly permeable (120) and without pericyte coverage (33). This may result in low restriction to protein transport across the capillary wall and high interstitial "counterpressure" or P_{if} (65) as well as high COP_{if} (439, 472, 494). Furthermore, there will be a low transmural pressure gradient and thereby reduced convection, and P_{if} will be strongly influenced by and dependent on intravascular pressure (65, 322, 515). That the increased permeability and vascular abnormality are central contributors to the high P_{if} is shown by the reduction in pressure in animal and human tumors after treatment with VEGF inhibitors resulting in "normalized" tumor vessels (e.g., reviewed in Refs. 142, 152). Other possible factors that may contribute to the high P_{if} are the lack of functioning lymphatics in central tumor areas (262, 350), intratumoral blood vessel compression due to solid stress from the growing tumor (351), and direct effects of growth factors like PDGF, TGF-β, and VEGF (187).

A strategy to overcome this therapeutic obstacle would thus be to reduce P_{if}, and that has proven successful in several instances. Targeting the VEGFR-2 with monoclonal antibodies results in "normalization" of the vasculature, a reduced P_{if} (e.g., Refs. 472, 516), and an increase in the initial uptake rate of macromolecular substances (472). Collagenase treatment also resulted in P_{if} reduction and increased transport rate of monoclonal antibodies (123). Another strategy to reduce P_{if} has been to inhibit the effect of PDGF-BB that exerts a tension on the ECM (see sect. IV*D*). A selective low-molecular-weight inhibitor of the PDGFR kinases, imatinib, and a DNA aptamer that specifically inhibits the PDGF B-chain reduced P_{if} by 2–4 mmHg, increased uptake of low-molecular-weight substances and chemotherapeutic agents, and reduced tumor growth (361–363). Similarly, PGE_1 was found to reduce tumor P_{if} and to increase the tumor concentration of small-molecular-weight substances (395, 406).

Other attempts to increase macromolecular uptake have been less successful. Flessner et al. (136) recorded how the monoclonal antibody trastuzumab entered experimental ovarian carcinomas after reducing P_{if} by various measures like PGE_1 and even decapsulation, but were unable to increase the transport into tumors even if the pressure was reduced from 12.5 mmHg to zero. Moreover, although treatment with pazopanib, a small-molecular-weight inhibitor of VEGF and PDGF receptors, resulted in vascular normalization and reduction in P_{if}, there was no increased uptake of liposomal doxyrubicin (456); instead, tissue penetration was reduced and hypoxia increased in pazopanib-treated animals.

Reduction of P_{if} should increase the transmural pressure gradient and thereby net filtration and bulk flow. One might therefore expect an increased uptake of macromolecules like monoclonal antibodies that are transported by bulk flow (387), but not small molecules transported by diffusion. It is therefore possible that a reduction in P_{if} is not the reason for the increased small-molecular-weight uptake in the studies discussed above. Since blood flow was unaffected after the induced pressure reduction by PGE_1 (406), another possibility would be that the P_{if} reduction increased the surface area available for exchange. When regarding macromolecules, initial uptake rate was increased after P_{if} reduction in some studies (123, 472), but not in other tumor types (136, 456). Interestingly, the transport of trastuzumab into an ovarian cancer model was found to be two to three times that of muscle (137). Moreover, in steady-state conditions, that may be more similar to the therapeutic situation with repeated injections of monoclonal antibodies, trastuzumab was available to a larger fraction of the interstitial fluid phase than albumin (498) in a mammary tumor model with high P_{if} (515), suggesting that uptake was not limited by P_{if}. Taken together, a reevaluation of available data suggest that P_{if} may not be such a significant barrier to therapy as has been proposed, and that other vascular factors might be more important in determining tumor drug uptake.

V. FORMATION AND TRANSPORT OF LYMPH

For the maintenance of fluid homeostasis in the interstitium, the net flux of filtered plasma must be balanced by

lymph formation into the initial lymphatic vessels. In the following sections we will briefly discuss the transport of interstitial fluid through the interstitium and the uptake of interstitial fluid into lymphatic capillaries (i.e., lymph formation). As this topic has been extensively reviewed earlier (25, 414), we present a condensed synopsis from these reviews and focus more on recent developments.

A. Passive Versus Active Mechanisms in Lymph Formation

1. Pressure gradients

For the net fluid filtrate to reach the initial lymphatics there has to be a downstream pressure gradient from capillaries to initial lymphatics, an issue addressed in a few studies only. Using micropipettes in the bat wing, Hogan (197) found that P_{if} adjacent to a lymphatic capillary averaged zero, while distant (116–224 μm) from the lymphatic capillary, P_{if} was 0.6 cmH_2O, resulting in an average pressure gradient of 3.7 cmH_2O/mm. Support for pressure gradients has also been shown with an estimated pressure gradient of 0.08 mmHg/mm in rat hindlimb skin (533). While much lower than gradients in the bat wing, such pressures can still drive lymph formation, since calculations by Schmid-Schönbein (414) suggest that a gradient of 0.09 mmHg/mm is sufficient to drive even a large filtrate from capillaries to the initial lymphatics. An even lower gradient may be sufficient in edema, which can increase the hydraulic conductivity five orders of magnitude or more (158, 172). Moreover, other factors such as tissue movement, arterial pulsations, or external tissue forces may affect fluid movement through the interstitium (25, 414).

2. Translymphatic transport

The uptake of interstitial fluid into initial lymphatics has been a subject of much controversy, but data gathered during the last decades have added clarity to the subject. Three mechanisms have been suggested: vesicular transport, osmotic pressure gradients, and hydraulic pressure gradients. After review of available data at that time, Aukland and Reed (25) concluded that little room was left for the vesicular transport mechanism, although new reports described below may challenge that hypothesis. With regard to the osmotic mechanism, advocated by Casley-Smith (77, 79), it was concluded "the weight of evidence against the osmotic theory for lymph formation is so great that it seems unlikely that it could be rehabilitated by future observations" (25).

In the hydraulic mechanism for initial lymphatic filling, which is most widely accepted, P_{if} is the main determinant of lymph flow. This assumption is based on consistent findings of increased lymph flow upon a rise in P_{if} caused by hyperfiltration, again assumed to raise pressure more in the interstitial fluid surrounding the initial lymphatic than within the lumen (reviewed in Ref. 25). What has been problematic with this mechanism has been to demonstrate a pressure gradient from the interstitium to the initial lymphatic, considering that time-averaged P_{if} is subatmospheric and pressure in initial lymphatics is close to ambient pressure (e.g., Ref. 197). The pressure gradient may, however, be variable, allowing for cyclic fluid uptake. Such cyclic pressure gradient variation was first shown by Hogan (196, 197), who found that the pressure in the lumen of contracting initial lymph bulbs of bat wings fell below P_{if} in diastole. In light of the fact that these initial lymphatics are contractile (199), one might argue this is a specific phenomenon for bat wings, but similar cyclic gradients have later been demonstrated for thoracic tissues (302, 315, 316) **(FIGURE 8)**, suggesting that this may be a general mechanism, at least in organs where lymphatics are regularly exposed to external forces and pulsations resulting in contraction/compression and relaxation cycles. For this mechanism to work, it requires that the initial lymphatic vessels do not collapse in spite of the pressure gradient, and it seems generally accepted that such support is provided by the anchoring filaments (24, 25, 376). Another requirement is that there is a functional one-way valve system that will allow fluid uptake during relaxation/expansion (diastole) and prevent or limit fluid loss during contraction/compression. Evidence for such a valve system in rat cremaster muscle has been found by Schmid-Schönbein and collaborators (476), who showed that microspheres (0.31 μm) that had entered the initial lymphatic could not be forced back into the interstitium by elevation of the initial lymphatic pressure by outflow obstruction. These experiments suggested that the initial lymphatics have a "primary" valve system at the level of the interstitium that in conjunction with the classical "secondary" valve system provide a system facilitating unidirectional flow during periodic compression and expansion of the initial lymphatics (476) **(FIGURE 5)**. As mentioned above, initial lymphatics having overlapping flaps at borders of endothelial cells that junction at the tip but are anchored on the sides by discontinuous button-like junctions (32) could act as the proposed primary valve system.

If we accept the hydraulic mechanism for initial lymph formation, the question is whether interstitial volume or pressure is the main driving force. As discussed in section IIIC, these parameters are interrelated in interstitial compliance, i.e., $C_i = \Delta V/\Delta P_{if}$, making it hard to differentiate between them. Strong evidence for a major role of V_i was found by Hogan and Unthank in the bat wing (198). A local increase of V_i gave a similar rise in mean P_{if} and pressure in the initial lymphatic. Still, in the diastole, there was an increased diastolic filling pressure gradient and increased contraction frequency and force, observations that can be explained by volume expansion of the interstitium and increased traction

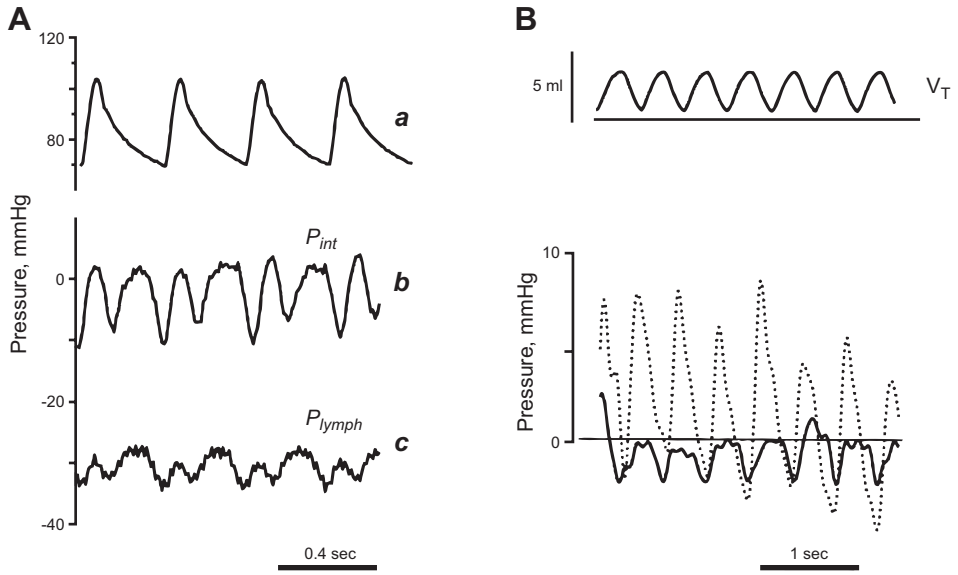

FIGURE 8. Effect of cardiac and respiratory activity on interstitial (P_{int}) and lymphatic (P_{lymph}) fluid pressure. *A*: cardiogenic oscillations of diaphragmatic interstitial (*b*, P_{int}) and intraluminar lymphatic pressure (*c*, P_{lymph}), measured with micropipettes in anesthetized rats under neuromuscular blockade. Both diaphragmatic P_{int} and P_{lymph} oscillate almost in phase with systemic arterial pressure (*a*), shifting from a minimum to a maximum value during cardiogenic oscillations. [Modified from Negrini et al. (316).] *B*: simultaneous recording of respiratory tidal volume (V_T, *top panel*) as well as lymphatic (P_{lymph}; continuous lines) and interstitial (P_{int}; dashed lines) pressures obtained in intercostal lymphatics of supine anesthetized rats during spontaneous breathing showing a (variable) pressure gradient from the interstitium to the lymphatic. [Modified from Moriondo et al. (302).]

of the anchoring filaments. Likewise, in the rat tail, chronic venous stasis, that increased P_{if} by 14 mmHg although at an unaltered V_i, gave less increase in lymph flow than a 3-mmHg increase in P_{if} induced by hypoproteinemia that increased V_i by 45% (2). These observations suggest it is the lymphatic transmural pressure and not P_{if} per se that is the stimulus for initial lymph formation.

3. Evidence for active regulation of lymph formation

For decades, electron microscopy studies have demonstrated intracellular vesicles carrying large solutes, lipids, and particles across lymphatic endothelium (31, 115, 130), yet the importance of active transport mechanisms in lymphatic endothelium remains nearly unexplored. As reviewed by Dixon (112), this question may be of particular interest in relation to lipids, where recent studies in mouse models have emphasized the importance of the lymphatic vasculature in lipid homeostasis and our lack of knowledge on how the lymphatic system is regulated to absorb and transport lipids. Heterozygous inactivation of Prox1 in mice suggested that lymph contains adipogenic stimuli and, moreover, that lymphatic vascular dysfunction may contribute to adult-onset obesity (183). Other studies have shown the importance of integrin $\alpha 9$ for chyle reabsorption (39).

Recently, new evidence has been provided for active regulation of transendothelial transport of solutes, lipids, and even water across lymphatic capillaries (69, 114, 298), which will hopefully spur more research on this important but overlooked aspect of functional lymphatic biology. In a tissue engineered model of small intestinal lymphatics, which are responsible for absorbing dietary lipids in the form of chylomicrons formed by enterocytes, Dixon et al. (114) used fluorescent lipid tracers with confocal microscopy along with transmission electron microscopy to demonstrate the abundant presence of lipid-filled vesicles within lymphatic endothelial cells that appeared to shuttle across from the basal to luminal side **(FIGURE 9)**. This apparent transcytosis mechanism was consistent with the earlier studies of Azzali et al. (31). Dixon then used this model to explore the active regulation of such transport, showing for example that basal-to-apical transport of chylomicrons was much more efficient than apical-to-basal transport, providing an alternative mechanism to one-way transport to the "second valve system"; in other words, one-way transport from the interstitium to the lymphatic capillary may be actively regulated in addition to physically regulated by valves.

In another study of dendritic cell and solute transport across lymphatic endothelial cells, Miteva et al. (298) demonstrated the importance of active transport and its regulation by transmural flow. In vivo, the effective permeability of lymphatic capillaries was increased in mice exposed to increased flow (via overhydration) for 24 h, reflecting the likelihood that effective permeability can be actively mod-

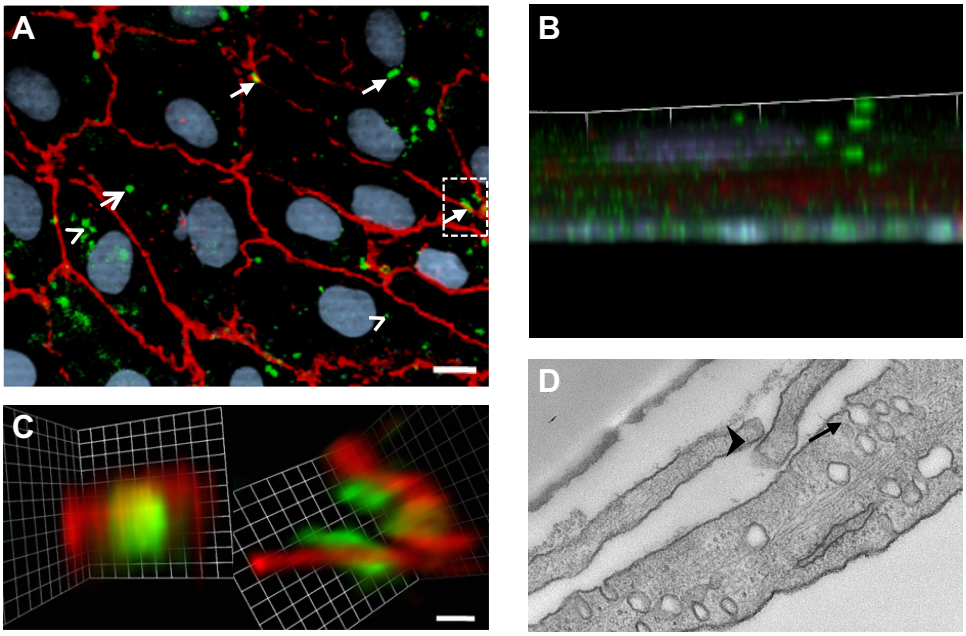

FIGURE 9. Fluorescent lipid particles (green) are transported across lymphatic endothelial cells (LECs) in vitro via both paracellular and transcellular pathways. *A*: maximum projection confocal image of LECs stained with VE-cadherin (red) show chylomicrons (green) being transported both transcellularly (arrowhead) and paracellularly (arrow). Bar, 10 μm. *B*: cross-section of a single LEC stained with VE-cadherin (red), showing transcytosis of chylomicrons (green) across the cell via vesicles in a chainlike fashion. Bar, 2.5 μm. *C*: enlarged view of the *inset* marked in *A* demonstrates chylomicrons (green) traversing through the cell and overlapping with VE-cadherin (red) as shown from two different perspectives: perpendicular to the imaging plane (*left*) and parallel to the imaging plane (*right*). Bar, 5 μm. *D*: transmission electron micrograph of lipid-containing vesicles (arrow) transcytosing across the LEC monolayer even in the proximity of an overlapping junction (arrowhead). Bar, 250 nm. [From Dixon et al. (114), with permission from John Wiley and Sons.].

ulated. In vitro, they found that transmural flow upregulated not only permeability but also aquaporin-2 (298). Since aquaporin-2 is a highly specific water transporter, this suggests that even water transport across lymphatic endothelium may be at least partially regulated by active mechanisms.

Active mechanisms of interstitial fluid transport across the lymphatic endothelium may seem unnecessary compared with passive transport, since lymphatic endothelial cell-cell junctions are overlapping and apparently extremely permissive. On the other hand, lymphatic endothelial cells are extremely attenuated, and thus the relative surface area for intercellular convection may be too small. More importantly, active mechanisms would allow rapid control over lymph formation rates without altering lymphatic vessel integrity, for example, in response to inflammatory cytokines or increased interstitial fluid load following tissue injury, consistent with the enormous capacity of lymphatics to immediately respond to heightened load during acute phases of inflammation. It is also consistent with the role of lymph flow in modulating immunity, which is discussed below.

The exact mechanisms and relative importance of active versus passive transendothelial transport remain to be determined, as well as how other cytokines or inflammatory signals may modulate these active transport functions of lymphatic vessels. Further research will hopefully shed more light on these processes and their potential roles in modulating immunity.

B. Lymph Propulsion

Having entered the initial noncontractile lymphatic, lymph is moved towards the valve-containing collecting vessels by external compression, a pressure gradient (force from behind) or by suction from downstream collecting lymphatics. A prerequisite for such propulsion is that collapse is prevented by anchoring filaments or by elastic forces in the vessel wall (25).

When the initial lymph enters the smooth muscle containing collecting vessels, it is driven centrally through the lymphatic bed by phasic coordinated contractions of the lymphatic smooth muscle cells. There is an extensive previous literature on this topic that was summarized in two earlier reviews in this journal (25, 414). Moreover, during the last decades, the field of functional and molecular control of lymphatic contractility has been an area of active research, and accumulated knowledge has been summarized recently in several comprehensive reviews (308, 482) and is therefore not discussed more extensively here.

C. Lymph Composition

The question whether lymph is modified in collecting lymphatics and lymph nodes is of relevance to decide whether sampled lymph is representative for free interstitial fluid. It appears well documented that lymph is modified by passage through the lymph node, whereas data with respect to possible changes in the collecting lymphatics are less conclusive.

The data on whether there is fluid and solute exchange in the collecting lymphatics are diverging, but such diversion may partly be due to variation in properties of lymphatic vessels in different vascular beds. Studies from other vascular beds than the mesentery suggest little or no exchange in collecting lymphatics. Thus Garlick and Renkin (145) found complete recovery of fluid volume, dextran, and dextrose after perfusion of a segment of a prenodal lymph vessel isolated from dog paw. Even more convincing are autoradiographic data from the mouse lung (328) showing uniform concentration of radiolabeled albumin in differently sized lymphatic vessels and thus no change in concentration as the lymph flows along the vessel. In line with these observations are recent data from Ono et al. (344) who found no exchange of albumin in lymphatic vessels isolated afferent to the iliac node even at a transmural pressure of 8 cmH_2O. They found, however, that there was some transfer of sodium fluorescein and dextrans, but this transport was not related to transmural (filtration) pressure and therefore most likely representing diffusion down a concentration gradient, probably not present for native substances. Moreover, since there was no change in albumin concentration with transmural pressure, it is likely that the hydraulic conductivity and thus fluid exchange of the isolated vessels was low.

Observations from the mesentery seem to contradict those of other lymphatic vascular beds. In cat and rabbit intestine, Hargens and Zweifach (181) found indications that lymph is concentrated during central passage, with protein concentration rising from 1.5 in small terminal (initial) to 2.6 g/dl in larger collecting vessels. These data are also supported by an increased concentration of macromolecular dextran passing from upstream to downstream in collecting lymphatics in rat mesentery (457). Contrasting these findings, in technically demanding experiments, Zawieja and Barber (532) measured protein concentration in nanoliter samples of initial lymph sampled from an intestinal villus and mesenteric collecting lymphatics in rats. Although they found a slightly lower concentration in superfused compared with oil-covered preparations, there was no difference between initial and collecting vessels, averaging 2.5 and 2.3 g/dl, respectively, in the oil-covered preparation. Recently, Scallan and Huxley (411) showed that collecting lymphatics in rat mesentery had a permeability to albumin and water similar to that of venules, suggesting that they could act as exchange vessels and thereby extravasate solute and filter fluid provided sufficient net driving pressure. Assuming that peritoneal fluid was similar in composition to mesentery IF, they found the average total protein concentration in collecting duct lymph (31.3 mg/ml) to be not different from peritoneal fluid (32.4 mg/ml). The albumin concentration and thus colloid osmotic pressure was however, slightly, but significantly, higher in lymph than in interstitial (peritoneal) fluid, averaging 9.4 and 7.2 cmH_2O, respectively. Taken together, although not conclusive, these studies from the mesentery indicate that the lymph may be slightly modified in prenodal vessels. These findings notwithstanding and as discussed in section VI*A*, it is still a question to what extent these data apply to other vascular beds, and the bulk of data from nonmesentery tissue suggest that there is no appreciable change in protein concentration and thus no addition or removal of water along prenodal collecting lymphatics. Accordingly, with the possible exception of the mesentery, and even in light of new data, there seems to be no reason to abandon the generally accepted view that prenodal lymph is not modified during its passage to the lymph node and may be considered as representative for IF (24, 25, 329, 386).

D. Lymph Modification in the Lymph Node

Whereas there appear to be minimal exchange of fluid and solutes in prenodal lymph, passage through the lymph node may strongly modify the lymph composition as shown in a series of studies by Adair and collaborators (reviewed in Ref. 3). They used a canine popliteal node preparation and found that water was removed from diluted and added to concentrated afferent lymph, resulting in more concentrated and more diluted efferent lymph, respectively (7). There was, however, an equilibrium lymph concentration of ~60% that in plasma where no change occurred between the efferent and afferent concentrations. A rise in nodal venous pressure increased efferent flow and reduced protein concentration (5), whereas increased pressure in the efferent lymphatic increased fluid reabsorption in the node (6). The change in concentration was due to the transfer of water except during very high efferent pressures (6). From these studies they concluded that the protein concentration in postnodal lymph is changed such as to establish equilibrium of the Starling forces acting across the blood-lymph barrier. Accordingly, the protein concentration in lymph may be increased or decreased depending on the direction of fluid transfer.

The obvious implication of these studies is that postnodal flow rate and protein concentration may deviate significantly from that of prenodal lymph and should not be considered as equivalent to initial lymph and IF. Rare exceptions to this rule would be an exceedingly high lymph flow through the node or that the afferent lymph has "equilibrium" concentration of ~60% that of plasma (3).

VI. COMPOSITION OF INTERSTITIAL FLUID

In this section we will discuss methods for IF isolation and their inherent strengths and weaknesses, and moreover how IF relates to prenodal (afferent) lymph. In light of the preponderance of data in other organs (with the possible exception of the mesentery) suggesting that IF and lymph are similar in composition (see sect. VC), we will here consider IF and prenodal lymph as equal representatives of the fluid microenvironment for cells in a tissue. The composition of IF and lymph in several organs and species have been reviewed previously (e.g., Refs. 25, 45, 341, 527). We will here give an update with respect to composition focusing on new knowledge regarding signaling substances and what can be learned about production in individual tissues from studies of absolute concentrations of substances and tissue-plasma gradients. It may be important to quantify known bioactive compounds in the IF since this fluid represents the microenvironment for most bodily cells. Moreover, numerous growth factors and cytokines are associated with and are sequestered in the ECM (e.g., Refs. 125, 131, 134, 209) that serve as a reservoir for freely diffusible bioactive molecules available to tissue cells by proteolytic cleavage (131, 201). There may accordingly be microenvironmental post-translational activation processes, and to be able to understand biological processes, it may be necessary to monitor substances in the compartment where they are biologically active, i.e., in the IF, rather than at the gene level. In support of such an assumption are studies by Garvin and Dabrosin (146) who observed that although estradiol and the antiandrogen tamoxifen increased mRNA and intracellular VEGF protein, the secreted VEGF to the extracellular phase and thereby angiogenesis was decreased by tamoxifen. We will first discuss IF in inflammatory conditions in experimental animals and humans and then specifically address the IF composition in tumors. The composition of IF with respect to plasma proteins and COP_{if} are considered when discussing the respective techniques.

A. Techniques for IF Isolation

To quantify one of the determinants of the transcapillary fluid transport, the IF protein concentration, and thus COP_{if}, it is imperative to have the appropriate methodologies that provide representative native IF. IF may, however, not be readily accessible, and therefore various techniques have been developed for fluid isolation. Although access to native fluid is required for COP_{if} determination, other substances may also affect filtration, e.g., cytokines, and we will therefore also discuss techniques that are used for sampling of derived IF, notably microdialysis. We will classify the techniques according to whether the isolated fluid is native or derived fluid, and will first describe methods for native (sect. VI*A*, *1–7*) and then derived fluid sampling (sect. VI*A*, *8–11*). The special characteristics of the tumor interstitium, e.g., the high vascularity and cellularity, result in special challenges when trying to gain access to the tumor IF as recently emphasized by one of us (514) and will therefore be addressed separately.

1. Lymph

Even though initial lymph cannot be defined as IF per se, it may be representative of true IF and is because of that fact discussed here. Previously, there have been vigorous discussions on whether the initial lymph is similar to IF and whether it is modified prior to reaching the lymph nodes (for review, see Refs. 24, 25, 329).

Previous direct comparisons between lymph and IF sampled with other techniques (127, 461, 484) suggest that the protein concentration and composition in IF and prenodal lymph is similar in steady-state conditions. This assumption is valid only if there are no changes in lymph protein concentration in prenodal lymphatics, and here the data are conflicting, as discussed in more detail in section VC. Recent studies from the mesentery suggesting that the lymph may be slightly modified in prenodal vessels (411) may question the use of prenodal lymph as representative for IF. Still, the mesentery is a highly specialized vascular bed, and until more data are available from other tissues than the mesentery, we may accept that prenodal lymph is representative for true IF (at least during steady-state conditions) and moreover that lymph measurements provide a good estimate for the concentration of a macromolecule of interest in its available space in the tissue. The only time, however, we can be certain that lymph is representative of true IF are those conditions where the sampling is made directly from the organ, e.g., skin (42), muscle (41), intestine (157), and lung (355).

The protein concentration in lymph is ~50% of that in plasma in skin and muscle (25), whereas for lung and spleen this ratio is significantly higher, ~0.65 (462) and ~0.9 (237, 421), respectively. An extensive review on the composition of lymph, especially relative to plasma, was given by Yoffey and Courtice (527) four decades ago and is still useful as a reference.

Lymphatics may not be cannulated in tumors, making lymph sampling inapplicable in this tissue.

2. Wick techniques

The wick technique was developed by Aukland and coworkers to allow simple and direct sampling of IF (21, 128). In the original version of the method, saline-soaked wicks were inserted into skin and muscle (22) using a needle. These authors also showed that the insertion resulted in an inflammatory reaction that was later avoided by performing experiments in rats after arresting the circulation (249, 499) in skin and combined with catheters for muscle im-

plantation (284, 511). In peritoneum, where pressures determining fluid flux are of special interest due to the importance for determining fluid exchange in peritoneal dialysis, COP_{if} was 60% of that in plasma in the control situation, falling to 28% after a 4-h peritoneal dialysis dwell (394). Moreover, the wick method has been applied successfully in the perivascular and peribronchial space in rabbit lungs (317).

As for several normal tissues, wicks have also been used in solid tumors to isolate IF. Stohrer et al. (439) implanted saline-soaked wicks either acutely into established tumors ("acute" wicks) or simultaneously with tumor implantation ("chronic" wicks). They evaluated the effect of acute and chronic insertion but also the effect of both implantation time and tumor type, and concluded that acute wick implantation requires a long time for equilibration (i.e., >120 min) and that chronic wicks should be preferred because then potential problems associated with bleeding and cellular damage are avoided. As pointed out by the Stohrer et al. (439), cellular proteins deriving from necrotic cells or cells disrupted during wick removal may enter the wick fluid and cause a higher protein concentration (and thus higher COP).

3. Pipettes

Whereas it is possible to drain fluid from edematous tissue by inserting a needle, fluid will not drain from a needle located in normally hydrated tissue. Nanoliter volumes have been isolated from euhydrated skin by applying suction to a micropipette (176). Later studies have shown that this fluid has a protein composition similar to that of prenodal lymph (399) and implanted wicks (398), suggesting that this is a technique that can be applied for studies of IF, although it has apparently not been used during the last decades.

Somewhat larger glass capillaries have also been used for sampling of IF in tumors, as initially described by Sylven and Bois (453). Admixture of fluid from the normal tissue surroundings, plasma and intracellular fluid that results from the cell damage by the sampling procedure are main disadvantages with this method that has not been used the last decades.

4. Catheters

Applying suction to empty wick catheters can also be used for isolation of IF (179). This method has been compared with the saline-soaked wick technique in human subcutis. Whereas the two techniques corresponded well when a low suction pressure was used, a pressure >10 mmHg lowered the COP, suggesting that the composition of the fluid was sensitive to suction pressure (330).

5. Implanted capsules

Another device that can be used for IF isolation is the perforated Guyton capsule (169). During steady-state conditions, fluid isolated from the lumen of capsules implanted subcutaneously in dogs had a COP of 8.4 mmHg (507), not different from that of wick fluid averaging 8.2 mmHg (506). These and lymph data (461) suggest that capsule fluid reaches a steady state with respect to composition of IF. This will, as pointed out by others (24), not be the case during perturbation of fluid balance. Although potentially useful, this technique has not been used during the last decades.

Gullino et al. (164) described a modified version of the Guyton capsule for sampling of tumor IF, and this technique has been pivotal in providing knowledge on the interstitial fluid phase in tumors. Although there are potential problems associated with the method (219), a main advantage is that fluid can be harvested for longer periods, e.g., to follow effects of therapy. One aspect that has not received much attention is that fluid was drained from the chambers to the atmosphere, and that a positive pressure of 8–16 mmHg was needed to stop the drainage. This means that the fluid drained to a lower pressure creating hyperfiltration that may again lead to sieving of macromolecules and a lowered tumor fluid protein concentration. One obvious problem is the inflammatory reaction and subsequent scarring that is induced by chamber insertion. Based on comparison of capsule and wick fluid in dogs, however (507), it is likely that the fluid reflects true tumor interstitial fluid in steady-state (nonfiltering) conditions, whereas this will not be the case during perturbations as described for the Guyton capsule above.

6. Suction blister technique

The suction blister technique, originally described by Kiistala (244), was developed as a way to separate epidermis from dermis and to study the pathogenesis of blister formation in human skin, but has frequently been applied to isolate IF from skin. With this technique, a hollow cup with typical diameter 20 mm with 5-mm bores is placed on the skin, and a negative pressure of 100–200 mmHg is applied. Fluid (~20 μl) can then be collected after 60–90 min. Recently, a variety of the technique was presented where micropores are made in the skin using a laser to allow mobilization of fluid when suction is applied in the next step (419). The traditional suction blister technique has been used widely for IF isolation in human skin, and isolated fluid has been found to have an electrolyte composition similar to serum (481), whereas the ratio of albumin in blister fluid relative to serum has ranged from 0.3 (480) through 0.40 (200) to 0.5 (435), and an inverse relation between blister fluid/serum ratio and molecular weight (480).

Clearly, the negative pressure will create hyperfiltration, and the blister formation induces an inflammatory reaction evidenced by high levels of the proinflammatory cytokines IL-6, IL-8, and RANTES in control blister fluid (537); release of neural and vascular peptides in human skin (162); and increased migration of Langerhans cells from epidermis (108), elements that will all contribute to increased protein permeability. There are hence factors that may influence the blister fluid protein concentration in opposite directions and moreover its composition, e.g., with respect to mediators, and it is doubtful whether samples will be representative for IF at least regarding composition of proteins. This is particularly important if the method is used to sample fluid for identification of protein biomarkers from the presumed extracellular fluid phase in skin (e.g., Ref. 248; see sect. VI*E*) as well as for estimating COP_{if}.

7. Tissue centrifugation

An alternative method to isolate native interstitial fluid that has gained increased use during the last years is to expose excised tissue to an increased G-force by centrifugation, first introduced by Aukland et al. (23) in rat tail tendon. Later, Wiig (492) exposed cornea to increased G-force and found that the COP of the isolated fluid was strongly dependent on G-force in such a way that the COP fell dramatically upon increasing the G-force.

In a later study designed to evaluate whether IF could be isolated from solid tumors by centrifugation that will be discussed in more detail below, skin from rats was used as a "control" tissue (494). On the basis of extracellular tracer experiments and a HPLC pattern of the isolated fluid similar to that of dry wicks implanted post mortem, it was concluded that exposure of skin to G ≤424 *g* gave fluid representative for undisturbed IF. Skin COP_{if} determined with this method averaged 13.8 mmHg in rats with COP_c of 23 mmHg. This method has later been used for several organs where the IF because of lack of available other methods has been difficult to access, like bone marrow (495), dental pulp (55), trachea (420), and salivary gland (47).

Recently, centrifugation was added to the armamentarium of methods for IF isolation in tumors (494). This might seem surprising considering that tumors are cell rich and richly vascularized, in contrast to cornea (492) and tail tendon (20, 28), where the technique had been used initially at that time. On the other hand, the two latter tissues are both rich in collagen, which may restrict the removal of macromolecules when high G-forces are applied. Tumor tissue has at least an order of magnitude higher hydraulic conductivity than cornea (219, 447) that will facilitate fluid removal by centrifugation. Wiig et al. (494) used the extracellular tracer ^{51}Cr-EDTA as a probe to show possible "contamination" of cellular fluid. Tumor cell fluid addition to the centrifuged volume should thus show up as a reduced ^{51}Cr-EDTA concentration in the centrifugate relative to plasma **(FIGURE 10)**. An observed ratio in peripheral tumor not significantly different from 1.0 for G ≤424 suggested no dilution of extracellular fluid, whereas the gradual reduc-

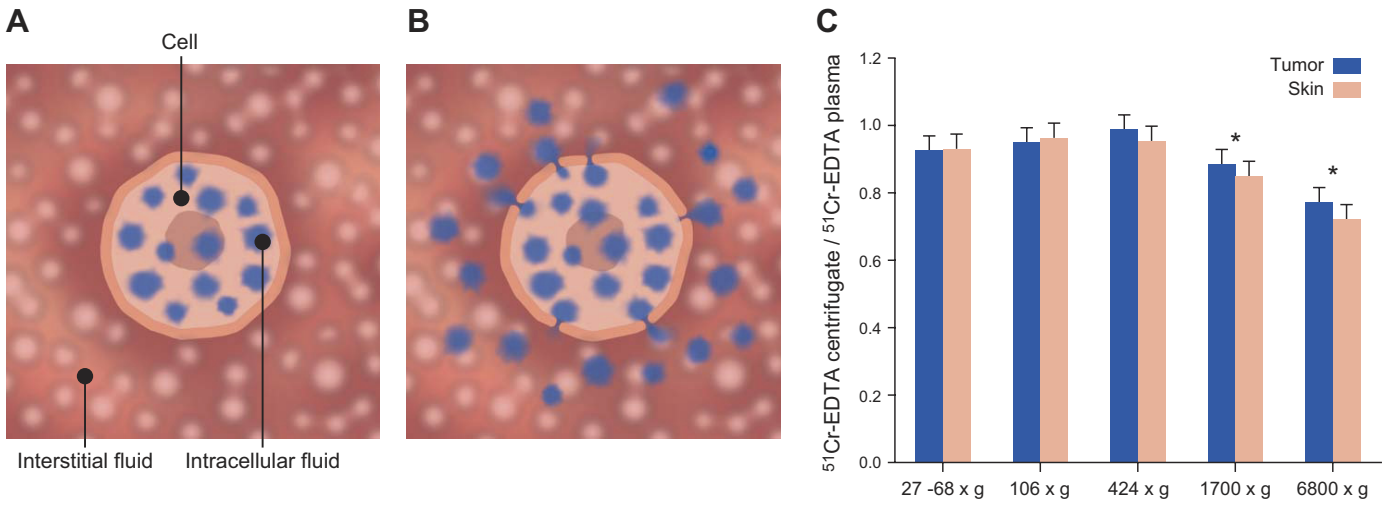

FIGURE 10. Determination of possible contamination of interstitial fluid. *A*: a tracer that does not pass intracellularly is equilibrated in the extracellular fluid phase. *B*: if undiluted interstitial fluid (IF) is isolated, the concentration in IF and plasma (P) will be equal, i.e., IF/P = 1.0. If, however, intracellular fluid (with dissolved proteins) not containing tracer is added to the interstitial fluid during the isolation process (e.g., centrifugation), the IF will become diluted and as a consequence IF/P <1.0. *C*: tissue-to-plasma distribution ratios (IF/P) of the extracellular tracer ^{51}Cr-ethylenediaminetetraacetic acid (EDTA) as a function of G-force for interstitial fluid isolated by centrifugation from intact tumor and skin (±SE). For $g < 424$, the IF/P ratio was not significantly different from 1.0, suggesting negligible dilution and thus contamination of IF. An IF/P <1.0 for $g > 424$ (*$P <$ 0.05 for tumor as well as skin) suggested contamination of IF with intracellular water and proteins. [From Wiig et al. (514).]

tion of this ratio when exposing the tissue to higher G-forces indicated an increasing dilution probably due to extrusion of cellular fluid and/or cell damage. Tumor fluid had an average COP of 16.6 mmHg, compared with 13.8 and 20.5 mmHg in skin and plasma, respectively (494).

Whereas only one model was evaluated initially, the procedure has later been found suitable for IF isolation in other tumor models (85, 405) and has been translated for use in human ovarian carcinomas, where the origin of the fluid was verified using Na^+ and creatinine as extracellular markers (184). In these tumors, the COP_{if} averaged 24 mmHg that was 79% of the corresponding pressure in plasma.

8. Microdialysis

Microdialysis is a frequently used method for sampling of endogenous and exogenous substances from the extracellular space, especially in the brain (e.g., Refs. 84, 268, 467), but also in other organs like muscle (e.g., Ref. 247) and in skin (e.g., Ref. 89). The sampling technique is based on the passive diffusion of substances across a semipermeable membrane. It has mainly been used for sampling of small molecular species. An extensive review on theoretical principles, available methods for estimating extracellular concentrations, and the various factors that affect in vivo relative recovery have recently been provided by Chefer et al. (84). During the last years the method has also been applied to study peptides and proteins dissolved in the IF (for recent reviews, see Refs. 18, 88). As pointed out by Clough (88), however, as a consequence of various physical restraints, the recovery of macromolecules in the dialysate may be very low (~1%), and it is therefore unlikely that the dialysate provides a representative concentration for the IF. Various techniques have been applied to enhance the recovery, like antibody-immobilized microspheres (17), heparin-immobilized microspheres (118), or adding albumin, modified starches, or lipids to the probe perfusate (reviewed in Ref. 88). Even though these modifications have increased the in vitro recovery, the effect in vivo is not well established. As pointed out by Stenken et al. (437), there are several caution-

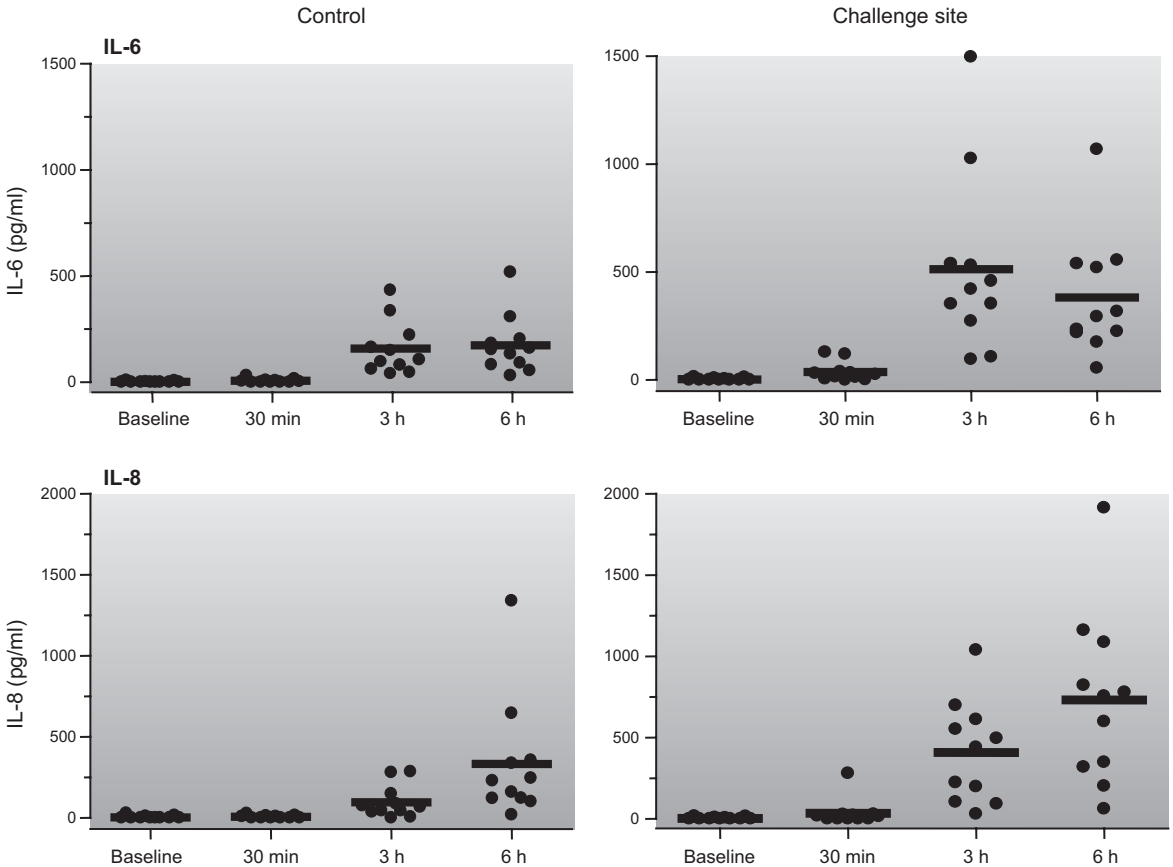

FIGURE 11. Cytokine recovery using 3,000-kDa molecular mass cutoff dialysis probes from 17 healthy volunteers with a positive skin prick test at two sites before and after intradermal injection of either allergen or saline control. The periods of dialysate collection were as follows: baseline, the 30-min period immediately before injection of allergen or saline (control); 30 min, the 30-min period immediately following injection of allergen or saline; 3 h, 3–3.5 h after injection of allergen or saline; and 6 h, 6–6.5 h after injection of allergen or saline. Bars represent median values. Insertion of the microdialysis probe results in increased levels of IL-6 and IL-8 also in control subjects injected with saline. [From Stenken et al. (437), copyright 2009 American Association of Pharmaceutical Scientists.]

ary notes in relation to tissue injury when using this technique for cytokine collection. Notably, an inflammatory reaction or wounding response is induced by implantation of the device, as shown in **FIGURE 11**. This is of course a special problem when investigating inflammatory responses, as shown in a study on temporal and spatial generation of cytokines in allergen-induced responses in human skin in vivo (89). Thus, although a significant increase in the level of several cytokines were observed in the challenged site, most pronounced for IL-6 and IL-8, there was also an increase in the control site **(FIGURE 11)**, which is important to consider when interpreting the results (437). Similarly, Clausen et al. (87) found a severalfold increase in the proinflammatory cytokines interleukin (IL)-1β, IL-6, IL-8, MCP-1, and tumor necrosis factor (TNF)-α during the first days of a 4-day subcutaneous large-pore microdialysis.

The microdialysis technique has been applied extensively also in tumors including those in the brain (for recent reviews, see Refs. 44, 62, 72, 86, 98–100, 534), and there has been an increased interest in using the technique for studies of pharmacokinetics and pharmacodynamics in tumors (72, 86, 535). In more recent work the method has also been applied in investigations of peptides and proteins dissolved in the interstitial fluid (43, 523).

9. Capillary ultrafiltration

Ultrafiltration is a technique traditionally used for separation or purification of chemicals. More recently, however, this method has also been applied to sample tissue fluid in vivo by implanting capillary ultrafiltration probes (reviewed in Ref. 261). Negative pressure is the driving force for sampling, and accordingly, fluid and solutes are removed from the interstitium by bulk flow. The characteristics of the semipermeable membrane used will affect the size of molecules that are allowed in the ultrafiltrate sample. For small molecules, the recovery is (as for microdialysis) close to 100% (261, 272), whereas the observed in vitro recovery for albumin has been 74–100% depending on dialysis time (415), indicating that ultrafiltration can be used for sampling of macromolecules. To better allow for sampling of interstitial proteins, membranes with a molecular mass cutoff of 400 kDa have been used, and tissue fluid has been collected from ear (206) and abdominal skin (205) in mice using this approach, yielding protein concentrations of 100 and 8.6 μg/ml, respectively.

Although the in vitro data suggest that the protein recovery is high and severalfold that of microdialysis (415), the protein concentration in the fluid sampled fluid is, however, 1/300 or less of the interstitial fluid concentration as estimated from COP_{if} in mouse subcutaneous wick fluid (284, 439) and the Landis-Pappenheimer equation for relationship between plasma protein concentration and COP (255). A likely explanation for this finding is that the negative pressure used during the ultrafiltration induces an increased capillary filtration, resulting in sieving of proteins at the capillary membrane, in the tissue, or at the tissue-membrane interface.

The capillary ultrafiltration technique has also been used for fibrosarcomas in mice (204), but the protein concentration is <1/2,000 of interstitial fluid in other tumors in mice (439) calculated as described above (255), and the explanation is again probably sieving at the capillary wall.

10. Tissue elution

Recently, tissue elution was proposed as a method to access the interstitial fluid phase of tumors (80), and later of fat tissue (81). With this method clean, fresh biopsies are cut into small pieces (1–3 mm^3), washed carefully, and placed in tubes containing phosphate-buffered saline. After incubation or elution for 1 h followed by centrifugation, the supernatant is collected and named IF. In the tumor study, they found that the IF contained some major serum proteins as might be expected, but that its overall protein profile was remarkably different from that of serum (80).

Clearly, fluid isolated this way will be dilute but may otherwise reflect the interstitial fluid phase. A potential problem is that dividing cell-rich tissues like tumors into small pieces will result in sectioning of a substantial fraction of cells resulting in addition of cell fluid to the eluate. This fact has consequences for the use of this method to measure, e.g., interstitial fluid protein concentration, and in search for proteins that are specific for the interstitial fluid phase.

11. Other methods

There are methods that have been used to determine COP_{if} directly without the need to isolate interstitial fluid. These are tissue osmometry (66) or implanted colloid osmometers (377, 441). None of these devices appears to have been used the last decades.

12. Summary of methods for isolating IF

In **TABLE 5**, we have summarized features with the various techniques used to access IF in selected normal tissues and tumors, elements that should be considered when planning experiments and interpreting data in this area. If the aim is isolation of native IF, isolation of prenodal lymph is a good alternative in many organs if this option is possible, even considering the recent observations related to possible modification of prenodal lymph (411). Wick implantation may also give representative samples if the inflammation can be controlled either by arresting the circulation or allowing sufficient time for the inflammatory reaction to subside. This also applies to implanted devices like capsules, although several weeks are needed for the inflammatory reaction to wear off, also taking into consideration that the

Table 5. *Methods for interstitial fluid isolation*

Method	Tissue	How Performed	What Is sampled	Advantages	Disadvantages	Remarks	Reference Nos.
Direct methods: native fluid isolation							
Lymph sampling	Skin, muscle, lung, intestine, other organs	Direct cannulation of prenodal lymphatic	Prenodal lymph	Atraumatic, no inflammation, in vivo	Origin of lymph, not applicable for regional sampling in small animals	Possible modification of interstitial fluid in collecting lymphatics, see Ref. 411	41, 42, 157, 355
Implanted wicks	Skin, muscle	Implanted in vivo or post mortem	Fluid absorbed during implantation	More versatile than lymph sampling	Implantation trauma, inflammation, bleeding	Trauma reduced by post mortem and catheter implantation	499, 511
	Tumor	Implanted acutely or chronically	Fluid absorbed during implantation	In vivo	Bleeding and inflammation, cellular disruption	Chronic implantation more representative than acute	439
Wick catheter	Skin	Suction applied to wick catheter	Fluid from subcutis	In vivo, versatile	Implantation trauma, suction necessary	Suction may induce filtration and dilution	180
Micropipettes	Skin	Sampled from a liquid paraffin cavity	Fluid from subcutaneous fascia	In vivo, relatively atraumatic	Small volume	Complicated sample handling	176
Glass capillaries	Tumor	Insertion by blunt dissection in vivo	Fluid from tumor periphery or sectioned surface	In vivo	Bleeding and inflammation, cellular disruption	High level of intracellular enzymes in isolated fluid	453
Implanted capsules/ chambers	Skin	Chronically implanted	Fluid sampled from center of capsules	In vivo	Scarring, aberrant dynamic response	Long equilibration times	507
	Tumors	Chronically implanted upon tumor implantation	Fluid draining from central part of tumor	In vivo, continuous and repeated sampling	Inflammation in early phases, scar formation	Requires chronic restraining of animal	164
Suction blisters	Skin, mucous membranes	Applying negative pressure	Fluid accumulating between epidermis-dermis	In vivo, convenient, noninvasive	Induce inflammation and hyperfiltration	Dilution of interstitial fluid	244
Tissue centrifugation	Skin	Exposure of excised tissue to increased G-force	Fluid from subcutis	Validated native fluid composition	Ex vivo, single samples	Composition validated by extracellular tracers	494
	Tumor	Exposure of excised tissue to increased G-force	Fluid from tumor periphery	Validated native fluid composition	Cell fluid contamination possible	Composition validated by extracellular tracers	494
Indirect methods: diluted samples							
Microdialysis	Skin and tumor	Insertion of semipermeable membrane	Substances diffusing across membrane	In vivo, continuous and repeated sampling	Inflammation, incomplete recovery, dilute fluid	Recovery especially low for macromolecules	Reviewed in 88, 98
Capillary ultrafiltration	Skin and tumor	Negative pressure applied to semipermeable membrane	Substances transported by bulk flow across membrane	In vivo, continuous and repeated sampling	Inflammation, incomplete recovery	Recovery especially low for macromolecules	204, 206
Tissue elution	Fat and tumor	Elution of minced tissue	Substances dissolved in elution buffer	Versatile, equilibration with extracellular phase	Ex vivo, single samples, dilute fluid	Contamination by intracellular fluid and proteins likely	80

dynamic response is very slow because the capsule fluid is sequestered in the tissue. Even though the suction blister technique is convenient and may be used in vivo and also in humans, the influence of inflammation and hyperfiltration should be bore in mind when interpreting the results. Tissue centrifugation has been validated as a method for isolation of native IF in several organs, including tumors, and may serve as a reference method if applicable. For tumors, blood contamination and cellular damage represent special challenges in relation to in vivo sampling with glass capillaries and wicks. This problem can at least partially be remedied by implanting wicks chronically.

If native fluid isolation is not a requirement, microdialysis and capillary ultrafiltration may represent alternatives allowing in vivo and repeated sampling to monitor dynamic responses. The techniques may reflect the concentration of small molecules in the IF, whereas the recovery may be reduced with increasing molecular size and be especially low for macromolecules. Full recovery may be achieved by tissue elution, but with that technique intracellular content may add to the eluted fluid.

B. The IF in Inflammation

1. Animal studies

By isolating native IF in small experimental animals, it has been possible to assess the quantitative importance of local production of inflammatory mediators in various organs and thereby get a better quantitative understanding of the mechanisms involved in inflammatory processes occurring at the tissue level. A central element in such considerations is to determine the ratio between the concentration in IF and serum/plasma, since any solute transported across the microvasculature from plasma will be present in a lower concentration in IF (and thus afferent lymph) than in plasma (96, 294). An IF/plasma ratio >1 will thus show local production.

After isolation of IF by centrifugation of rat skin, Nedrebø et al. (314) were able to demonstrate a differential response of two proinflammatory cytokines during endotoxemia and ischemia-reperfusion (I/R). Whereas the concentration of IL-1β increased dramatically in interstitial fluid upon lipopolysaccharide (LPS) stimulation, averaging close to 300 times that of serum 30 min after LPS injection, the corresponding concentration ratio for TNF-α was ~0.1, clearly showing that the IL-1β was produced locally whereas there was a strong gradient from plasma to interstitium of TNF-α **(FIGURE 12)**. In I/R, both of these cytokines were produced locally in skin, although the increase in IL-1β was less prominent in endotoxemia. Immunohistochemistry suggested that the sources of IL-1β were cells in epidermis and around hair follicles as well as fibroblast-like cells in the interstitium. Interestingly, by applying the observed concentrations directly to subcutis, the authors were able to elicit a reduction in P_{if} shown to induce fluid flux and edema formation in endotoxemia (312) and I/R (313), strongly suggesting a mechanistic role of these cytokines in the inflammatory edema formation.

A differential cytokine response in serum and IF was also found in the rat dental pulp, where LPS-induced inflammation resulted in IL-1α and IL-1β IF concentrations up to 11 times that of serum, whereas other proinflammatory cytokines, notably interferon (IFN)-γ, were higher in serum and thus derived from other tissues (55). The observed response was interpreted as being the result of a high abundance of macrophages in the normal dental pulp (337) that were

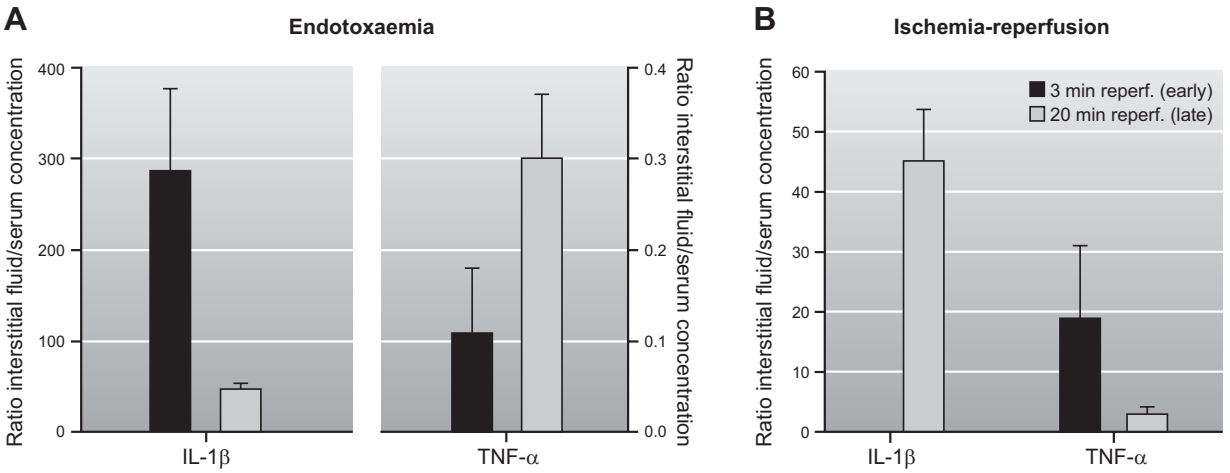

FIGURE 12. Ratio of skin interstitial fluid and serum concentrations in endotoxemia. *A:* ratio of concentration of TNF-α and IL-1β in interstitial fluid over serum in early (30 min, black bar) and late (210 min, gray bar) phase of the endotoxemia. *B*: ratio of concentration of TNF-α and IL-1β in interstitial fluid over serum in early (3 min, black bar) and late (20 min, gray bar) phase of ischemia-reperfusion injury. Early phase of IL-1β is missing due to undetectable amounts in serum. Data are means ± SE. [From Nedrebo et al. (314).]

activated by the LPS stimulation and known to be the major source of IL-1 (55). As suggested by the authors, the high local concentration of IL-1 (and TNF-α) relative to serum may actually induce a pain and illness response via a neural route during development of pulpitis, an assumption supported by the finding of IL-1 receptor on sensory nerves in the pulp (56). One might expect that the high local production of proinflammatory cytokines should result in increased capillary permeability and edema formation (e.g., Refs. 101, 285, 490), but the V_i was unaltered after LPS in the pulp as well as trachea (420) and skeletal muscle (61) having comparable cytokine patterns. A lack of edema formation is likely a result of a reduced blood pressure and blood flow as observed in the dental pulp (55), since cytokine-induced increased capillary permeability is insufficient to cause edema unless capillary pressure is elevated (143).

2. Human studies

Much of the accumulated data on the assumed composition of the IF phase derives from studies on thoracic duct lymph (reviewed in Ref. 527), thereby representing most organs of the body. More recent knowledge on composition of the microenvironment in skin is from studies of afferent lymph in the leg, a technique that was pioneered by Engeset and Olszewski (124, 340). In a review based on many years work in the field, Olszewski (341) has summarized data on normal afferent leg lymph plasma protein and cytokine concentrations as well as cellular content. The total protein concentration is highly variable, ranging from 0.1 to 0.39 relative to serum, depending on capillary filtration rate, activity, and positions of the limb. Of note, normal leg lymph contains severalfold higher concentration of many proinflammatory cytokines, showing local production in uninflamed skin and likely reflecting an immune alert situation (341).

By sampling lymph draining inflamed joints, Olszewski et al. (343) have also provided insight into the mediators involved in the inflammatory process occurring in rheumatoid arthritis. Although several protein fractions, including IgM and IgG, were significantly increased compared with control, their lymph/serum (L/S) ratio was unchanged and remained <1 and was thus likely a consequence of an increased plasma concentration and not local production. In contrast, cytokine and chemokine levels in lymph draining the inflamed joints and foot connective tissue of rheumatoid arthritis patients exceeded those of plasma severalfold, showing a local production by cells in the synovium and affected tissue in the drainage area. Observing that glucocorticoids rapidly decreased lymph but not serum concentrations further supported the notion of local cytokine production (343) **(FIGURE 13)** and emphasizing the importance of studying disease processes at the local level.

Analysis of human prenodal lymph has also provided new knowledge on lipoprotein metabolism, as pioneered by Reichl and collaborators (reviewed in Ref. 383) and more recently by Miller et al. The latter group verified what had been suggested by Reichl et al. that lipoproteins and lipids in lymph did not correlate well with concentrations in plasma (310) amounting to ~10% of the plasma level. Moreover, they were able to show that high-density lipoproteins undergo extensive remodeling and acquire cholesterol in human tissue fluid (311). In this context, we might consider that interstitial lipid accumulation seems to negatively affect lymphatic function, as suggested by recent experiments in apolipoprotein E-deficient (apoE$^{-/-}$) mice (270). ApoE$^{-/-}$ mice fed a high-fat diet had substantial lipid accumulation in the interstitium, edema of the paw and tail, hyperplastic initial lymph vessels, and reduced lymphatic conductance. The reduced conductance due to interstitial lipids may thus be part of a vicious circle that will aggravate the lipid accumulation.

Recently, Miller et al. (295) studied how peptides secreted by adipose tissue (adipokines) enter the systemic circulation

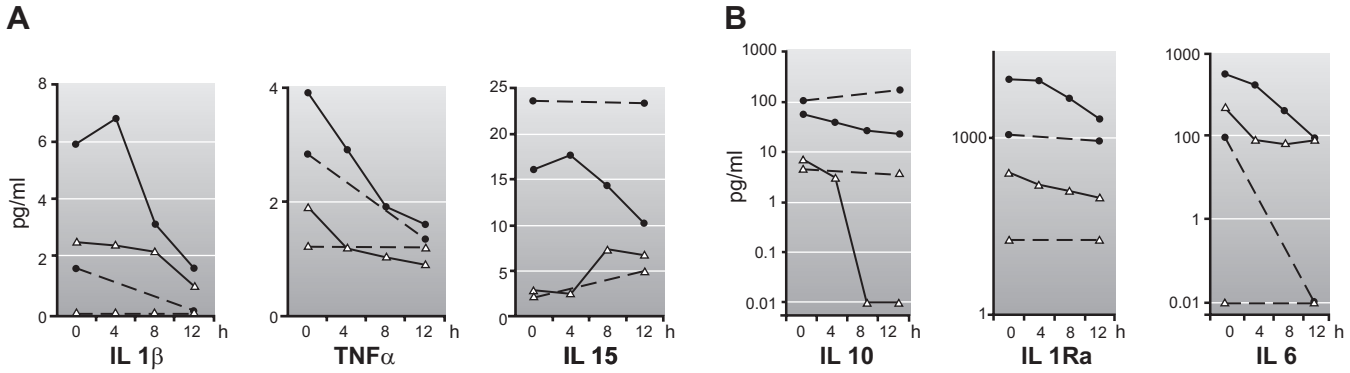

FIGURE 13. Lower leg lymph (solid lines) and serum (broken lines) cytokine levels of two patients with rheumatoid arthritis [named patient 1 (●) and patient 2 (△)] before (time 0) and after intravenous infusion of 1.0 g methylprednisolone. *A*: arithmetic scale. *B*: logarithmic scale. A substantial decrease occurred in lymph concentrations, but not in serum concentrations, of interleukin-1β (IL 1β), tumor necrosis factor-α (TNF-α), IL-10, IL-1 receptor antagonist (IL 1Ra), and IL-6. Only a small effect of methylprednisolone on IL-15 concentration was recorded. [From Olszewski et al. (343), with permission from John Wiley and Sons.]

and their production rate. They used nonsecreted proteins to derive indexes of vascular permeability and thus to estimate the fraction of adipokines leaving via capillaries, and lymph adipokine concentrations and flow to measure lymph flux. With the exception of adiponectin, adipokine concentrations were always higher in lymph than in plasma, showing local production in the tissue drained. Surprisingly, the average concentration of IL-6 in normal lymph was ~40 times that reported in normal subjects in other studies from some of the contributing authors using the same approach, and even ~6 times higher than in lymph draining joints affected by rheumatoid arthritis (341, 343). Still, the other cytokines were within normal range, suggesting that local inflammation, which one might suspect from the high level of IL-6, was not a problem. Since the cannulated vessel drains superficial tissues of the foot and ankle (310), the origin of the sampled lymph is mixed and not adipose tissue only, but clearly some adipose tissue was drained since there were higher concentrations in lymph of glycerol and leptin, substances produced specifically by adipocytes (295). Based on current pore theory, they were able to predict that the proportion of an adipokine transported via lymph was directly related to its molecular radius, increasing from 14 to 100% as radius increased from 1.18 nm for IL-8 to 3.24 for TNF-α **(FIGURE 14)**, the latter approaching the size of albumin (3.56 nm). The observed partitioning between lymph and plasma may have functional importance and influence the biological effect of secreted substances, also applying to other tissues secreting peptides. Moreover, accepting that prenodal lymph is representative for IF, the study also delineates actual concentrations that the various cell types in adipose tissue (and in other tissues in the drainage area) as well as draining lymph nodes are exposed to.

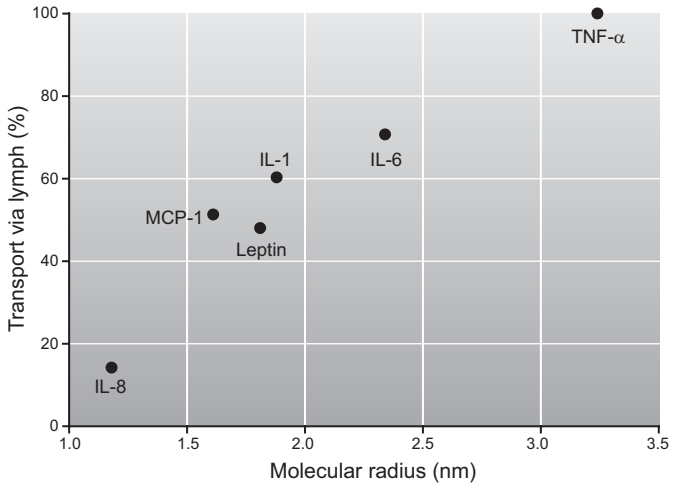

FIGURE 14. Relation between molecular radius and percentage transport via lymph for six adipokines. Values for percentage transport via lymph were calculated from the mean values for lymphatic and total transport. Spearman rank correlation coefficient = 0.94, $P = 0.025$. [From Miller et al. (295), with permission.]

Collectively, these studies on IF and lymph in experimental animals and humans show that the quantification of substances and mediators in plasma/serum does not give a representative picture of concomitant conditions in the interstitium and accordingly that tissue fluid may have to be used to investigate processes occurring in the local microenvironment.

C. IF in Lymphedema

Lymphedema, i.e., IF accumulation due to insufficient lymph drainage, may affect the composition of the interstitial fluid, and further analysis of such fluid may add to knowledge on the pathomechanisms of the condition. Since the removal of filtered proteins is impeded, one might expect an accumulation of plasma proteins in the IF, which was already suggested by Drinker et al. (117) after inducing a chronic lymphatic obstruction in dogs. A rise in lymph protein concentration was, however, not observed in dogs with chronic limb lymphedema even after 6 yr of duration, where the lymph protein concentration averaged 37 and 34% of that in serum in lymph on the lymphedema and control side, respectively (339). In early studies in primary lymphedema patients, Taylor et al. (463) found that protein concentration in lymphedema fluid increased with the severity of the disease, from 2.5 g/dl in moderate to 3.2 g/dl in severe cases, agreeing with the protein concentration range of 2.1–3.6 g/dl in primary lymphedema fluid observed by Crockett (94). The latter data correspond to a range in COP_{if} of 5.2–10 mmHg according to the Landis-Pappenheimer equation (255), i.e., rather low compared with what has been obtained with the wick technique in the lower leg of 11.1 mmHg in normal humans (331) and suggesting that COP_{if} in lymphedema is not increased. Interestingly, whereas primary lymphedema patients had a similar protein concentration in afferent lymph as normals (28 and 24% of serum, respectively), the lymph/serum ratio in patients with obstructive lymphatic disease was doubled (53%) (339), suggesting that the pathogenic mechanism may affect the composition of the IF and lymph. Still, there may also be species variation, as indicated by a significantly higher COP_{if} in hindlimb skin that was 87% of serum in the Chy mouse model of primary lymphedema, with a corresponding value of 75% in wild-type mice (232). Similar data were found in K14-VEGFR3-Ig mice (C.E. Markus, T.V. Karlsen, Ø.S. Svendsen, K. Alitalo, and H. Wiig, unpublished data), another model of primary lymphedema (281).

More recent data from obstructive/secondary lymphedema in humans indicate, contrary to expectations, that the protein centration and COP_{if} is not increased but may rather be reduced. In postsurgical and postinflammatory edema, Olszewski (342) found lower leg afferent lymph protein concentration similar to that of controls. Much to their surprise, Bates et al. (36) observed a lower COP_{if} in postmas-

tectomy lymphedema fluid isolated by wicks of 14.1 mmHg compared with wick fluid from the normal arm of 15.7 mmHg, and that there was a negative correlation between edema fluid COP_{if} and the percentage increase in arm volume. They proposed that a rise in capillary pressure might explain their results. The same group has, however, in a more recent study shown that lymphatic pump failure may contribute to the swelling (301) and thus a reduced protein concentration and COP_{if} in secondary lymphedema.

The pathogenetic role of inflammation in lymphedema is debated, and a widely held view is that high interstitial protein concentration induces an inflammatory reaction resulting in fibrosis and tissue degeneration (e.g., Refs. 12, 388). This question might be addressed by assessing inflammatory markers in lymphedema interstitial fluid. In support of such a role, Olszewski (342) observed a moderately increased level of IL-1β and strongly increased IL-6 in afferent lymph draining a limb with secondary lymphedema. In contrast, there was no increase in proinflammatory cytokines in IF in the Chy primary lymphedema model in young mice (3–4 mo) (232) and rather a reduction in proinflammatory cytokines in the K14-VEGFR3-Ig primary lymphedema model (Markhus et al., unpublished data). Since these two latter models as discussed above both have a high COP_{if}, cytokine data suggest that a high IF concentration per se does not result in inflammation and that alternative mechanisms are required.

D. IF in Tumors

1. Fluid composition

Although the functional importance the tumor IF for the understanding of tumor biology has been acknowledged (e.g., Refs. 139, 514), there are surprisingly few studies addressing this topic specifically. We will therefore include some old data in the discussion before we turn to new developments. Our focus is analyses on native IF that may serve as a reference for the noninvasive methodologies that are emerging in this area.

In **TABLE 6**, we have summarized examples of data on some characteristics of tumor IF. When compared with plasma and subcutaneous IF, tumor IF has high H^+, CO_2, and lactic acid and low glucose and O_2. In rats, the pH of the tumor IF has also been found to be related to tumor size, decreasing linearly from pH 7.3 to 6.2 with increasing tumor mass up to 50 g (220), the P_{CO_2} 16–39 mmHg higher, and the concentration of bicarbonate 4–6 mM higher when compared with afferent plasma. Gullino et al. (164) also assessed Na^+, K^+, and Cl^- in tumor IF and found the composition to be not different from serum except for a few instances where Na^+ was increased, but this change was "neither constant nor significant," suggesting that the ionic composition of tumor IF is similar to plasma.

Table 6. *Composition of interstitial fluid in tumors*

Tumor Type	Host	P_{O_2}, mmHg		P_{CO_2}, mmHg			pH			Lactic Acid, mg/l		Reference Nos.
		TIF		TIF	SIF	Plasma	TIF	SIF	Plasma (arterial)	TIF	Plasma	
Carcinoma (Walker 256)	Rat			79 ± 6	50 ± 2	31 ± 1	7.044 ± 0.044	7.341 ± 0.30	7.313 ± 0.041	12 ± 3	5.1 ± 4	164, 166
Chinese hamster lung fibroblasts	Mouse			76.9 ± 7.9			6.85 ± 0.05			20 ± 1.2		190
Carcinoma (Walker 256)	Rat						6.98 ± 0.13	7.30 ± 0.11				220
Colon adenocarcinoma (LS174T)	Mouse	8.3 ± 1.6				8.3 ± 1.6	7.04 ± 0.02					191
Cervical cancer	Human	<10				<10						195
Various	Human	<10				<10						478

TIF, tumor interstitial fluid; SIF, subcutaneous interstitial fluid. If no value is given, value was not determined.

In light of the invasive character of malignant tumors, it is also of interest to study activities of proteolytic and lysozymal enzymes in IF. A generally increased activity of such enzymes has been found (167, 453, 454). Furthermore, an increased hyaluronidase activity has been observed (132, 133) that could explain the lower concentration of hyaluronan in tumor compared with subcutaneous IF.

During the last years data have emerged regarding the macromolecular composition and COP_{if} and thus of importance for our understanding of transcapillary fluid exchange in tumors. Although tumor vessels are known to be highly permeable for water and proteins (e.g., Refs. 119, 142, 187, 422 and references therein) suggesting a low σ and thus a low, if any, COP gradient between interstitial fluid and plasma, exact knowledge of this parameter is important for understanding transcapillary fluid transport in tumors. Whereas there are numerous studies addressing tumor P_{if} (for review, see Ref. 187 and sect. IV*E*), data on COP_{if} in tumors are more scarce **(TABLE 7)**. Most extensive are studies by Stohrer et al. (439), who measured COP_{if} in four different human tumor xenografts in mice after implanting wicks. With "chronic" wicks inserted at the time of tumor implantation (see sect. III*C2*), they found a generally higher COP than in subcutaneous tissue. COP_{if} was not significantly different from plasma (or actually tended to be higher) in three out of four tumor types, while in a colon adenocarcinoma (LS174T) the COP_{if} was 82% of that in plasma and significantly higher than in subcutaneous IF, which amounted to 41% of the plasma value. More recently, Wiig and co-workers found a tumor IF/plasma COP ratio of 0.75–0.79 in chemically induced mammary tumors in rats (494) and ovarian carcinomas in humans (184), again significantly higher than the corresponding subcutaneous ratio of 0.60 and close to the value for LS174T colon adenocarcinomas. The high COP observed in these two studies and that of Tong et al. (472) corresponds well to the high protein concentration relative to plasma of 0.8–1.0 found by Sylven et al. (453), although not so well to the data from Gullino et al. (164). The latter authors found a protein concentration in IF of 3.2 g/100 ml (average of 4 tumor types), with corresponding concentrations of 4.1 g/100 ml in fluid draining from subcutaneous capsules and 4.8 and 5.2 g/100 ml in serum flowing into and out of the tumor, respectively. In general, the protein concentration in IF was lower than in subcutaneous fluid and on average 67% of that in serum. It is, however, likely that the concentration was underestimated in the study of Gullino et al. due to sieving at the interface between capsule and tissue. This may have occurred since fluid was drained to atmospheric pressure from an area with high P_{if} as discussed in section VI*A5*. Of note, whereas it is possible to reliably calculate COP from total protein concentration in plasma and normal IF using, e.g., the Landis-Pappenheimer equation (255) to translate these protein concentrations to COP_{if}, such calculations will probably not be valid for tumor due to a different protein distribution pattern relative to plasma, especially with respect to low-molecular-weight proteins (439).

The potential contamination by intracellular and plasma proteins during capillary and wick sampling notwithstanding (see sect. VI*A2*), all data suggest that there is a high colloid osmotic pressure and protein concentration in IF and thus that the colloid osmotic pressure gradient across the tumor microvascular wall is low. This conclusion is also consistent with the findings of increased permeability of tumor vessels and may together with the lack of functional lymphatics result in an elevated tumor P_{if} (see sect. IV*E*). Together, all these factors contribute to reducing the filtration and thus the delivery of macromolecular therapeutic agents.

The protein distribution pattern in IF in general and in tumor IF specifically is also a function of the tissue microen-

Table 7. *Protein concentration and colloid osmotic pressure of interstitial fluid in tumors*

Tumor Type	Host	Protein, mg/ml			COP, mmHg			Reference Nos.
		TIF	Subcutis	Plasma	TIF	Subcutis	Plasma	
Carcinoma (Walker 256)	Rat	32 ± 1	41 ± 2	48 ± 1				164, 166
Mammary carcinoma	Mouse	54		55–60				453
Carcinoma (Walker 256)	Rat							220
Colon adenocarcinoma (LS174T)	Mouse				16.7 ± 3.0			439
Small cell lung carcinoma (54A)					21.1 ± 2.8	8.2 ± 2.3	20.0 ± 1.6	
Mammary carcinoma MCaIV					17.1 ± 0.8		19.5 ± 0.5	472
Mammary carcinoma (chemically induced)	Rat	44.7		54.9	16.6 ± 1.0	13.8 ± 1.0	20.5 ± 0.8	494
Ovarian carcinoma	Human				24.0 ± 3.0		30.3 ± 2.0	184

TIF, tumor interstitial fluid. If no value is given, value was not determined.

vironment as it is a consequence of fluid exchange as well as the local production of substances. Gullino et al. (164) subjected tumor IF to paper electrophoresis. Interestingly, they found that the fluid did not contain any fibrinogen. The relative proportions of electrophoretic components were similar to that of serum except for α-globulins (i.e., α-lipoproteins, α1-antitrypsin, α2-macroglobulin, α1-glycoprotein, ceruloplasmin, and orosomucoid; Ref. 372) that was moderately smaller than that of plasma. Of note, these proteins have higher as well as lower molecular mass compared with albumin. The albumin-to-globulin ratio of tumor IF was similar to that of afferent blood. Stohrer et al. (439) observed a somewhat deviating pattern after separation by SDS-gel electrophoresis. Compared with plasma, tumor IF had a significantly lower fraction of proteins with molecular mass >75 kDa and not different fraction for proteins 25–75 kDa, indicating some size selectivity of the tumor vessels. For proteins with molecular mass <25 kDa, the concentration in IF was on average 2.4 times higher than in plasma, and these smaller proteins can be breakdown products from necrotic areas and tumor-derived cell proteins as well as cellular enzymes (439, 453). Similar relative protein distribution pattern, i.e., a larger fraction of molecules eluting in the lower molecular mass region, has later been found by gel chromatography (494). The latter authors concluded that a prominent peak observed was a specific tumor protein. It is, however, likely that there are a plethora of proteins in this fraction.

Obviously, identification of proteins in tumor IF is useful to better characterize the microenvironment and to look for tissue-specific proteins as discussed in following sections. The importance of studying signaling substances locally in the target organ was recently shown for bone marrow. By isolation of bone marrow IF from acute myeloid leukemia patients at the time of diagnosis and 2–4 wk after start of induction therapy, Iversen and Wiig (213) observed that leukemia-derived bone marrow IF, but not plasma, repressed hematopoietic cell growth, an effect that was lost by successful induction treatment. Moreover, TNF-α and adiponectin concentrations were higher in bone marrow IF showing that these substances were produced locally, leading to the conclusion that these two cytokines had a central role in the disease process (213). This assumption was further supported by the observation that TNF-α and adiponectin fell significantly in bone marrow IF in patients entering remission, whereas their plasma levels were unaffected by therapy. The therapeutic importance of addressing substances in the local microenvironment has also been shown for other hematological cancers (239, 524). Moreover, recent data on autologous chemotaxis in the inflammatory and tumor microenvironments (discussed in sect. VIIIC) further emphasize the importance of studying signaling occurring locally in the interstitial fluid phase.

E. Tissue-Specific Proteins in IF

Although our main focus is the fluid phase of the interstitium and the composition of this phase in the context of fluid exchange and local signaling, we will briefly discuss this fluid in the context of biomarker discovery, the reason being that IF has emerged as an important source for disease- or biomarkers, i.e., molecular indicators of disease-related processes and/or disease outcomes (223). The most commonly used source for searches is plasma/serum, but due to the complexity of this fluid and the dynamic range in the proteins sampled, techniques have emerged to enrich and study subproteomes in an attempt to reduce the complexity and to be able to detect low abundant proteins (149, 360, 479). This fact notwithstanding, the potential biomarkers deriving from a local disease process like solid cancer will be diluted by several orders of magnitude even if subproteomes of plasma/serum are used as substrate (431) that moreover represents an integration of cellular processes of the body. Accordingly will the chances of finding disease specific biomarkers that may eventually end up in plasma and there be detected by a specific approach be greater if the search is performed closer to the disease process, i.e., in the local IF.

Several authors have searched for proteins in the IF phase in diseased tissues having used various methods for fluid isolation (see sect. VI*A*). Some of the first studies were those of Celis and co-workers in breast carcinomas (80) and adipose tissue from breast carcinoma patients (81) using the tissue elution method, that has later also been used, e.g., in liver (443). A proteomics approach has also been applied on IF isolated by centrifugation in rat bone marrow (488), pig skin (68) and human ovarian carcinomas (184), by capillary ultrafiltration in fibrosarcomas in mice (204), a human head and neck squamous carcinoma (440) and by the suction blister technique in human skin (248). The available data suggest that this is an emerging area with significant potential. Prevailing candidate proteins should, however, be interpreted in light of validation studies and inherent strengths and weaknesses of the methods applied and whether they sample fluid representative of IF, as discussed in section VI*A*.

VII. LOCAL REGULATION OF INTERSTITIAL FLUID VOLUME ("AUTOREGULATION")

Above we have discussed P_{if} and COP_{if} and their role in formation and flow of lymph. These determinants of fluid volume will also adapt to oppose primary perturbations in COP_c and P_c and thus to maintain a stable V_i. A general finding in all tissues studied is that an increase in the net filtration will increase P_{if} (i.e., hydrostatic buffering) and reduce COP_{if} (colloidosmotic or oncotic buffering), but their relative changes and thus contributions to fluid volume regulation may vary substantially among organs (25). Moreover, an increased lymph drainage induced by the increased filtration may also

contribute to prevent edema formation. Together, these factors are "safety factors against edema," a term introduced by Guyton (171) and that is useful when discussing the maintenance of V_i. This relates to another useful concept in normal V_i control, namely, "autoregulation" of V_i (24, 25), i.e., that normal control of V_i is obtained via changes in interstitial fluid hydrostatic and colloid osmotic pressures to counteract changes in capillary fluid filtration to restore normal filtration. In relation to maintenance of V_i, it is also pertinent to consider interstitial compliance, as discussed in section III*C*, that gives a measure of the change in P_{if} and net filtration pressure created by a given change in V_i that will vary depending on the interstitial matrix and the "encapsulation" of the organ. This was previously an area of active research, and an analysis of V_i autoregulation and safety factors against edema was provided by Aukland and Reed (25). During the last two decades, however, the interest in this topic has been moderate, briefly summarized here focusing on recent developments.

A. Hydrostatic Buffering

In early experiments by Guyton using the implanted perforated capsule in dogs (170), he found that P_{if} rose from the normal level of −7 to +2 mmHg when overt edema developed, suggesting a maximal hydrostatic buffering in skin/subcutis of 9 mmHg. Even though this pressure is still referred to as the level of hydrostatic buffering (410), more recent data show that the control P_{if} in these experiments was too negative (493, 507) and that the maximal hydrostatic counterpressure is ~2 mmHg in dog skin and muscle (506) as in the same tissues in other species. It may, however, increase more in excessive overhydration in dogs (506), and in human skin where accumulated data suggest a counterpressure of ~5 mmHg (reviewed in Ref. 25). That the hydrostatic counterpressure in human skin is higher than that of other species is supported by data from Bates et al. (36, 37), finding a rise in subcutaneous P_{if} measured with wick-in-needle of ~5 cmH_2O from control level upon development of edema.

A more pronounced increase in P_{if} may occur if the edema formation is rapid, as shown by the increment in P_{if} from −1 to 25 mmHg in rat frostbite injury (46) as the fluid volume increased to two to three times control (see sect. IV*D*). Moreover, in lymphedema mice, a rise in P_{if} of ~6 mmHg was recorded after volume expansion (232), suggesting that skin compliance is altered in these conditions since similar changes in volume result in severalfold lower increment in P_{if} if edema develops slowly (e.g., Ref. 504). Clearly, the counterpressure against edema formation is dependent on compliance of the tissue. Thus, in the myocardium, P_{if} rose by 12.6 mmHg when abolishing lymph flow (438), although this may represent an overestimate due to the use of porous polyethylene capsules during an acute perturbation (507) (see sect. III*B2*). Moreover, counterpressures in this range have also been found in encapsulated organs in rats like bone marrow (212) and brain (505) and even higher in the tail where this pressure may exceed 15 mmHg (1, 27). To summarize, if developing slowly, P_{if} will counteract edema formation by ~2 mmHg, but may be severalfold higher in rapidly generated edemas or if developing in enclosed organs.

B. Oncotic Buffering

As pointed out previously (25), the maximal edema-preventive effect of lowering COP_{if} is determined as the difference between the normal COP_{if} and its minimal value corresponding to a protein concentration of $C_p(1 - \sigma)$. When reviewing a number of studies in humans (ankle), dogs, cats, rats, and sheep and tissues including skin, skeletal muscle, intestine and lung (25), the data were remarkably consistent showing an oncotic edema prevention by dilution/washout of interstitial proteins in the range of 6–9 mmHg. The exception was human chest where the maximal counterpressure was 14 mmHg that may be explained by a higher control COP_{if}.

In apparent contrast to these data are observations from the myocardium, where a 5.6-fold rise in lymph flow induced by partial coronary sinus occlusion resulted in a halved protein concentration but a reduction in COP_{lymph} of 2.9 mmHg only. Apparently, this was due to an increased albumin fraction in lymph, thereby limiting the edema preventive effect of protein washout/washdown. The fact that we do not know at what COP_{if} edema develops notwithstanding, recent data suggest that the interstitium in this organ can compensate for a significantly higher increase in net filtration pressure than skin and muscle discussed above because of a higher control COP_{if}. After isolation of interstitial fluid by centrifugation, Semaeva et al. (420) found a control COP_{if} of 18.8 mmHg that was 3.2 mmHg lower, only, than the corresponding COP_c. In support of the assumption of an important role in edema prevention was the finding of a dramatic reduction during induced hypervolemia. Even though the data reviewed above all suggest that washout/dilution of protein will contribute in edema prevention, the presented recent studies indicate a wide span of variation between organs.

C. Lymphatic Buffering

Clearly, the lymphatics will by removal of fluid and proteins also contribute in edema prevention during increased net filtration. Although Aukland and Reed in their review called for more studies to address this question quantitatively (25), there appear to be a lack of new data in this field. For completeness we will briefly summarize a few of their main points.

In steady state (i.e., constant V_i), the net filtration J_v will equal lymph flow (J_l), and by rearrangement of the Starling equation (see sect. IV*A*), it can be shown that J_l relates to the

net filtration pressure ΔP as $J_l/L_pA = \Delta P$, and accordingly that J_l/L_pA can tell us how much imbalance of the Starling pressure that can be compensated by lymph flow (25). Alternatively, ΔP can also be determined from J_l estimated from the removal rate of albumin (k_{alb}) from the interstitium, in such a way that $\Delta P = k_{alb}/L_pA_a$, where L_pA_a is the L_pA per milliliter available volume for albumin (25). By careful review of available data either based on direct measurement of J_l or by its estimation via k_{alb}, they concluded that "it seems safe to assume that lymph flow in various tissues normally neutralizes a net filtration pressure of only a few tenths of a millimeter of mercury" (25). No new data seem to dispute that statement.

During increased filtration, lymphatic compensation may be higher, estimated to 6–12 mmHg for lung, intestine, and hindpaw in response to venous stasis (329). By reanalysis of data from Landis and Gibbon (254), lymph flow was found to compensate for 15 mmHg increase in net filtration pressure (25). In contrast to these studies are data discussed above where a net filtration pressure of 10–15 mmHg can be compensated by the combination of hydrostatic and oncotic buffering without the need of lymphatic buffering. Clearly, the contribution of lymphatic buffering is variable but may have its most important role in preventing edema in tissues exposed to orthostasis (25).

VIII. INTERSTITIAL FLOW AND ITS BIOLOGICAL EFFECTS

A. Measurements of IF and Shear Stress

Interstitial flow, caused by Starling forces between the capillary, interstitial, and lymphatic compartments, is highly heterogeneous, and few direct measurements exist. Early estimates of average interstitial flow within the tumor microenvironment were made by Butler and Gullino, who compared hematocrit in the afferent versus efferent blood vasculature of the tumor (75). Chary and Jain (83) measured interstitial flow directly in the rabbit ear window model and found a wide range of velocities between 0 and 2 μm/s with an average of 0.6 μm/s. Measurements in anesthetized mice using magnetic resonance imaging found similar, albeit slower (0.1–0.5 μm/s), flows (103); whether this is due to differences in measurement techniques or animal species remains to be determined.

Importantly, interstitial flow may be substantially increased in peritumoral tissue (103) and in acute stages of inflammation, as evidenced by dramatically increased lymph flow rates draining these regions (186, 286, 300, 304). Increased lymphatic drainage to the sentinel lymph node of tumors has also been demonstrated (182, 369, 396), again inferring increased interstitial flow since interstitial and lymph flow are coupled. The increased flow in the tumor microenvironment is presumed to be due to the high P_{if} in tumors, and subsequently high gradients in P_{if} at the tumor margin, as discussed in section IV*E*. Increased interstitial flow in acute inflammation may be due to temporarily increased blood vessel permeability, but we will show below in section VIII*E* that increased fluid flow can induce lymphatic endothelial cells to increase their effective permeability via active transport mechanisms, thereby further increasing interstitial and lymphatic flow.

How might interstitial flow affect interstitial cells? Of course, interstitial flow imparts mechanical stresses on ECM fibers and cells embedded in the matrix, including shear stress and drag forces. These stresses can be estimated by the hydraulic conductivity *K* of the interstitium (discussed in section III*D*), since the latter is governed by the flow resistance of the solid phase of the material, i.e., the fluid-solid interactions in the pores or at the ECM fiber boundaries (487). In physiologically relevant interstitial flow rates, average shear stresses have been estimated at <0.1 dyn/cm^2 (423). These are much lower than those found in the blood vasculature, for example, but similar to shear stress estimates in lymph vessels (113, 449).

On the other hand, flow through porous media is heterogeneous, and thus peak shear stresses and shear gradients can be high when fluid is forced through confined and tortuous spaces like the ECM (455), particularly when considering ECM remodeling near the cell that can substantially shield local shear stress (358, 359). Drag forces on the ECM need also to be considered (358, 359), which can transmit stress to nearby cells through tethering forces on integrin attachments. Thus mechanical stresses imposed by interstitial flow are complex and heterogeneous, and depend on the specific architecture of the ECM and organization of the interstitium.

B. Effects of Interstitial Flow on Fibroblastic Cells

Fibroblasts are responsible for maintaining and remodeling the ECM. In some types of inflammation, namely, those leading to fibrosis and cancer, fibroblasts can differentiate into myofibroblasts, which are more contractile and synthetic, and are characterized by α-smooth muscle actin expression, increased secretion of matrix proteins, and MMPs and can also secrete angiogenic growth factors and tumor-promoting cytokines (107, 193, 194, 345). Myofibroblast differentiation depends on TGF-β, which is secreted by the myofibroblast and can also be activated from latent stores in the matrix by mechanical stress (10, 517, 518).

Interestingly, it was found that superphysiological or pathological levels of interstitial flow, i.e., 3–10 μm/s, could induce fibroblast motility through MMP-1 upregulation (423, 424) as well as drive myofibroblast differentiation and matrix alignment (325–327) **(FIGURE 15)**. This matrix alignment was more rapid (within 12–24 h after flow onset) than the myofibroblast differentiation (1–5 days). Interest-

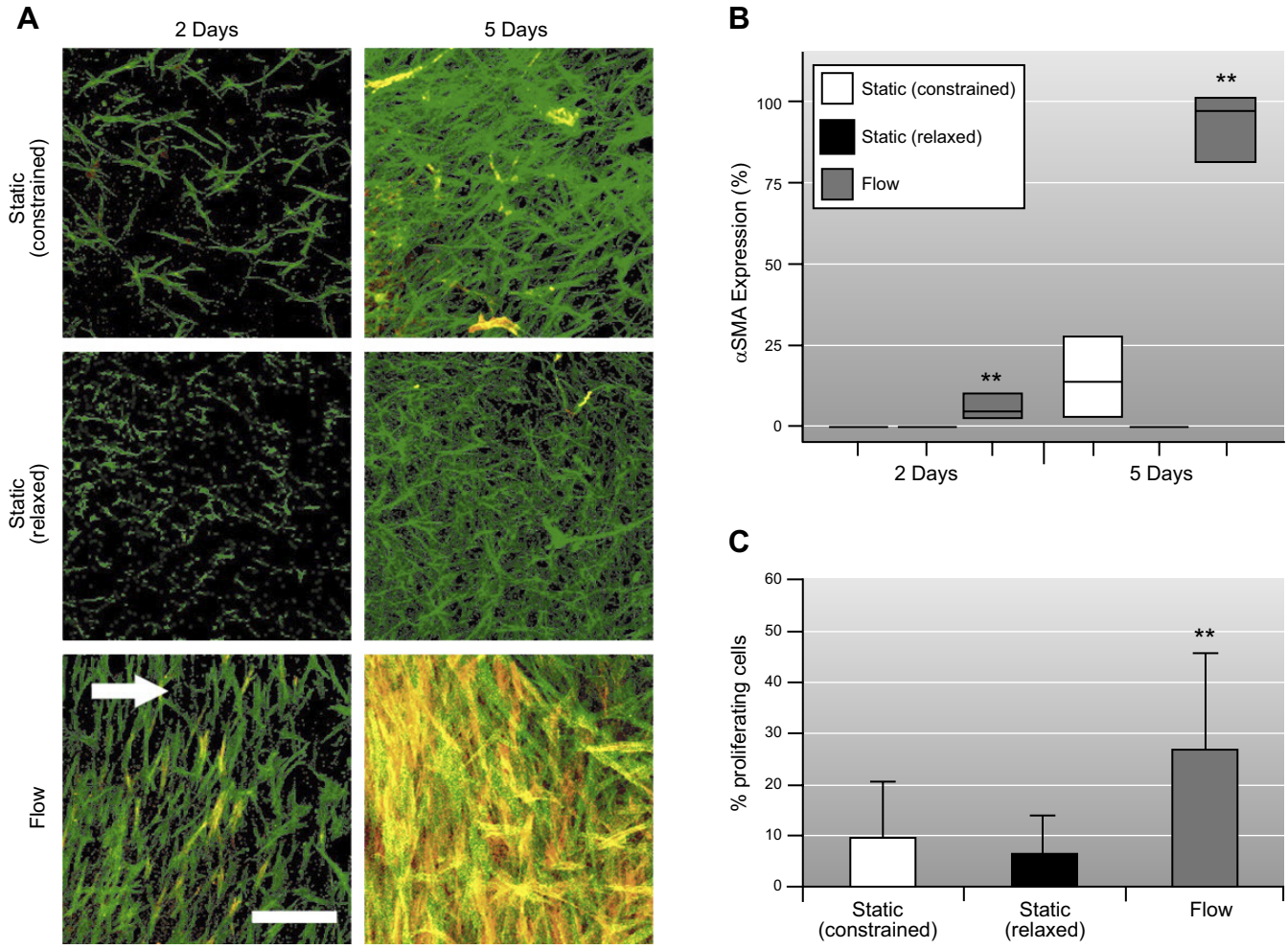

FIGURE 15. Interstitial flow induces α-SMA expression in fibroblasts. *A*: confocal images of fibroblasts exposed to flow for 2 and 5 days showing α-SMA expression under mechanically constrained static and interstitial flow conditions (green, factin; red, α-SMA; arrow indicates flow direction). Bar, 200 μm. *B*: significantly higher levels of α-SMA expression are seen in fibroblasts under interstitial flow at both time points ($^{**}P < 0.01$). Box plot shows 95% confidence intervals with midline showing the median. *C*: the percentage of proliferating (Ki67+) cells after 2 days was higher under interstitial flow conditions than either constrained or relaxed static controls (bar represents the mean value and error bars represent SD; $^{**}P < 0.01$). [From Ng et al. (325), with permission.]

ingly, the alignment was perpendicular to flow (326), rather than parallel, and corresponded to a decrease in hydraulic conductivity (326, 327). The alignment and myofibroblast differentiation were both dependent on TGF-β, which was increased by flow (325).

Why is flow-induced ECM alignment significant? ECM alignment is commonly seen in tissue remodeling and wound healing (470), where interstitial flow is increased, and in response to all types of mechanical signals. A matrix made of perpendicularly aligned fibers should experience greater drag force than matrices parallel to the direction of flow (178, 215), so when matrices align perpendicular to interstitial flow, the shear stress is increased on the ECM fibers but, as computational fluid dynamics studies revealed, decreased on the cells (358, 359). In other words, perpendicular matrix alignment transfers fluid stresses away from the cells and onto the matrix fibers, thereby shielding fluid stress from the cell. This occurs even if the fiber rearrangement does not alter the bulk tissue porosity (359).

In addition to altering the hydraulic conductivity, matrix alignment and ECM compaction from by fibroblast contraction can increase the ECM stiffness, which communicates mechanical stresses to cells. Interstitial flow can induce matrix tension to which cells may respond by aligning and stiffening the ECM. Fibroblasts appear to be highly sensitive to interstitial flow, and heightened flow drives myofibroblast differentiation and ECM remodeling that recapitulates certain pathological features of fibrosis (325–327). These in vitro findings suggest that chronically increased interstitial flow may contribute to ECM stiffening and alignment, as well as myofibroblast differentiation, hallmarks of interstitial fibrosis as well as tumor stroma.

C. Pericellular Gradient Formation by Interstitial Flow

Another effect of interstitial flow on cells is that it may bias the local extracellular distribution of secreted molecules like proteases, cytokines, or growth factors. Even when interstitial flow rates are very small (such that diffusion still dominates mass transport distances), convective forces due to interstitial flow can bias the local gradients of these factors around individual cells (138). And since cells often respond to local concentration gradients of such factors rather than absolute amounts, such forces may theoretically direct growth or migration **(FIGURE 16)**.

This concept was first demonstrated experimentally with microvascular endothelial cells cultured in 3D fibrin matrices to which a growth factor, VEGF, was covalently tethered (189). Cells could liberate the growth factor (required for its function) by secreting proteases. Under flow conditions, theoretical modeling predicted that the secreted pro-

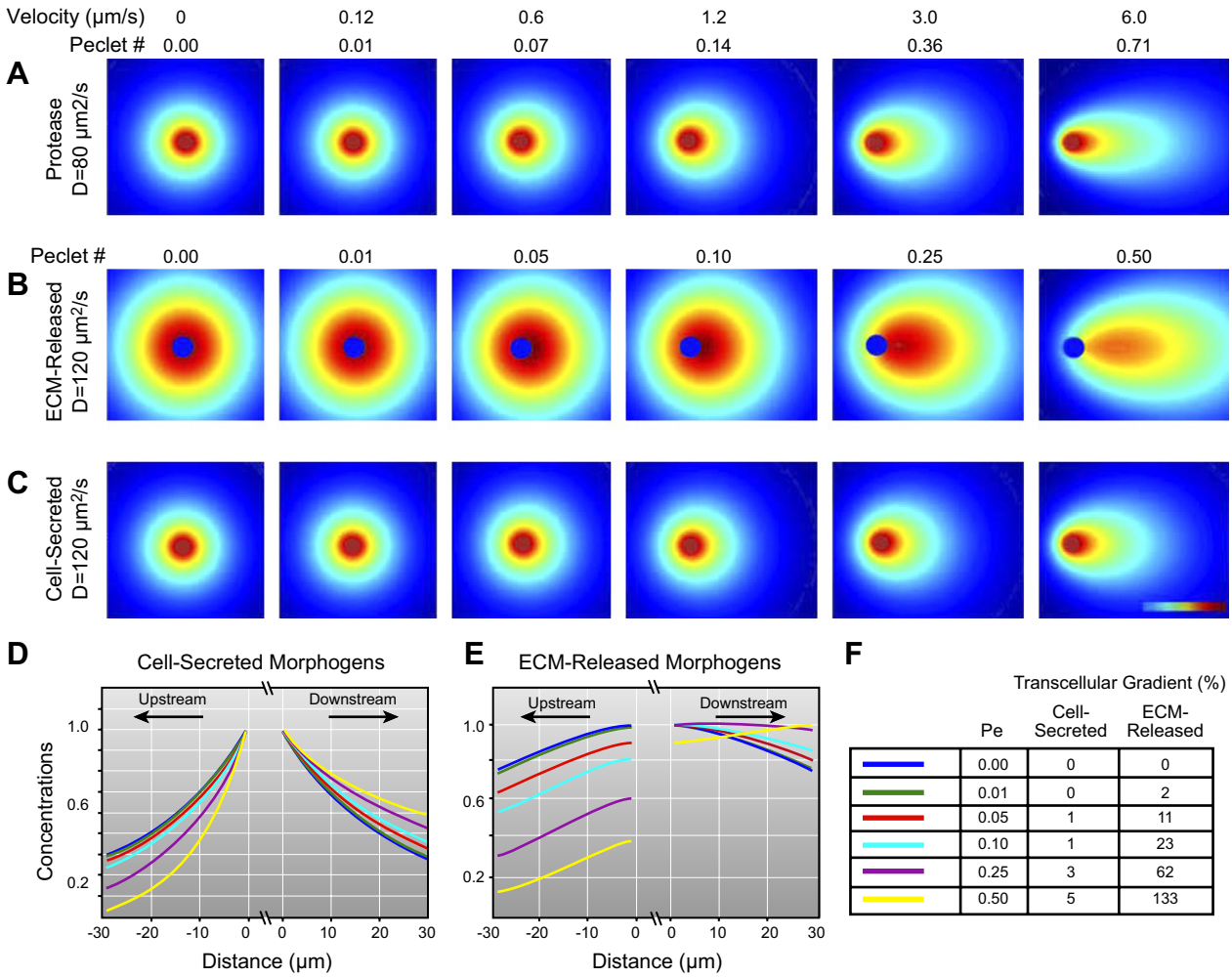

FIGURE 16. Creation and amplification of autologous morphogen gradients by subtle physiological flows and matrix-binding properties of morphogen. *A*: dimensionless concentration gradients of cell-released proteases calculated using a constant surface concentration are increasingly skewed in the direction of flow with increasing flow velocities. Red, 1 (maximum concentration); dark blue, 0. *B*: dimensionless concentration gradients of liberated morphogen are released from the ECM through the action of the cell-secreted protease whose profiles are shown in *A*. *C*: distributions of cell-released morphogen demonstrate, when compared with the corresponding profiles in *B*, the marked gradient amplification effect in matrix-released versus cell-secreted morphogen properties under otherwise identical conditions. *D*: cell-secreted morphogen concentrations as calculated along a line parallel to flow and passing through the cell midlines. All flow conditions result in cell concentrations that decrease with increasing distance from the cell. *E*: ECM-released morphogen concentrations show greater asymmetry compared with those of cell-secreted morphogens for the same flow conditions. Interestingly, the higher Peclet numbers (0.25 and 0.5) show increasing concentration gradients with increasing distance downstream from the cell. *F*: calculated transcellular gradients (percentage difference between the downstream and upstream sides of the cell) reveal the degree of gradient amplification that is achieved when morphogen is secreted into matrix-binding form and demonstrate the potential for autologous chemotaxis gradients. [From Fleury et al. (138), with permission from Elsevier.]

tease distribution would be skewed by flow so that more protease was downstream of the cell, and thus liberated more VEGF in the downstream direction. Furthermore, the newly soluble VEGF would also be skewed by flow in the downstream direction, with the net effect of amplified pericellular gradients. The experimental data supported this hypothesis, and directed capillary formation only occurred when both flow and VEGF were present (189).

The concept was then applied in special cases of chemotaxis, when the chemotacting cell both secretes a chemokine as well as expresses its receptor. Such is the case for dendritic cells, which use the receptor CCR7 to chemotact to lymphatic vessels, but also secrete its ligand. Some tumor cells also express both CCR7 and its ligands, and it was shown that such cells can use interstitial flow to chemotact, so-called "autologous chemotaxis," by secreting the chemokine and then following the gradient that is skewed by flow (427). Thus autologous gradients created by interstitial flow may provide morphogenic and chemotactic cues related to direction in some cell behaviors.

As a side note, since autologous chemotaxis requires both the chemokine receptor and its ligand to be expressed by the same cell, it may only apply to a small subset of certain cell populations. For example, both dendritic cells and certain tumor cells express heterogeneous levels of CCR7 and its ligand, rendering a subpopulation to be flow-responsive. A recent report has demonstrated that in addition to autologous chemotaxis, interstitial flow can also drive competing mechanisms in tumor cells, including strain-induced migration in the upstream direction (367). Thus autologous chemotaxis is only one of many biophysical effects that interstitial flow may have on cells.

D. Effects of Interstitial Flow on Lymphatic Growth and Function

1. Lymphangiogenesis

The formation of new lymphatic vessels, or lymphangiogenesis, is also affected by interstitial flow. Lymphangiogenesis occurs during development as well as in wound healing, inflammation, and cancer (459, 522); it occurs both in the inflamed tissue as well as in their draining lymph nodes (16, 175, 182, 235, 396, 430). In some models of experimental inflammation, VEGFR-3-dependent lymphangiogenesis has been shown to play a role in the resolution of inflammation and edema, including in a mouse model of chronic airway inflammation (34) and inflammation in mouse skin (228, 229). Other studies have lent further support to this, showing, for example, that VEGF-D and VEGF-A are important for the resolution of inflammation in mouse skin (207, 208, 234). In arthritis models, inhibition of lymphangiogenesis via blockade of VEGFR-3 reduced lymph drainage and aggravated inflammation (168), while intra-articular delivery of VEGF-C improved lymph drainage and attenuated the joint tissue damage (536). Collectively, these studies in mice suggest that inflammatory lymphangiogenesis plays a key role in clearing edema fluid and antigens, and that local delivery of VEGF-C may be useful in treating certain types of inflammatory disorders.

In tumors, lymphangiogenesis has obvious importance as a route for cancer cells to disseminate to lymph nodes, and lymphatic vessels are known to secrete a wide range of chemokines that attract tumor cells, including CCL5 and CCL21 (210, 426, 459). At the same time, tumor-associated lymphangiogenesis leads to a more extensive drainage network to capture IF flowing from the tumor and through the microenvironment. Since fluid drainage is one of the main functions of lymphatic capillaries, it is perhaps not surprising that interstitial fluid flow might regulate lymphatic capillary regeneration.

The role of interstitial flow in adult lymphangiogenesis was first explored in 2003, using a model of circumferential dermal regeneration in the tail of the mouse (450). While epidermal regeneration and blood angiogenesis occurred equally in both ends of the regenerating skin, lymphatic vessels organized around fluid channels, and only in the lymph flow direction (distal to proximal) (58). Without "forcing" lymph flow through the regenerating region, lymphatic vessels failed to organize (400). Furthermore, while VEGF-C was found to be required for lymphatic endothelial cell proliferation and migration, interstitial flow was required for capillary organization and functionality (perfusion) (153–155).

In vitro, interstitial flow was also found to play an organization role in lymphatic capillary morphogenesis, stimulating lymphatic endothelial cells in three-dimensional cultures to organize into structures (155, 324). Similar effects were found for blood endothelial cells in culture, in a manner synergistic with the growth factor VEGF (155, 324). These studies highlight the importance of interstitial flow in driving morphogenesis of lymphatic and blood capillaries and can be used as the basis for interstitial flow as a design principle for in vitro capillary tissue engineering.

2. Lymphatic function

In addition to guiding lymphatic morphogenesis, interstitial flow can also affect lymphatic endothelial cell function. In vitro, lymphatic endothelial cells cultured in a monolayer at the bottom of a culture insert are very sensitive to transmural flow, responding by upregulating expression of the lymphoid homing chemokine CCL21 and the cell adhesion molecules ICAM-1, VCAM-1, and E-selectin (298), all important for dendritic cell transmigration and homing to the lymph node (224, 375). Such changes have also been observed upon stimulation by cytokines like TNF-α and -β and IL-1 (224, 366, 409), implying that heightened flow

may act as an inflammatory cue, perhaps as an early cue, since it is almost immediately increased upon tissue injury or insult (35, 67, 186, 304). Transmural flow also maintained the organization of the cell-cell junctional molecules PECAM-1 and VE-cadherin, and increased fluid and solute transport rates across lymphatic vessels (298), indicating active regulation to some extent of lymph formation.

Since increased interstitial flow correlates with increased lymph flow, increased interstitial flow may also have important consequences on the collecting lymphatics. Studies from isolated rat mesenteric vessels have demonstrated that lymph pump function is sensitive to fluid flow via both stretch and shear stress-activated mechanisms (45, 308). Shear stress in collecting vessels was estimated to average <1 dyn/cm^2, but throughout normal functioning, peaks of 4–12 dyn/cm^2 (113) were estimated due to pump-induced fluctuations in flow velocity and diameter. Shear-sensitive pump function of collecting lymphatic vessels is thought to be primarily regulated by shear-modulated nitric oxide release from lymphatic endothelium (60, 116, 174, 373, 477), particularly in the valve regions (60). However, when very high lymph flow rates are imposed, pump function decreases and the vessels switch to conduit-like behavior to more efficiently move fluid (373). Thus, since interstitial flow and lymph formation is inherently and obviously coupled to lymph flow downstream, lymphatic pump function helps to determine interstitial flow velocity and lymph formation rates, and all three have positive-feedback control loops in sensing and responding to fluid loads.

Finally, interstitial flow may also affect the lymph node. Fibroblastic reticular cells secrete matrix proteins and chemokines that are critical for guiding adaptive immune responses, including CCL21 and CCL19, both ligands to the lymphoid homing chemokine receptor CCR7. With the use of a tissue-engineered model of the lymph node stroma, it was demonstrated that CCL21 regulation and stromal organization by these fibroblastic cells depended on IF flow (471). In vivo, blocking afferent flow to the lymph node led to rapid downregulation of CCL21 gene expression (471) and was also found to drive collapse of high endothelial cells and reduce lymphocyte entry (289). Interestingly, lymph node lymphangiogenesis has also been correlated to increased lymph flow, at least in tumor-bearing mice (102, 182, 369, 397). Thus interstitial flow appears to have important functional consequences on both the lymphatic vessels as well as the draining lymph nodes, implying key roles for flow in modulating immunity in secondary lymphoid organs. And although it is fascinating to consider, the role of altered lymph flow into the tumor-draining lymph node on tumor immunity has yet to be elucidated (275).

E. Interstitial Flow in the Tumor Microenvironment

As described above, interstitial flow can have important effects on stromal fibroblasts, immune cells, lymphangiogenesis, and lymphatic transport functions. All these are important in the tumor microenvironment, and thus interstitial flow may have important implications for tumor invasion and metastasis.

For one, interstitial flow may promote tumor cell invasion via autologous chemotaxis, which was described above. Some tumor cells express chemokine/receptor pairs, including CCR7/CCL21 and CXCR4/CXCL12, which in the presence of interstitial fluid flow may generate pericellular gradients that in turn guide cell migration in the flow direction, i.e., towards the nearest draining lymphatic vessel (367, 427). For example, invasive human breast cancer cells that expressed CCL21 and CCR7 were found to polarize and directionally migrate in the flow direction, but this directionality was lost when either CCR7 signaling was blocked or when exogenous CCL21 was added so as to overpower any local gradients (427).

Of course, in vivo tumor cells do not migrate as single cells in a collagen gel, but rather in a complex microenvironment where they are often seen following migratory fibroblasts (140, 243). As explained above, fibroblasts are also sensitive to interstitial flow and in enhanced flow environments can become myofibroblasts and align their ECM (325–327). When human melanoma cells were cocultured with dermal fibroblasts in three-dimensional cultures under flow, tumor cell invasion was markedly compared with that without flow or without fibroblasts; however, in the absence of flow, the fibroblasts did not affect tumor cell migration (425). It was found that while interstitial flow increased TGF-β1 levels by fibroblast upregulation and enhanced liberation from latent stores in the matrix, as described above (325), the fibroblasts migrated up the flow-induced gradients of TGF-β in the flow direction, remodeling the ECM along the way, facilitating tumor cells to follow them. This was consistent with other reports of fibroblast-led tumor cell invasion in live imaging studies of the tumor microenvironment (144, 243), but showed for the first time how interstitial flow might influence such behaviors. Such a mechanism may also synergize (or compete) with other proposed mechanisms of interstitial flow-enhanced migration via MMP upregulation (423, 424) or ECM stress-mediated effects (367).

Finally, the fact that interstitial flow can drive ECM alignment and stiffening, as described above in section VIII*B*, may also have implications in tumor cell invasion and metastasis. This is because interstitial flow-induced ECM alignment and myofibroblast formation are associated with matrix stiffening, and stromal stiffening can promote tumor initiation, progression, and invasion, at least in breast can-

cer (356, 371, 390, 529). For example, increased mammary tissue density correlates with poor prognosis of patients with breast cancer, and collagen alignment in the stroma of breast tumors negatively correlates with survival (92). Expression levels of the collagen cross-linking enzyme lysyl oxidase, which stiffens the tumor stroma, are correlated with tumor cell invasion both in experimental mice as well as in human biopsies (263). Fibroblasts and tumor cells can also migrate along bundled collagen fibers radiating outward from the tumor (140, 370). Thus ECM stiffening in the tumor stroma is associated with tumor invasion, and since interstitial flow drives stiffening via the upregulation of TGF-β expression and myofibroblast differentiation, interstitial flow may promote tumor cell invasion via indirect actions on fibroblasts that tumor cells follow.

IX. INTERSTITIAL AND LYMPH FLOW IN IMMUNITY

A. Immunological Roles of Lymphangiogenesis

In addition to cancer, lymphangiogenesis occurs in chronic inflammation and in lymph nodes draining the inflamed regions (175, 207, 483, 522, 526). Currently, very little is known about how inflammatory lymphangiogenesis affects immunity, and the literature is puzzling. In cancer, we know that cancer progression is positively correlated with both lymphangiogenesis and immune suppression and tolerance (274). In mouse models of acute inflammation, lymphangiogenesis was important in resolving the inflammation, as discussed in section VIII*D1* (207). On the other hand, lymphangiogenesis is also frequently seen in autoimmunity-related chronic inflammatory disorders (483, 522) and in transplant rejection (241), suggesting that lymphangiogenesis may somehow contribute to immune rejection. Blocking lymphangiogenesis before experimental corneal or islet transplantation was found to decrease graft rejection (271, 526), but 1-yr follow-ups of renal transplant patients found a positive correlation between transplant function and lymphangiogenesis (442). Such apparently contradictory findings raise questions of how inflammatory lymphangiogenesis affects immune response in different types of inflammation.

The inflammatory context may be critically important in considering the roles of lymphangiogenesis in inflammation. In particular, the stromal changes, cytokines, and cells present differ in acute versus chronic inflammation or in cancer. Lymph node lymphangiogenesis, at least in acute inflammation, is driven by B cells (16, 430) and inhibited by cytotoxic T cells and their cytolytic cytokines like IFN-γ (235). Tertiary lymphoid structures that may arise during inflammation are rich in B cells and produce autoantibodies, such as those seen in renal interstitial injury (188). It is unclear whether lymphatic drainage in such cases goes to the tertiary lymphoid structures or the lymph node (465).

In the tumor microenvironment, lymphangiogenesis has been correlated with metastasis, but not necessarily B-cell recruitment. VEGF-C can recruit VEGFR-3$^+$ tumor-associated macrophages (433), which are tumor-promoting (109) and which secrete VEGF-C when stimulated by tumor-derived factors like TNF-α (417). Lymphangiogenic tumors have increased lymph flow to the draining lymph node (182, 369, 396, 397), which would increase the transport of tumor antigens to lymph node lymphatic endothelial cells that can dampen dendritic cell maturation (366) and may suppress tumor antigen-specific T cells (90, 274). Thus, while the immunological implications of lymphangiogenesis are unclear in acute and chronic inflammatory conditions, tumor lymphangiogenesis appears to be correlated with immunological tolerance.

B. Possible Roles of Interstitial and Lymph Flow in Immunity

Proteins, proteases, ECM fragments, processed peptides, and cytokines are among the soluble factors that are communicated from the periphery to the local draining lymph node by lymph flow. These may be sampled by lymph node-resident DCs as well as blood or lymphatic endothelial cells, which in turn can affect the immunological outcome (38, 211, 253). While DCs activated in the periphery have time during transit to the lymph node to upregulate costimulatory molecules and cytokines before activating T cells, lymph node-resident DCs interact with T cells on a shorter timescale relative to antigen uptake and in the presence of a different cytokine milieu, leading to a different quality of T-cell activation (211).

It is likely that the lymph node-resident DCs play essential roles in maintaining peripheral tolerance, since they constantly sample lymph-borne antigens as well as constitutively expressing endogenous autoantigens (413). Early studies comparing response to dermal contact hypersensitivity in transplanted skin with or without lymphatic connection to the skin-draining lymph nodes suggested that lymphatic flow may be required for immunological tolerance (141). In the tumor-draining lymph node, resident DCs are more tolerogenic (306). Therefore, lymph flow regulation may help to control the balance between immunity and tolerance in the lymph node.

C. Lymph Flow Through the Lymph Node

Several afferent lymphatic vessels drain towards a single lymph node, but only a single efferent lymphatic vessel drains away. Lymph flows mostly around the lymph node in the subcapsular sinus, but also through the regions of the

lymph node, carrying different sized particles to different regions and in turn helping to regulate appropriate immune responses to different types of stimuli (225, 253, 392, 432) (see also section V*D*). Subcapsular macrophages line the subcapsular sinus and phagocytose large particles, pathogens, and molecular aggregates and can present these to B cells (225, 253, 392). Lymph is also directed from the sinus into the cortex by narrow conduits (200 nm to 3 μm), lined by fibroblastic reticular cells, that regulate the flow of unopsonized small molecules (<70 kDa) to the T-cell zone (159, 253, 392, 393). Therefore, flow pathways within the lymph node help to direct different types of molecules to different regions, which in turn affect immunity. Given the renewed interest in active transport mechanisms of fluid and soluble antigen by local lymphatic vessels (114, 298), future studies will hopefully elucidate how such flow pathways might be altered under conditions of inflammation. Such detailed studies will be important for revealing the likely critical roles of lymph flow, and the mechanisms of lymph flow regulation, on fine-tuning immune responses to peripheral inflammation.

X. SUMMARY AND FUTURE PERSPECTIVES

In this review, we attempted to illustrate how the biochemical, biomechanical, and biological functions of IF and its regulation can affect cell function in physiology, pathology, and immunity. When addressing the formation of IF and lymph we found it useful first to describe the molecular structure and biophysical aspects of the interstitium and lymphatics to place the topic in a framework, well aware that these are large and important fields in their own right, and that including the tumor interstitium makes limitation of this part even more challenging. Our focus has been on the interstitial structure from a functional perspective, inasmuch as affecting IF formation and transport, and the major structural components collagen and GAGs both have such effects. Moreover, the tumor interstitium in general contains increased amounts of both collagen and GAGs, which in turn influences fluid exchange and substance uptake in such tissues. The various components of the interstitium, notably the GAGs, carry charges that can affect the IF composition and exchange, and recent data suggest that GAGs provide an actively regulated interstitial cation exchange function contributing in fluid volume and blood pressure regulation. The major structural molecules also restrict the space available to macromolecules due to their inherent size and charge, resulting in an excluded volume effect of importance for plasma volume regulation. During the last years it has been shown that excluded volume has a strong inverse relation to hydration, and that the relative importance of charge effects on excluded volume is significant, amounting to ~40% in skin. Recent data also indicate that there is a significant charge effect on distribution volume of macromolecular substances in tumors that may be exploited to enhance the uptake of therapeutic agents by targeting either the GAGs or the net charge of the substances to be delivered.

The mechanical properties of the interstitium and the stresses imposed by fluid pressure gradients (which drive interstitial flow and lymph formation and which can be dramatically altered in inflammation and cancer) have critically important consequences for a variety of cell functions. Pathological changes in these properties often drive tissue remodeling, cell migration, stem cell differentiation, and malignant transformation. One of these, the P_{if} of different tissue compartments, relates V_i with transendothelial, interstitial, and lymph flow, thereby also affecting the delivery of drugs to the interstitium and antigens and cytokines to the lymph node. P_{if} also relates tissue hydration with interstitial compliance (C_i) determining the hydrostatic counterpressure to a given V_i. Recent advances include elucidating the importance of structural components, most notably hyaluronan, as determinants of tissue compliance, and demonstrating that stress relaxation may contribute to a high C_i in long-standing edema. Another interstitial mechanical property, hydraulic conductivity, determines IF flow for given pressure gradients, and recent evidence has accumulated for its importance in matrix remodeling, cell migration, and morphogenetic processes as well as in regulating immune responses. This new area of research was facilitated by novel in vitro systems allowing slow interstitial flow through three-dimensional cultures of cells, and the strongly nonlinear behavior of hydraulic conductivity during tissue swelling and compaction has recently been quantified in vivo.

Whereas exchange and formation of IF is determined by structural properties of the capillary wall, transcapillary pressure differences, and protein concentrations, we have mainly focused on the importance of interstitial tissue factors for filtration. Several recent studies have questioned the importance of the colloid osmotic pressure exerted by interstitial proteins, COP_{if}, in the general (global) interstitial fluid, but a closer examination of these data suggest that although this may be the case for high filtration states, COP_{if} is a major determinant of normal fluid filtration. During the last two decades, it has become increasingly clear that P_{if} plays an active role in edema formation in inflammation and in tumor fluid exchange and biology. Tissue injury and inflammation induce a strongly negative P_{if} that is a major factor responsible for acute edema formation, an effect that is mediated via the collagen-binding integrins $\alpha_2\beta_1$ and $\alpha_{11}\beta_1$, and attenuated by PDGF-BB. In tumors, it is now well established that P_{if} is high compared with normal tissues, and widely held that this compromises the delivery of therapeutic agents across the vasculature. After re-evaluation of the available data, however, we conclude that P_{if} may not be such a significant barrier to therapy as has been proposed, and that other vascular factors are important in determining tumor drug uptake.

Lymph formation is facilitated by small, cyclically variable hydraulic pressure gradients between the interstitium and initial lymphatics, as well as by vesicular transport, although the importance of active transport mechanisms in lymph formation has yet to be elucidated. Aiding this process is a functional one-way valve system that has been suggested by structural as well as functional studies. Lymph composition is modified in the draining lymph node, due to selective size-dependent filtration through different compartments and into the blood via high endothelial venules, and whether there is modification also in collecting lymphatics is currently debated. Having reviewed available data it seems that, with the possible exception of the mesentery, that prenodal lymph is not modified during its passage to the lymph node and may be considered as representative of IF.

IF may not be readily accessible, and we discuss established methods for fluid isolation in normal tissue and solid tumors, and their strengths and weaknesses. An important question is whether the experimental situation requires sampling of native or derived IF. By analysis of native IF and lymph, in experimental animals as well as humans, it has been possible to assess the quantitative importance of local production of mediators and thus knowledge on the mechanisms involved at the tissue level. These studies show that there can be dramatic gradients from tissue to plasma. When compared with plasma and subcutaneous IF, tumor IF has high H^+, CO_2, and lactic acid, and low glucose and O_2. Moreover, tumor IF has a high protein concentration and COP_{if}, as determined in experimental as well as human tumors, and is representative for the fluid part of the tissue microenvironment.

In the overall regulation of V_i, COP_{if} and P_{if} will adapt to maintain a stable V_i in such a way that an increase in filtration will increase P_{if} (hydrostatic buffering) and reduce COP_{if} (colloid osmotic or oncotic buffering) that together with an increased lymph flow will act as "safety factors against edema formation" and contribute to "autoregulation" of V_i. The effect of an increase in P_{if} may be modest if edema develops slowly, but may be significant in rapidly generated edemas or in enclosed organs. A reduction in COP_{if} by washout/dilution of interstitial proteins will contribute in edema prevention, but the relative importance of this mechanism depends strongly on the organ. The effect of lymphatic buffering, i.e., increased lymph flow, is also variable but especially important in preventing edema due to orthostasis.

The biological effects of interstitial flow have begun to be explored in the last decade. The mechanical stresses imposed are complex and heterogeneous and depend on the specific architecture of the ECM and the organization of the interstitium. In vitro data suggest that chronically increased interstitial flow may contribute to ECM stiffening and alignment as well as myofibroblast differentiation. Another important effect of interstitial flow on cells is that it may bias local extracellular distribution of secreted molecules like proteases, cytokines, and growth factors, thus skewing gradients and affecting direction of cell behaviors. It may additionally drive morphogenesis of lymphatic and blood capillaries, as well as affecting the lymph node implying a key role in modulating immunity in secondary lymphoid organs. In tumors, interstitial flow may have important implications for tumor invasion and metastasis, since it drives stroma stiffening associated with tumor invasion via upregulation of TGF-β expression and myofibroblast differentiation.

It has also become increasingly clear that interstitial flow and lymph flow influence immunity and peripheral tolerance. It appears that there are positive-feedback loops in the tumor stroma between lymphangiogenesis, interstitial fluid flow, and the upregulation of TGF-β, which is important for promoting T-cell tolerance in the tumor stroma. Lymph flowing to the tumor draining lymph nodes induces modifications that make the node a key component of the tumor microenvironment, also inducing immune tolerance and providing a permissive environment of metastatic growth. Within the tumor itself, interstitial flow may promote lymphoid-like features to develop in the stroma, which may mimic the lymph node T-cell zone that is critical for attracting, recruiting, and educating T cells in the tumor microenvironment, being another example of the many and diverse biological effects of interstitial fluid flow.

ACKNOWLEDGMENTS

Address for reprint requests and other correspondence: H. Wiig, Dept. of Biomedicine, Jonas Lies vei 91, N-5009 Bergen, Norway (e-mail: helge.wiig@biomed.uib.no).

GRANTS

Financial support from The Research Council of Norway and Locus on Cardiovascular Research, University of Bergen, Swiss National Science Foundation (135756), and the European Research Council (206653-2) is gratefully acknowledged.

DISCLOSURES

No conflicts of interest, financial or otherwise, are declared by the authors.

REFERENCES

1. Aarli V, Aukland K. Oedema-preventing mechanisms in a low-compliant tissue: studies on the rat tail. *Acta Physiol Scand* 141: 489–495, 1991.

2. Aarli V, Reed RK, Aukland K. Effect of longstanding venous stasis and hypoproteinaemia on lymph flow in the rat tail. *Acta Physiol Scand* 142: 1–9, 1991.

3. Adair TH. Studies of lymph modification by lymph nodes. *Microcirc Endothelium Lymphatics* 2: 251–269, 1985.

4. Adair TH, Guyton AC. Measurement of subcutaneous tissue fluid pressure using a skin-cup method. *J Appl Physiol* 58: 1528–1535, 1985.

5. Adair TH, Guyton AC. Modification of lymph by lymph nodes. II. Effect of increased lymph node venous blood pressure. *Am J Physiol Heart Circ Physiol* 245: H616–H622, 1983.

6. Adair TH, Guyton AC. Modification of lymph by lymph nodes. III. Effect of increased lymph hydrostatic pressure. *Am J Physiol Heart Circ Physiol* 249: H777–H782, 1985.

7. Adair TH, Moffatt DS, Paulsen AW, Guyton AC. Quantitation of changes in lymph protein concentration during lymph node transit. *Am J Physiol Heart Circ Physiol* 243: H351–H359, 1982.

8. Adamson RH, Lenz JF, Zhang X, Adamson GN, Weinbaum S, Curry FE. Oncotic pressures opposing filtration across non-fenestrated rat microvessels. *J Physiol* 557: 889–907, 2004.

9. Adamson RH, Michel CC. Pathways through the intercellular clefts of frog mesenteric capillaries. *J Physiol* 466: 303–327, 1993.

10. Ahamed J, Burg N, Yoshinaga K, Janczak CA, Rifkin DB, Coller BS. In vitro and in vivo evidence for shear-induced activation of latent transforming growth factor-beta1. *Blood* 112: 3650–3660, 2008.

11. Alitalo K. The lymphatic vasculature in disease. *Nat Med* 17: 1371–1380, 2011.

12. Alitalo K, Tammela T, Petrova TV. Lymphangiogenesis in development and human disease. *Nature* 438: 946–953, 2005.

13. Allen SJ, Gunnar Sedin E, Jonzon A, Wells AF, Laurent TC. Lung hyaluronan during development: a quantitative and morphological study. *Am J Physiol Heart Circ Physiol* 260: H1449–H1454, 1991.

14. Ameye L, Young MF. Mice deficient in small leucine-rich proteoglycans: novel in vivo models for osteoporosis, osteoarthritis, Ehlers-Danlos syndrome, muscular dystrophy, and corneal diseases. *Glycobiology* 12: 107R–116R, 2002.

15. Anand S, Wu JH, Diamond SL. Enzyme-mediated proteolysis of fibrous biopolymers: dissolution front movement in fibrin or collagen under conditions of diffusive or convective transport. *Biotechnol Bioeng* 48: 89–107, 1995.

16. Angeli V, Ginhoux F, Llodra J, Quemeneur L, Frenette PS, Skobe M, Jessberger R, Merad M, Randolph GJ. B cell-driven lymphangiogenesis in inflamed lymph nodes enhances dendritic cell mobilization. *Immunity* 24: 203–215, 2006.

17. Ao X, Sellati TJ, Stenken JA. Enhanced microdialysis relative recovery of inflammatory cytokines using antibody-coated microspheres analyzed by flow cytometry. *Anal Chem* 76: 3777–3784, 2004.

18. Ao X, Stenken JA. Microdialysis sampling of cytokines. *Methods* 38: 331–341, 2006.

19. Aszodi A, Legate KR, Nakchbandi I, Fassler R. What mouse mutants teach us about extracellular matrix function. *Annu Rev Cell Dev Biol* 22: 591–621, 2006.

20. Aukland K. Distribution volumes and macromolecular mobility in rat tail tendon interstitium. *Am J Physiol Heart Circ Physiol* 260: H409–H419, 1991.

21. Aukland K, Fadnes HO. Protein concentration of interstitial fluid collected from rat skin by a wick method. *Acta Physiol Scand* 88: 350–358, 1973.

22. Aukland K, Johnsen HM. Protein concentration and colloid osmotic pressure of rat skeletal muscle interstitial fluid. *Acta Physiol Scand* 91: 354–364, 1974.

23. Aukland K, Kramer GC, Renkin EM. Protein concentration of lymph and interstitial fluid in the rat tail. *Am J Physiol Heart Circ Physiol* 247: H74–H79, 1984.

24. Aukland K, Nicolaysen G. Interstitial fluid volume: local regulatory mechanisms. *Physiol Rev* 61: 556–643, 1981.

25. Aukland K, Reed RK. Interstitial-lymphatic mechanisms in the control of extracellular fluid volume. *Physiol Rev* 73: 1–78, 1993.

26. Aukland K, Tenstad O, Wiig H. Distribution spaces for hyaluronan and albumin in rat tail tendons. *Am J Physiol Heart Circ Physiol* 281: H1589–H1597, 2001.

27. Aukland K, Wiig H. Hemodynamics and interstitial fluid pressure in the rat tail. *Am J Physiol Heart Circ Physiol* 247: H80–H87, 1984.

28. Aukland K, Wiig H, Tenstad O, Renkin EM. Interstitial exclusion of macromolecules studied by graded centrifugation of rat tail tendon. *Am J Physiol Heart Circ Physiol* 273: H2794–H2803, 1997.

29. Azzali G. Structure, lymphatic vascularization and lymphocyte migration in mucosa-associated lymphoid tissue. *Immunol Rev* 195: 178–189, 2003.

30. Azzali G. Transendothelial transport and migration in vessels of the apparatus lymphaticus perihericus absorbens (ALPA). *Int Rev Cytol* 230: 41–87, 2003.

31. Azzali G. The ultrastructural basis of lipid transport in the absorbing lymphatic vessel. *J Submicrosc Cytol* 14: 45–54, 1982.

32. Baluk P, Fuxe J, Hashizume H, Romano T, Lashnits E, Butz S, Vestweber D, Corada M, Molendini C, Dejana E, McDonald DM. Functionally specialized junctions between endothelial cells of lymphatic vessels. *J Exp Med* 204: 2349–2362, 2007.

33. Baluk P, Morikawa S, Haskell A, Mancuso M, McDonald DM. Abnormalities of basement membrane on blood vessels and endothelial sprouts in tumors. *Am J Pathol* 163: 1801–1815, 2003.

34. Baluk P, Tammela T, Ator E, Lyubynska N, Achen MG, Hicklin DJ, Jeltsch M, Petrova TV, Pytowski B, Stacker SA, Yla-Herttuala S, Jackson DG, Alitalo K, McDonald DM. Pathogenesis of persistent lymphatic vessel hyperplasia in chronic airway inflammation. *J Clin Invest* 115: 247–257, 2005.

35. Bates DO, Hillman NJ, Williams B, Neal CR, Pocock TM. Regulation of microvascular permeability by vascular endothelial growth factors. *J Anat* 200: 581–597, 2002.

36. Bates DO, Levick JR, Mortimer PS. Starling pressures in the human arm and their alteration in postmastectomy oedema. *J Physiol* 477: 355–363, 1994.

37. Bates DO, Levick JR, Mortimer PS. Subcutaneous interstitial fluid pressure and arm volume in lymphoedema. *Int J Microcirc Clin Exp* 11: 359–373, 1992.

38. Batista FD, Harwood NE. The who, how and where of antigen presentation to B cells. *Nat Rev Immunol* 9: 15–27, 2009.

39. Bazigou E, Xie S, Chen C, Weston A, Miura N, Sorokin L, Adams R, Muro AF, Sheppard D, Makinen T. Integrin-alpha9 is required for fibronectin matrix assembly during lymphatic valve morphogenesis. *Dev Cell* 17: 175–186, 2009.

40. Becker BF, Chappell D, Jacob M. Endothelial glycocalyx and coronary vascular permeability: the fringe benefit. *Basic Res Cardiol* 105: 687–701, 2010.

41. Bell DR, Mullins RJ. Effects of increased venous pressure on albumin- and IgG-excluded volumes in muscle. *Am J Physiol Heart Circ Physiol* 242: H1044–H1049, 1982.

42. Bell DR, Mullins RJ. Effects of increased venous pressure on albumin- and IgG-excluded volumes in skin. *Am J Physiol Heart Circ Physiol* 242: H1038–H1043, 1982.

43. Bendrik C, Dabrosin C. Estradiol increases IL-8 secretion of normal human breast tissue and breast cancer in vivo. *J Immunol* 182: 371–378, 2009.

44. Benjamin RK, Hochberg FH, Fox E, Bungay PM, Elmquist WF, Stewart CF, Gallo JM, Collins JM, Pelletier RP, de Groot JF, Hickner RC, Cavus I, Grossman SA, Colvin OM. Review of microdialysis in brain tumors, from concept to application: first annual Carolyn Frye-Halloran symposium. *Neuro Oncol* 6: 65–74, 2004.

45. Benoit JN, Zawieja DC. Gastrointestinal lymphatics. In: *Physiology of the Gastrointestinal Tract*, edited by Johnson LR. New York: Raven, 1994, p. 1669–1692.

46. Berg A, Aas P, Gustafsson T, Reed RK. Effect of alpha-trinositol on interstitial fluid pressure, oedema generation and albumin extravasation in experimental frostbite in the rat. *Br J Pharmacol* 126: 1367–1374, 1999.

47. Berggreen E, Wiig H. Lowering of interstitial fluid pressure in rat submandibular gland: a novel mechanism in saliva secretion. *Am J Physiol Heart Circ Physiol* 290: H1460–H1468, 2006.

48. Bert J, Reed RK. Hyaluronan, hydration and flow conductivity of rat dermis. *Biorheology* 35: 211–219, 1998.

49. Bert JL, Mathieson JM, Pearce RH. The exclusion of human serum albumin by human dermal collagenous fibres and within human dermis. *Biochem J* 201: 395–403, 1982.

50. Bert JL, Pearce RH. The interstitium and microvascular exchange. In: *Handbook of Physiology. The Cardiovascular System. Microcirculation*. Bethesda, MD: Am. Physiol. Soc., 1984, sect. 2, vol. IV, pt. 1, chapt. 12, p. 521–547.

51. Bert JL, Pearce RH, Mathieson JM. Concentration of plasma albumin in its accessible space in postmortem human dermis. *Microvasc Res* 32: 211–223, 1986.

52. Bert JL, Reed RK. Flow conductivity of rat dermis is determined by hydration. *Biorheology* 32: 17–27, 1995.

53. Bert JL, Reed RK. Pressure-volume relationship for rat dermis: compression studies. *Acta Physiol Scand* 160: 89–94, 1997.

54. Blackhall FH, Merry CL, Davies EJ, Jayson GC. Heparan sulfate proteoglycans and cancer. *Br J Cancer* 85: 1094–1098, 2001.

55. Bletsa A, Berggreen E, Fristad I, Tenstad O, Wiig H. Cytokine signalling in rat pulp interstitial fluid and transcapillary fluid exchange during lipopolysaccharide-induced acute inflammation. *J Physiol* 573: 225–236, 2006.

56. Bletsa A, Fristad I, Berggreen E. Sensory pulpal nerve fibres and trigeminal ganglion neurons express IL-1RI: a potential mechanism for development of inflammatory hyperalgesia. *Int Endod J* 42: 978–986, 2009.

57. Bletsa A, Nedrebo T, Heyeraas KJ, Berggreen E. Edema in oral mucosa after LPS or cytokine exposure. *J Dent Res* 85: 442–446, 2006.

58. Boardman KC, Swartz MA. Interstitial flow as a guide for lymphangiogenesis. *Circ Res* 92: 801–808, 2003.

59. Bockris JOM, Reddy AKN. Ion-ion interactions. In: *Modern Electrochemistry 1, Ionics*, edited by Bockris JOM, Reddy AKN. New York: Plenum, 1998, p. 225–347.

60. Bohlen HG, Wang W, Gashev A, Gasheva O, Zawieja D. Phasic contractions of rat mesenteric lymphatics increase basal and phasic nitric oxide generation in vivo. *Am J Physiol Heart Circ Physiol* 297: H1319–H1328, 2009.

61. Borge BA, Kalland KH, Olsen S, Bletsa A, Berggreen E, Wiig H. Cytokines are produced locally by myocytes in rat skeletal muscle during endotoxemia. *Am J Physiol Heart Circ Physiol* 296: H735–H744, 2009.

62. Boschi G, Scherrmann J. Microdialysis in mice for drug delivery research. *Adv Drug Deliv Rev* 45: 271–281, 2000.

63. Boucher Y, Baxter LT, Jain RK. Interstitial pressure gradients in tissue-isolated and subcutaneous tumors: implications for therapy. *Cancer Res* 50: 4478–4484, 1990.

64. Boucher Y, Brekken C, Netti PA, Baxter LT, Jain RK. Intratumoral infusion of fluid: estimation of hydraulic conductivity and implications for the delivery of therapeutic agents. *Br J Cancer* 78: 1442–1448, 1998.

65. Boucher Y, Jain RK. Microvascular pressure is the principal driving force for interstitial hypertension in solid tumors: implications for vascular collapse. *Cancer Res* 52: 5110–5114, 1992.

66. Brace RA, Guyton AC. Interstitial fluid pressure: capsule, free fluid, gel fluid, and gel absorption pressure in subcutaneous tissue. *Microvasc Res* 18: 217–228, 1979.

67. Brand CU, Hunziker T, Braathen LR. Isolation of human skin-derived lymph: flow and output of cells following sodium lauryl sulphate-induced contact dermatitis. *Arch Dermatol Res* 284: 123–126, 1992.

68. Brekke HK, Oveland E, Kolmannskog O, Hammersborg SM, Wiig H, Husby P, Tenstad O, Nedrebo T. Isolation of interstitial fluid in skin during volume expansion: evaluation of a method in pigs. *Am J Physiol Heart Circ Physiol* 299: H1546–H1553, 2010.

69. Breslin JW, Yuan SY, Wu MH. VEGF-C alters barrier function of cultured lymphatic endothelial cells through a VEGFR-3-dependent mechanism. *Lymphat Res Biol* 5: 105–113, 2007.

70. Brinkman HC. A calculation of the viscous force exerted by a flowing fluid on a dense swarm of particles. *Appl Sci Res* A1: 27–34, 1947.

71. Brown LF, Guidi AJ, Schnitt SJ, Van De Water L, Iruela-Arispe ML, Yeo TK, Tognazzi K, Dvorak HF. Vascular stroma formation in carcinoma in situ, invasive carcinoma, and metastatic carcinoma of the breast. *Clin Cancer Res* 5: 1041–1056, 1999.

72. Brunner M, Muller M. Microdialysis: an in vivo approach for measuring drug delivery in oncology. *Eur J Clin Pharmacol* 58: 227–234, 2002.

73. Burch GE, Sodeman WA. The estimation of the subcutaneous tissue pressure by a direct method. *J Clin Invest* 16: 845–850, 1937.

74. Butcher DT, Alliston T, Weaver VM. A tense situation: forcing tumour progression. *Nat Rev Cancer* 9: 108–122, 2009.

75. Butler TP, Grantham FH, Gullino PM. Bulk transfer of fluid in interstitial compartment of mammary tumors. *Cancer Res* 35: 3084–3088, 1975.

76. Canty EG, Kadler KE. Procollagen trafficking, processing and fibrillogenesis. *J Cell Sci* 118: 1341–1353, 2005.

77. Casley-Smith JR. Lymph and lymphatics. In: *Microcirculation*, edited by Kaley G, Altura BM. Baltimore, MD: University Park Press, 1977, p. 423–502.

78. Casley-Smith JR. "Prelymphatic': a question of terminology? *Experientia* 38: 1123–1124, 1982.

79. Casley-Smith JR. A theoretical support for the transport of macromolecules by osmotic flow across a leaky membrane against a concentration gradient. *Microvasc Res* 9: 43–48, 1975.

80. Celis JE, Gromov P, Cabezon T, Moreira JM, Ambartsumian N, Sandelin K, Rank F, Gromova I. Proteomic characterization of the interstitial fluid perfusing the breast tumor microenvironment: a novel resource for biomarker and therapeutic target discovery. *Mol Cell Proteomics* 3: 327–344, 2004.

81. Celis JE, Moreira JM, Cabezon T, Gromov P, Friis E, Rank F, Gromova I. Identification of extracellular and intracellular signaling components of the mammary adipose tissue and its interstitial fluid in high risk breast cancer patients: toward dissecting the molecular circuitry of epithelial-adipocyte stromal cell interactions. *Mol Cell Proteomics* 4: 492–522, 2005.

82. Chapple C, Bowen BD, Reed RK, Xie SL, Bert JL. A model of human microvascular exchange: parameter estimation based on normals and nephrotics. *Comput Methods Programs Biomed* 41: 33–54, 1993.

83. Chary SR, Jain RK. Direct measurement of interstitial convection and diffusion of albumin in normal and neoplastic tissues by fluorescence photobleaching. *Proc Natl Acad Sci USA* 86: 5385–5389, 1989.

84. Chefer VI, Thompson AC, Zapata A, Shippenberg TS. Overview of brain microdialysis. *Curr Protoc Neurosci* 7: 1, 2009.

85. Choi J, Credit K, Henderson K, Deverkadra R, He Z, Wiig H, Vanpelt H, Flessner MF. Intraperitoneal immunotherapy for metastatic ovarian carcinoma: resistance of intratumoral collagen to antibody penetration. *Clin Cancer Res* 12: 1906–1912, 2006.

86. Chu J, Gallo JM. Application of microdialysis to characterize drug disposition in tumors. *Adv Drug Deliv Rev* 45: 243–253, 2000.

87. Clausen TS, Kaastrup P, Stallknecht B. Proinflammatory tissue response and recovery of adipokines during 4 days of subcutaneous large-pore microdialysis. *J Pharmacol Toxicol Methods* 60: 281–287, 2009.

88. Clough GF. Microdialysis of large molecules. *AAPS J* 7: E686–692, 2005.

89. Clough GF, Jackson CL, Lee JJ, Jamal SC, Church MK. What can microdialysis tell us about the temporal and spatial generation of cytokines in allergen-induced responses in human skin in vivo? *J Invest Dermatol* 127: 2799–2806, 2007.

90. Cohen JN, Guidi CJ, Tewalt EF, Qiao H, Rouhani SJ, Ruddell A, Farr AG, Tung KS, Engelhard VH. Lymph node-resident lymphatic endothelial cells mediate peripheral tolerance via Aire-independent direct antigen presentation. *J Exp Med* 207: 681–688, 2010.

91. Comper WD, Laurent TC. Physiological function of connective tissue polysaccharides. *Physiol Rev* 58: 255–315, 1978.

92. Conklin MW, Eickhoff JC, Riching KM, Pehlke CA, Eliceiri KW, Provenzano PP, Friedl A, Keely PJ. Aligned collagen is a prognostic signature for survival in human breast carcinoma. *Am J Pathol* 178: 1221–1232, 2011.

93. Coussens LM, Werb Z. Inflammation and cancer. *Nature* 420: 860–867, 2002.

94. Crockett DJ. The protein levels of oedema fluids. *Lancet* 271: 1179–1182, 1956.

95. Curry FE, Michel CC. A fiber matrix model of capillary permeability. *Microvasc Res* 20: 96–99, 1980.

96. Curry FR. Microvascular solute and water transport. *Microcirculation* 12: 17–31, 2005.

97. D'Arcy H, Bazin H. *Recherches hydrauliques, Enterprises par M.H. D'Arcy*. Paris: Imprimerie Nationale, 1865.

98. Dabrosin C. Microdialysis: an in vivo technique for studies of growth factors in breast cancer. *Front Biosci* 10: 1329–1335, 2005.

99. Dabrosin C. Positive correlation between estradiol and vascular endothelial growth factor but not fibroblast growth factor-2 in normal human breast tissue in vivo. *Clin Cancer Res* 11: 8036–8041, 2005.

100. Dabrosin C, Margetts PJ, Gauldie J. Estradiol increases extracellular levels of vascular endothelial growth factor in vivo in murine mammary cancer. *Int J Cancer* 107: 535–540, 2003.

101. Daffonchio L, Novellini R, Bertuglia S. Protective effect of ketoprofen lysine salt on interleukin-1beta and bradykinin induced inflammatory changes in hamster cheek pouch microcirculation. *Inflamm Res* 51: 223–228, 2002.

102. Dafni H, Cohen B, Ziv K, Israely T, Goldshmidt O, Nevo N, Harmelin A, Vlodavsky I, Neeman M. The role of heparanase in lymph node metastatic dissemination: dynamic contrast-enhanced MRI of Eb lymphoma in mice. *Neoplasia* 7: 224–233, 2005.

103. Dafni H, Israely T, Bhujwalla ZM, Benjamin LE, Neeman M. Overexpression of vascular endothelial growth factor 165 drives peritumor interstitial convection and induces lymphatic drain: magnetic resonance imaging, confocal microscopy, and histological tracking of triple-labeled albumin. *Cancer Res* 62: 6731–6739, 2002.

104. Davies Cde L, Berk DA, Pluen A, Jain RK. Comparison of IgG diffusion and extracellular matrix composition in rhabdomyosarcomas grown in mice versus in vitro as spheroids reveals the role of host stromal cells. *Br J Cancer* 86: 1639–1644, 2002.

105. Davies Cde L, Engesaeter BB, Haug I, Ormberg IW, Halgunset J, Brekken C. Uptake of IgG in osteosarcoma correlates inversely with interstitial fluid pressure, but not with interstitial constituents. *Br J Cancer* 85: 1968–1977, 2001.

106. Davis MJ, Rahbar E, Gashev AA, Zawieja DC, Moore JE Jr. Determinants of valve gating in collecting lymphatic vessels from rat mesentery. *Am J Physiol Heart Circ Physiol* 301: H48–H60, 2011.

107. De Wever O, Westbroek W, Verloes A, Bloemen N, Bracke M, Gespach C, Bruyneel E, Mareel M. Critical role of N-cadherin in myofibroblast invasion and migration in vitro stimulated by colon-cancer-cell-derived TGF-beta or wounding. *J Cell Sci* 117: 4691–4703, 2004.

108. Dearman RJ, Bhushan M, Cumberbatch M, Kimber I, Griffiths CE. Measurement of cytokine expression and Langerhans cell migration in human skin following suction blister formation. *Exp Dermatol* 13: 452–460, 2004.

109. DeNardo D, Andreu P, Coussens LM. Interactions between lymphocytes and myeloid cells regulate pro- versus anti-tumor immunity. *Cancer Metastasis Rev* 29: 309–316, 2010.

110. Desgrosellier JS, Cheresh DA. Integrins in cancer: biological implications and therapeutic opportunities. *Nat Rev Cancer* 10: 9–22, 2010.

111. Diamond SL. Engineering design of optimal strategies for blood clot dissolution. *Annu Rev Biomed Eng* 1: 427–462, 1999.

112. Dixon JB. Lymphatic lipid transport: sewer or subway? *Trends Endocrinol Metab* 21: 480–487, 2010.

113. Dixon JB, Greiner ST, Gashev AA, Cote GL, Moore JE, Zawieja DC. Lymph flow, shear stress, and lymphocyte velocity in rat mesenteric prenodal lymphatics. *Microcirculation* 13: 597–610, 2006.

114. Dixon JB, Raghunathan S, Swartz MA. A tissue-engineered model of the intestinal lacteal for evaluating lipid transport by lymphatics. *Biotechnol Bioeng* 2009.

115. Dobbins WO, Rollins EL. Intestinal mucosal lymphatic permeability: an electron microscopic study of endothelial vesicles and cell junctions. *J Ultrastruct Res* 33: 29–59, 1970.

116. Dougherty PJ, Davis MJ, Zawieja DC, Muthuchamy M. Calcium sensitivity and cooperativity of permeabilized rat mesenteric lymphatics. *Am J Physiol Regul Integr Comp Physiol* 294: R1524–R1532, 2008.

117. Drinker CK, Field ME, Homans J. The experimental production of edema and elephantiasis as a result of lymphatic obstruction. *Am J Physiol* 108: 509–520, 1934.

118. Duo J, Stenken JA. In vitro and in vivo affinity microdialysis sampling of cytokines using heparin-immobilized microspheres. *Anal Bioanal Chem* 399: 783–793, 2011.

119. Dvorak HF. Vascular permeability factor/vascular endothelial growth factor: a critical cytokine in tumor angiogenesis and a potential target for diagnosis and therapy. *J Clin Oncol* 20: 4368–4380, 2002.

120. Dvorak HF, Brown LF, Detmar M, Dvorak AM. Vascular permeability factor/vascular endothelial growth factor, microvascular hyperpermeability, and angiogenesis. *Am J Pathol* 146: 1029–1039, 1995.

121. Dvorak HF, Sioussat TM, Brown LF, Berse B, Nagy JA, Sotrel A, Manseau EJ, Van de Water L, Senger DR. Distribution of vascular permeability factor (vascular endothelial growth factor) in tumors: concentration in tumor blood vessels. *J Exp Med* 174: 1275–1278, 1991.

122. Egeblad M, Rasch MG, Weaver VM. Dynamic interplay between the collagen scaffold and tumor evolution. *Curr Opin Cell Biol* 22: 697–706, 2010.

123. Eikenes L, Bruland OS, Brekken C, Davies CL. Collagenase increases the transcapillary pressure gradient and improves the uptake and distribution of monoclonal antibodies in human osteosarcoma xenografts. *Cancer Res* 64: 4768–4773, 2004.

124. Engeset A, Hager B, Nesheim A, Kolbenstvedt A. Studies on human peripheral lymph. I. Sampling method. *Lymphology* 6: 1–5, 1973.

125. Esko JD, Selleck SB. Order out of chaos: assembly of ligand binding sites in heparan sulfate. *Annu Rev Biochem* 71: 435–471, 2002.

126. Ethier CR, Johnson M, Ruberti J. Ocular biomechanics and biotransport. *Annu Rev Biomed Eng* 6: 249–273, 2004.

127. Fadnes HO. Colloid osmotic pressure in interstitial fluid and lymph from rabbit subcutaneous tissue. *Microvasc Res* 21: 390–392, 1981.

128. Fadnes HO, Aukland K. Protein concentration and colloid osmotic pressure of interstitial fluid collected by the wick technique: analysis and evaluation of the method. *Microvasc Res* 14: 11–25, 1977.

129. Fadnes HO, Reed RK, Aukland K. Interstitial fluid pressure in rats measured with a modified wick technique. *Microvasc Res* 14: 27–36, 1977.

130. Feng D, Nagy JA, Dvorak HF, Dvorak AM. Ultrastructural studies define soluble macromolecular, particulate, and cellular transendothelial cell pathways in venules, lymphatic vessels, and tumor-associated microvessels in man and animals. *Microsc Res Technique* 57: 289–326, 2002.

131. Ferrara N, Gerber HP, LeCouter J. The biology of VEGF and its receptors. *Nat Med* 9: 669–676, 2003.

132. Fiszer-Szafarz B, Gullino PM. Hyaluronic acid content of the interstitial fluid of Walker carcinoma 256. *Proc Soc Exp Biol Med* 133: 597–600, 1970.

133. Fiszer-Szafarz B, Gullino PM. Hyaluronidase activity of normal and neoplastic interstitial fluid. *Proc Soc Exp Biol Med* 133: 805–807, 1970.

134. Fjeldstad K, Kolset SO. Decreasing the metastatic potential in cancers–targeting the heparan sulfate proteoglycans. *Curr Drug Targets* 6: 665–682, 2005.

135. Fleischmajer R, Perlish JS, Timpl R, Olsen BR. Procollagen intermediates during tendon fibrillogenesis. *J Histochem Cytochem* 36: 1425–1432, 1988.

136. Flessner MF, Choi J, Credit K, Deverkadra R, Henderson K. Resistance of tumor interstitial pressure to the penetration of intraperitoneally delivered antibodies into metastatic ovarian tumors. *Clin Cancer Res* 11: 3117–3125, 2005.

137. Flessner MF, Choi J, He Z, Credit K. Physiological characterization of human ovarian cancer cells in a rat model of intraperitoneal antineoplastic therapy. *J Appl Physiol* 97: 1518–1526, 2004.

138. Fleury ME, Boardman KC, Swartz MA. Autologous morphogen gradients by subtle interstitial flow and matrix interactions. *Biophys J* 91: 113–121, 2006.

139. Freitas I, Baronzio GF, Bono B, Griffini P, Bertone V, Sonzini N, Magrassi GR, Bonandrini L, Gerzeli G. Tumor interstitial fluid: misconsidered component of the internal milieu of a solid tumor. *Anticancer Res* 17: 165–172, 1997.

140. Friedl P, Gilmour D. Collective cell migration in morphogenesis, regeneration and cancer. *Nature Rev Mol Cell Biol* 10: 445–457, 2009.

141. Friedlaender MH, Baer H. Immunologic tolerance: Role of the regional lymph node. *Science* 176: 312–314, 1972.

142. Fukumura D, Jain RK. Tumor microenvironment abnormalities: causes, consequences, and strategies to normalize. *J Cell Biochem* 101: 937–949, 2007.

143. Gabel JC, Hansen TN, Drake RE. Effect of endotoxin on lung fluid balance in unanesthetized sheep. *J Appl Physiol* 56: 489–494, 1984.

144. Gaggioli C, Hooper S, Hidalgo-Carcedo C, Grosse R, Marshall JF, Harrington K, Sahai E. Fibroblast-led collective invasion of carcinoma cells with differing roles for RhoGTPases in leading and following cells. *Nature Cell Biol* 9: 1392–1400, 2007.

145. Garlick DG, Renkin EM. Transport of large molecules from plasma to interstitial fluid and lymph in dogs. *Am J Physiol* 219: 1595–1605, 1970.

146. Garvin S, Dabrosin C. Tamoxifen inhibits secretion of vascular endothelial growth factor in breast cancer in vivo. *Cancer Res* 63: 8742–8748, 2003.

147. Gelse K, Poschl E, Aigner T. Collagens–structure, function, and biosynthesis. *Adv Drug Deliv Rev* 55: 1531–1546, 2003.

148. Gerli R, Solito R, Weber E, Agliano M. Specific adhesion molecules bind anchoring filaments and endothelial cells in human skin initial lymphatics. *Lymphology* 33: 148–157, 2000.

149. Gerszten RE, Asnani A, Carr SA. Status and prospects for discovery and verification of new biomarkers of cardiovascular disease by proteomics. *Circ Res* 109: 463–474, 2011.

150. Gilanyi M, Ikrenyi C, Fekete J, Ikrenyi K, Kovach AG. Ion concentrations in subcutaneous interstitial fluid: measured versus expected values. *Am J Physiol Renal Fluid Electrolyte Physiol* 255: F513–F519, 1988.

151. Gilanyi M, Kovach AG. Effect of local pH on interstitial fluid pressure. *Am J Physiol Heart Circ Physiol* 261: H627–H631, 1991.

152. Goel S, Duda DG, Xu L, Munn LL, Boucher Y, Fukumura D, Jain RK. Normalization of the vasculature for treatment of cancer and other diseases. *Physiol Rev* 91: 1071–1121, 2011.

153. Goldman J, Conley KA, Raehl A, Bondy DM, Pytowski B, Swartz MA, Rutkowski JM, Jaroch DB, Ongstad EL. Regulation of lymphatic capillary regeneration by interstitial flow in skin. *Am J Physiol Heart Circ Physiol* 292: H2176–H2183, 2007.

154. Goldman J, Le TX, Skobe M, Swartz MA. Overexpression of VEGF-C causes transient lymphatic hyperplasia but not increased lymphangiogenesis in regenerating skin. *Circ Res* 96: 1193–1199, 2005.

155. Goldman J, Rutkowski JM, Shields JD, Pasquier M, Cui Y, Schmoekel HG, Wiley S, Hicklin DJ, Pytowski B, Swartz MA. Cooperative and redundant roles of VEGFR-2 and VEGFR-3 signaling in adult lymphangiogenesis. *FASEB J* 21: 1003–1012, 2007.

156. Gotte M, Yip GW. Heparanase, hyaluronan, and CD44 in cancers: a breast carcinoma perspective. *Cancer Res* 66: 10233–10237, 2006.

157. Granger DN, Taylor AE. Permeability of intestinal capillaries to endogenous macromolecules. *Am J Physiol Heart Circ Physiol* 238: H457–H464, 1980.

158. Granger HJ, Laine GA, Barnes GE, Lewis RE. Dynamics and control of transmicrovascular fluid exchange. In: *Edema*, edited by Staub NC, Taylor AE. New York: Raven, 1984, p. 189–228.

159. Gretz JE, Norbury CC, Anderson AO, Proudfoot AE, Shaw S. Lymph-borne chemokines and other low molecular weight molecules reach high endothelial venules via specialized conduits while a functional barrier limits access to the lymphocyte microenvironments in lymph node cortex. *J Exp Med* 192: 1425–1440, 2000.

160. Grodzinsky AJ. Electromechanical and physicochemical properties of connective tissue. *Crit Rev Biomed Eng* 9: 133–199, 1983.

161. Grodzinsky AJ, Melcher JR. Electromechanical transduction with charged polyelectrolyte membranes. *IEEE Trans Biomed Eng* 23: 421–433, 1976.

162. Gu XH, Terenghi G, Purkis PE, Price DA, Leigh IM, Polak JM. Morphological changes of neural and vascular peptides in human skin suction blister injury. *J Pathol* 172: 61–72, 1994.

163. Gullino PM, Grantham FH. The influence of the host and the neoplastic cell population on the collagen content of a tumor mass. *Cancer Res* 23: 648–653, 1963.

164. Gullino PM, Clark SH, Grantham FH. The interstitial fluid of solid tumors. *Cancer Res* 24: 780–798, 1964.

165. Gullino PM, Grantham FH, Clark SH. The collagen content of transplanted tumors. *Cancer Res* 22: 1031–1037, 1962.

166. Gullino PM, Grantham FH, Smith SH, Haggerty AC. Modifications of the acid-base status of the internal milieu of tumors. *J Natl Cancer Inst* 34: 857–869, 1965.

167. Gullino PM, Lanzerotti RH. Mammary tumor regression. II. Autophagy of neoplastic cells. *J Natl Cancer Inst* 49: 1349–1356, 1972.

168. Guo R, Zhou Q, Proulx ST, Wood R, Ji RC, Ritchlin CT, Pytowski B, Zhu Z, Wang YJ, Schwarz EM, Xing L. Inhibition of lymphangiogenesis and lymphatic drainage via vascular endothelial growth factor receptor 3 blockade increases the severity of inflammation in a mouse model of chronic inflammatory arthritis. *Arthritis Rheum* 60: 2666–2676, 2009.

169. Guyton AC. A concept of negative interstitial pressure based on pressure in implanted perforated capsules. *Circ Res* 12: 399–413, 1963.

170. Guyton AC. Interstitial fluid pressure. II. Pressure-volume curves of interstitial space. *Circ Res* 16: 452–460, 1965.

171. Guyton AC, Granger HJ, Taylor AE. Interstitial fluid pressure. *Physiol Rev* 51: 527–563, 1971.

172. Guyton AC, Scheel K, Murphree D. Interstitial fluid pressure. 3. Its effect on resistance to tissue fluid mobility. *Circ Res* 19: 412–419, 1966.

173. Gyenge CC, Tenstad O, Wiig H. In vivo determination of steric and electrostatic exclusion of albumin in rat skin and skeletal muscle. *J Physiol* 552: 907–916, 2003.

174. Hagendoorn J, Padera TP, Kashiwagi S, Isaka N, Noda F, Lin MI, Huang PL, Sessa WC, Fukumura D, Jain RK. Endothelial nitric oxide synthase regulates microlymphatic flow via collecting lymphatics. *Circ Res* 95: 204–209, 2004.

175. Halin C, Tobler NE, Vigl B, Brown LF, Detmar M. VEGF-A produced by chronically inflamed tissue induces lymphangiogenesis in draining lymph nodes. *Blood* 110: 3158–3167, 2007.

176. Haljamae H, Freden H. Comparative analysis of the protein content of local subcutaneous tissue fluid and plasma. *Microvasc Res* 2: 163–171, 1970.

177. Haljamae H, Linde A, Amundson B. Comparative analyses of capsular fluid and interstitial fluid. *Am J Physiol* 227: 1199–1205, 1974.

178. Happel J, Brenner H. *Low Reynolds Number Hydrodynamics*. Englewood Cliffs, NJ: Prentice-Hall, 1965.

179. Hargens AR, Akeson WH, Mubarak SJ, Owen CA, Evans KL, Garetto LP, Gonsalves MR, Schmidt DA. Fluid balance within the canine anterolateral compartment and its relationship to compartment syndromes. *J Bone Joint Surg Am* 60: 499–505, 1978.

180. Hargens AR, Cologne JB, Menninger FJ, Hogan JS, Tucker BJ, Peters RM. Normal transcapillary pressures in human skeletal muscle and subcutaneous tissues. *Microvasc Res* 22: 177–189, 1981.

181. Hargens AR, Zweifach BW. Transport between blood and peripheral lymph in intestine. *Microvasc Res* 11: 89–101, 1976.

182. Harrell MI, Iritani BM, Ruddell A. Tumor-induced sentinel lymph node lymphangiogenesis and increased lymph flow precede melanoma metastasis. *Am J Pathol* 170: 774–786, 2007.

183. Harvey NL, Srinivasan RS, Dillard ME, Johnson NC, Witte MH, Boyd K, Sleeman MW, Oliver G. Lymphatic vascular defects promoted by Prox1 haploinsufficiency cause adult-onset obesity. *Nat Genet* 37: 1072–1081, 2005.

184. Haslene-Hox H, Oveland E, Berg KC, Kolmannskog O, Woie K, Salvesen HB, Tenstad O, Wiig H. A new method for isolation of interstitial fluid from human solid tumors applied to proteomic analysis of ovarian carcinoma tissue. *PLoS One* 6: e19217, 2011.

185. Hauck G, Castenholz A. Contribution of prelymphatic structures to lymph drainage. *Z Lymphol* 16: 6–9, 1992.

186. He C, Young AJ, West CA, Su M, Konerding MA, Mentzer SJ. Stimulation of regional lymphatic and blood flow by epicutaneous oxazolone. *J Appl Physiol* 93: 966–973, 2002.

187. Heldin CH, Rubin K, Pietras K, Ostman A. High interstitial fluid pressure: an obstacle in cancer therapy. *Nat Rev Cancer* 4: 806–813, 2004.

188. Heller F, Lindenmeyer MT, Cohen CD, Brandt U, Draganovici D, Fischereder M, Kretzler M, Anders HJ, Sitter T, Mosberger I, Kerjaschki D, Regele H, Schlondorff D, Segerer S. The contribution of B cells to renal interstitial inflammation. *Am J Pathol* 170: 457–468, 2007.

189. Helm CE, Fleury ME, Zisch AH, Boschetti F, Swartz MA. Synergy between 3D flow and VEGF directs capillary morphogenesis in vitro: experiments and theoretical mechanisms. *Proc Natl Acad Sci USA* 44: 15779–15784, 2005.

190. Helmlinger G, Sckell A, Dellian M, Forbes NS, Jain RK. Acid production in glycolysis-impaired tumors provides new insights into tumor metabolism. *Clin Cancer Res* 8: 1284–1291, 2002.

191. Helmlinger G, Yuan F, Dellian M, Jain RK. Interstitial pH and pO_2 gradients in solid tumors in vivo: high-resolution measurements reveal a lack of correlation. *Nat Med* 3: 177–182, 1997.

192. Heuchel R, Berg A, Tallquist M, Ahlen K, Reed RK, Rubin K, Claesson-Welsh L, Heldin CH, Soriano P. Platelet-derived growth factor beta receptor regulates interstitial fluid homeostasis through phosphatidylinositol-3′ kinase signaling. *Proc Natl Acad Sci USA* 96: 11410–11415, 1999.

193. Hinz B, Gabbiani G. Mechanisms of force generation and transmission by myofibroblasts. *Curr Opin Biotechnol* 14: 538–546, 2003.

194. Hinz B, Gabbiani G, Chaponnier C. The NH_2-terminal peptide of alpha-smooth muscle actin inhibits force generation by the myofibroblast in vitro and in vivo. *J Cell Biol* 157: 657–663, 2002.

195. Hockel M, Schlenger K, Hockel S, Vaupel P. Hypoxic cervical cancers with low apoptotic index are highly aggressive. *Cancer Res* 59: 4525–4528, 1999.

196. Hogan RD. The initial lymphatics and tissue fluid pressure. In: *Tissue Fluid Pressure and Composition*, edited by Hargens AR. Baltimore, MD: Williams & Wilkins, 1981, p. 155–163.

197. Hogan RD. Lymph formation in the bat wing. In: *Progress in Microcirculation Research First Australasian Symposium on the Microcirculation Sydney 1980*, edited by Garlick D. Kensington: Univ. of New South Wales, 1981, p. 261–282.

198. Hogan RD, Unthank JL. The initial lymphatics as sensors of interstitial fluid volume. *Microvasc Res* 31: 317–324, 1986.

199. Hogan RD, Unthank JL. Mechanical control of initial lymphatic contractile behavior in bat's wing. *Am J Physiol Heart Circ Physiol* 251: H357–H363, 1986.

200. Hommel E, Mathiesen ER, Aukland K, Parving HH. Pathophysiological aspects of edema formation in diabetic nephropathy. *Kidney Int* 38: 1187–1192, 1990.

201. Houck KA, Leung DW, Rowland AM, Winer J, Ferrara N. Dual regulation of vascular endothelial growth factor bioavailability by genetic and proteolytic mechanisms. *J Biol Chem* 267: 26031–26037, 1992.

202. Hu X, Adamson RH, Liu B, Curry FE, Weinbaum S. Starling forces that oppose filtration after tissue oncotic pressure is increased. *Am J Physiol Heart Circ Physiol* 279: H1724–H1736, 2000.

203. Hu X, Weinbaum S. A new view of Starling's hypothesis at the microstructural level. *Microvasc Res* 58: 281–304, 1999.

204. Huang CM, Ananthaswamy HN, Barnes S, Ma Y, Kawai M, Elmets CA. Mass spectrometric proteomics profiles of in vivo tumor secretomes: capillary ultrafiltration sampling of regressive tumor masses. *Proteomics* 6: 6107–6116, 2006.

205. Huang CM, Wang CC, Barnes S, Elmets CA. In vivo detection of secreted proteins from wounded skin using capillary ultrafiltration probes and mass spectrometric proteomics. *Proteomics* 6: 5805–5814, 2006.

206. Huang CM, Wang CC, Kawai M, Barnes S, Elmets CA. In vivo protein sampling using capillary ultrafiltration semi-permeable hollow fiber and protein identification via mass spectrometry-based proteomics. *J Chromatogr A* 1109: 144–151, 2006.

207. Huggenberger R, Siddiqui SS, Brander D, Ullmann S, Zimmermann K, Antsiferova M, Werner S, Alitalo K, Detmar M. An important role of lymphatic vessel activation in limiting acute inflammation. *Blood* 117: 4667–4678, 2011.

208. Huggenberger R, Ullmann S, Proulx ST, Pytowski B, Alitalo K, Detmar M. Stimulation of lymphangiogenesis via VEGFR-3 inhibits chronic skin inflammation. *J Exp Med* 207: 2255–2269, 2010.

209. Hynes RO. The extracellular matrix: not just pretty fibrils. *Science* 326: 1216–1219, 2009.

210. Issa A, Le TX, Shoushtari AN, Shields JD, Swartz MA. Vascular endothelial growth factor-C and C-C chemokine receptor 7 in tumor cell-lymphatic cross-talk promote invasive phenotype. *Cancer Res* 69: 349–357, 2009.

211. Itano AA, McSorley SJ, Reinhardt RL, Ehst BD, Ingulli E, Rudensky AY, Jenkins MK. Distinct dendritic cell populations sequentially present antigen to CD4 T cells and stimulate different aspects of cell-mediated immunity. *Immunity* 19: 47–57, 2003.

212. Iversen PO, Berggreen E, Nicolaysen G, Heyeraas K. Regulation of extracellular volume and interstitial fluid pressure in rat bone marrow. *Am J Physiol Heart Circ Physiol* 280: H1807–H1813, 2001.

213. Iversen PO, Wiig H. Tumor necrosis factor alpha and adiponectin in bone marrow interstitial fluid from patients with acute myeloid leukemia inhibit normal hematopoiesis. *Clin Cancer Res* 11: 6793–6799, 2005.

214. Jackson D, Cleary E. The determination of collagen and elastin. In: *Methods of Biochemical Analysis*, edited by Glick D. New York: Interscience, 1976, p. 25–76.

215. Jackson GW, James DF. The permeability of fibrous porous media. *Can J Chem Eng* 64: 1986.

216. Jackson RL, Busch SJ, Cardin AD. Glycosaminoglycans: molecular properties, protein interactions, and role in physiological processes. *Physiol Rev* 71: 481–539, 1991.

217. Jain RK. The next frontier of molecular medicine: delivery of therapeutics. *Nat Med* 4: 655–657, 1998.

218. Jain RK. Normalization of tumor vasculature: an emerging concept in antiangiogenic therapy. *Science* 307: 58–62, 2005.

219. Jain RK. Transport of molecules in the tumor interstitium: a review. *Cancer Res* 47: 3039–3051, 1987.

220. Jain RK, Shah SA, Finney PL. Continuous noninvasive monitoring of pH and temperature in rat Walker 256 carcinoma during normoglycemia and hyperglycemia. *J Natl Cancer Inst* 73: 429–436, 1984.

221. Jain RK, Stylianopoulos T. Delivering nanomedicine to solid tumors. *Nat Rev Clin Oncol* 7: 653–664, 2010.

222. Ji RC. Lymphatic endothelial cells, lymphangiogenesis, and extracellular matrix. *Lymphat Res Biol* 4: 83–100, 2006.

223. Jimenez CR, Piersma C, Pham TV. High-throughput and targeted in-depth mass spectrometry-based approaches for biofluid profiling and biomarker discovery. *Biomarkers Med* 1: 541–565, 2007.

224. Johnson LA, Clasper S, Holt AP, Lalor PF, Baban D, Jackson DG. An inflammation-induced mechanism for leukocyte transmigration across lymphatic vessel endothelium. *J Exp Med* 203: 2763–2777, 2006.

225. Junt T, Moseman EA, Iannacone M, Massberg S, Lang PA, Boes M, Fink K, Henrickson SE, Shayakhmetov DM, Di Paolo NC, van Rooijen N, Mempel TR, Whelan SP, von Andrian UH. Subcapsular sinus macrophages in lymph nodes clear lymph-borne viruses and present them to antiviral B cells. *Nature* 450: 110–114, 2007.

226. Kadar A, Tokes AM, Kulka J, Robert L. Extracellular matrix components in breast carcinomas. *Semin Cancer Biol* 12: 243–257, 2002.

227. Kadler KE, Baldock C, Bella J, Boot-Handford RP. Collagens at a glance. *J Cell Sci* 120: 1955–1958, 2007.

228. Kajiya K, Detmar M. An important role of lymphatic vessels in the control of UVB-induced edema formation and inflammation. *J Invest Dermatol* 126: 919–921, 2006.

229. Kajiya K, Sawane M, Huggenberger R, Detmar M. Activation of the VEGFR-3 pathway by VEGF-C attenuates UVB-induced edema formation and skin inflammation by promoting lymphangiogenesis. *J Invest Dermatol* 129: 1292–1298, 2009.

230. Kalluri R. Basement membranes: structure, assembly and role in tumour angiogenesis. *Nat Rev Cancer* 3: 422–433, 2003.

231. Kalluri R, Zeisberg M. Fibroblasts in cancer. *Nat Rev Cancer* 6: 392–401, 2006.

232. Karlsen TV, Karkkainen MJ, Alitalo K, Wiig H. Transcapillary fluid balance consequences of missing initial lymphatics studied in a mouse model of primary lymphoedema. *J Physiol* 574: 583–596, 2006.

233. Karpakka J, Virtanen P, Vaananen K, Orava S, Takala TE. Collagen synthesis in rat skeletal muscle during immobilization and remobilization. *J Appl Physiol* 70: 1775–1780, 1991.

234. Kataru RP, Jung K, Jang C, Yang H, Schwendener RA, Baik JE, Han SH, Alitalo K, Koh GY. Critical role of CD11b+ macrophages and VEGF in inflammatory lymphangiogenesis, antigen clearance, and inflammation resolution. *Blood* 113: 5650–5659, 2009.

235. Kataru RP, Kim H, Jang C, Choi DK, Koh BI, Kim M, Gollamudi S, Kim YK, Lee SH, Koh GY. T lymphocytes negatively regulate lymph node lymphatic vessel formation. *Immunity* 34: 96–107, 2011.

236. Katz EP, Wachtel EJ, Maroudas A. Extrafibrillar proteoglycans osmotically regulate the molecular packing of collagen in cartilage. *Biochim Biophys Acta* 882: 136–139, 1986.

237. Kaufman S, Deng Y. Splenic control of intravascular volume in the rat. *J Physiol* 468: 557–565, 1993.

238. Keene DR, Sakai LY, Lunstrum GP, Morris NP, Burgeson RE. Type VII collagen forms an extended network of anchoring fibrils. *J Cell Biol* 104: 611–621, 1987.

239. Kelly T, Miao HQ, Yang Y, Navarro E, Kussie P, Huang Y, MacLeod V, Casciano J, Joseph L, Zhan F, Zangari M, Barlogie B, Shaughnessy J, Sanderson RD. High heparanase activity in multiple myeloma is associated with elevated microvessel density. *Cancer Res* 63: 8749–8756, 2003.

240. Kerin A, Patwari P, Kuettner K, Cole A, Grodzinsky A. Molecular basis of osteoarthritis: biomechanical aspects. *Cell Mol Life Sci* 59: 27–35, 2002.

241. Kerjaschki D, Regele HM, Moosberger I, Nagy-Bojarski K, Watschinger B, Soleiman A, Birner P, Krieger S, Hovorka A, Silberhumer G, Laakkonen P, Petrova T, Langer B, Raab I. Lymphatic neoangiogenesis in human kidney transplants is associated with immunologically active lymphocytic infiltrates. *J Am Soc Nephrol* 15: 603–612, 2004.

242. Kessenbrock K, Plaks V, Werb Z. Matrix metalloproteinases: regulators of the tumor microenvironment. *Cell* 141: 52–67, 2010.

243. Khalil AA, Friedl P. Determinants of leader cells in collective cell migration. *Integr Biol* 2: 568–574, 2010.

244. Kiistala U. Suction blister device for separation of viable epidermis from dermis. *J Invest Dermatol* 50: 129–137, 1968.

245. Kinsky MP, Guha SC, Button BM, Kramer GC. The role of interstitial starling forces in the pathogenesis of burn edema. *J Burn Care Rehabil* 19: 1–9, 1998.

246. Kjaer M. Role of extracellular matrix in adaptation of tendon and skeletal muscle to mechanical loading. *Physiol Rev* 84: 649–698, 2004.

247. Kjaer M, Magnusson P, Krogsgaard M, Boysen Moller J, Olesen J, Heinemeier K, Hansen M, Haraldsson B, Koskinen S, Esmarck B, Langberg H. Extracellular matrix adaptation of tendon and skeletal muscle to exercise. *J Anat* 208: 445–450, 2006.

248. Kool J, Reubsaet L, Wesseldijk F, Maravilha RT, Pinkse MW, D'Santos CS, van Hilten JJ, Zijlstra FJ, Heck AJ. Suction blister fluid as potential body fluid for biomarker proteins. *Proteomics* 7: 3638–3650, 2007.

249. Kramer GC, Sibley L, Aukland K, Renkin EM. Wick sampling of interstitial fluid in rat skin: further analysis and modifications of the method. *Microvasc Res* 32: 39–49, 1986.

250. Krol A, Dewhirst MW, Yuan F. Effects of cell damage and glycosaminoglycan degradation on available extravascular space of different dextrans in a rat fibrosarcoma. *Int J Hyperthermia* 19: 154–164, 2003.

251. Krol A, Maresca J, Dewhirst MW, Yuan F. Available volume fraction of macromolecules in the extravascular space of a fibrosarcoma: implications for drug delivery. *Cancer Res* 59: 4136–4141, 1999.

252. Kubik S, Manestar M. Anatomy of the lymph capillaries and precollectors of the skin. In: *The Initial Lymphatics*, edited by Bollinger A, Partsch H, Wolfe JHN. Stuttgart: Thieme-Verlag, 1985, p. 66–74.

253. Lammermann T, Sixt M. The microanatomy of T-cell responses. *Immunol Rev* 221: 26–43, 2008.

254. Landis EM, Gibbon JH. The effects of temperature and of tissue pressure on the movement of fluid through the human capillary wall. *J Clin Invest* 12: 105–138, 1933.

255. Landis EM, Pappenheimer JR. Exchange of substances through the capillary wall. In: *Handbook of Physiology. Circulation*. Washington, DC: Am. Physiol. Soc., 1963, sect. 2, p. 961–1034.

256. Lareu RR, Subramhanya KH, Peng Y, Benny P, Chen C, Wang Z, Rajagopalan R, Raghunath M. Collagen matrix deposition is dramatically enhanced in vitro when crowded with charged macromolecules: the biological relevance of the excluded volume effect. *FEBS Lett* 581: 2709–2714, 2007.

257. Laurent TC. The interaction between polysaccharides and other macromolecules. 9. The exclusion of molecules from hyaluronic acid gels and solutions. *Biochem J* 93: 106–112, 1964.

258. Leak LV. The structure of lymphatic capillaries in lymph formation. *Federation Proc* 35: 1863–1871, 1976.

259. Leak LV, Burke JF. Fine structure of the lymphatic capillary and the adjoining connective tissue area. *Am J Anat* 118: 785–810, 1966.

260. Leak LV, Burke JF. Ultrastructural studies on the lymphatic anchoring filaments. *J Cell Biol* 36: 129–149, 1968.

261. Leegsma-Vogt G, Janle E, Ash SR, Venema K, Korf J. Utilization of in vivo ultrafiltration in biomedical research and clinical applications. *Life Sci* 73: 2005–2018, 2003.

262. Leu AJ, Berk DA, Lymboussaki A, Alitalo K, Jain RK. Absence of functional lymphatics within a murine sarcoma: a molecular and functional evaluation. *Cancer Res* 60: 4324–4327, 2000.

263. Levental KR, Yu H, Kass L, Lakins JN, Egeblad M, Erler JT, Fong SF, Csiszar K, Giaccia A, Weninger W, Yamauchi M, Gasser DL, Weaver VM. Matrix crosslinking forces tumor progression by enhancing integrin signaling. *Cell* 139: 891–906, 2009.

264. Levick JR. An analysis of the interaction between interstitial plasma protein, interstitial flow, fenestral filtration and its application to synovium. *Microvasc Res* 47: 90–125, 1994.

265. Levick JR. Flow through interstitium and other fibrous matrices. *Q J Exp Physiol* 72: 409–437, 1987.

266. Levick JR, Michel CC. Microvascular fluid exchange and the revised Starling principle. *Cardiovasc Res* 87: 198–210, 2010.

267. Li ST, Katz EP. An electrostatic model for collagen fibrils. The interaction of reconstituted collagen with Ca^{2+}, Na^{+}, and Cl. *Biopolymers* 15: 1439–1460, 1976.

268. Li Y, Peris J, Zhong L, Derendorf H. Microdialysis as a tool in local pharmacodynamics. *Aaps J* 8: E222–235, 2006.

269. Liden A, Berg A, Nedrebo T, Reed RK, Rubin K. Platelet-derived growth factor BB-mediated normalization of dermal interstitial fluid pressure after mast cell degranulation depends on beta3 but not beta1 integrins. *Circ Res* 98: 635–641, 2006.

270. Lim HY, Rutkowski JM, Helft J, Reddy ST, Swartz MA, Randolph GJ, Angeli V. Hypercholesterolemic mice exhibit lymphatic vessel dysfunction and degeneration. *Am J Pathol* 175: 1328–1337, 2009.

271. Ling S, Qi C, Li W, Xu J, Kuang W. Crucial role of corneal lymphangiogenesis for allograft rejection in alkali-burned cornea bed. *Clin Exp Ophthalmol* 37: 874–883, 2009.

272. Linhares MC, Kissinger PT. Determination of endogenous ions in intercellular fluid using capillary ultrafiltration and microdialysis probes. *J Pharm Biomed Anal* 11: 1121–1127, 1993.

273. Liotta LA, Kohn EC. The microenvironment of the tumour-host interface. *Nature* 411: 375–379, 2001.

274. Lund AW, Duraes FV, Hirosue S, Raghavan VR, Nembrini C, Thomas SN, Hugues S, Swartz MA. VEGF-C promotes immune tolerance in B16 melanomas and cross-presentation of tumor antigen by lymph node lymphatics. *Cell Reports* 1: 191–199, 2012.

275. Lund AW, Swartz MA. Role of lymphatic vessels in tumor immunity: passive conduits or active participants? *J Mammary Gland Biol Neoplasia* 15: 341–352, 2010.

276. Lund T, Onarheim H, Wiig H, Reed RK. Mechanisms behind increased dermal imbibition pressure in acute burn edema. *Am J Physiol Heart Circ Physiol* 256: H940–H948, 1989.

277. Lund T, Wiig H, Reed RK. Acute postburn edema: role of strongly negative interstitial fluid pressure. *Am J Physiol Heart Circ Physiol* 255: H1069–H1074, 1988.

278. Lunt SJ, Fyles A, Hill RP, Milosevic M. Interstitial fluid pressure in tumors: therapeutic barrier and biomarker of angiogenesis. *Future Oncol* 4: 793–802, 2008.

279. Machnik A, Neuhofer W, Jantsch J, Dahlmann A, Tammela T, Machura K, Park JK, Beck FX, Muller DN, Derer W, Goss J, Ziomber A, Dietsch P, Wagner H, van Rooijen N, Kurtz A, Hilgers KF, Alitalo K, Eckardt KU, Luft FC, Kerjaschki D, Titze J. Macrophages regulate salt-dependent volume and blood pressure by a vascular endothelial growth factor-C-dependent buffering mechanism. *Nat Med* 15: 545–552, 2009.

280. Mahfouz SM, Chevallier M, Grimaud JA. Distribution of the major connective matrix components of the stromal reaction in breast carcinoma. An immunohistochemical study. *Cell Mol Biol* 33: 453–467, 1987.

281. Makinen T, Jussila L, Veikkola T, Karpanen T, Kettunen MI, Pulkkanen KJ, Kauppinen R, Jackson DG, Kubo H, Nishikawa S, Yla-Herttuala S, Alitalo K. Inhibition of lymphangiogenesis with resulting lymphedema in transgenic mice expressing soluble VEGF receptor-3. *Nat Med* 7: 199–205, 2001.

282. Mantovani A, Allavena P, Sica A, Balkwill F. Cancer-related inflammation. *Nature* 454: 436–444, 2008.

283. Marin-Padilla M, Knopman DS. Developmental aspects of the intracerebral microvasculature and perivascular spaces: insights into brain response to late-life diseases. *J Neuropathol Exp Neurol* 70: 1060–1069, 2011.

284. Markhus CE, Wiig H. Isolation of interstitial fluid from skeletal muscle and subcutis in mice using a wick method. *Am J Physiol Heart Circ Physiol* 287: H2085–H2090, 2004.

285. Martin S, Maruta K, Burkart V, Gillis S, Kolb H. IL-1 and IFN-gamma increase vascular permeability. *Immunology* 64: 301–305, 1988.

286. Matsumoto N, Koike K, Yamada S, Staub NC. Caudal mediastinal node lymph flow in sheep after histamine or endotoxin infusions. *Am J Physiol Heart Circ Physiol* 258: H24–H28, 1990.

287. McDonald JN, Levick JR. Effect of extravascular plasma protein on pressure-flow relations across synovium in anaesthetized rabbits. *J Physiol* 465: 539–559, 1993.

288. McGuire S, Zaharoff D, Yuan F. Nonlinear dependence of hydraulic conductivity on tissue deformation during intratumoral infusion. *Ann Biomed Eng* 34: 1173–1181, 2006.

289. Mebius RE, Streeter PR, Breve J, Duijvestijn AM, Kraal G. The influence of afferent lymphatic vessel interruption on vascular addressin expression. *J Cell Biol* 115: 85–95, 1991.

290. Mehta D, Malik AB. Signaling mechanisms regulating endothelial permeability. *Physiol Rev* 86: 279–367, 2006.

291. Meyer FA. Macromolecular basis of globular protein exclusion and of swelling pressure in loose connective tissue (umbilical cord). *Biochim Biophys Acta* 755: 388–399, 1983.

292. Michel C. Fluid movement through capillary walls. In: *Handbook of Physiology. The Cardiovascular System. Microcirculation.* Bethesda, MD: Am. Physiol. Soc., 1984, sect. 2, vol. IV, pt. 1, chapt. 9, p. 375–409.

293. Michel CC. Starling: the formulation of his hypothesis of microvascular fluid exchange and its significance after 100 years. *Exp Physiol* 82: 1–30, 1997.

294. Michel CC, Curry FE. Microvascular permeability. *Physiol Rev* 79: 703–761, 1999.

295. Miller NE, Michel CC, Nanjee MN, Olszewski WL, Miller IP, Hazell M, Olivecrona G, Sutton P, Humphreys SM, Frayn KN. Secretion of adipokines by human adipose tissue in vivo: partitioning between capillary and lymphatic transport. *Am J Physiol Endocrinol Metab* 301: E659–E667, 2011.

296. Miner JH, Yurchenco PD. Laminin functions in tissue morphogenesis. *Annu Rev Cell Dev Biol* 20: 255–284, 2004.

297. Miserocchi G, Negrini D, Del Fabbro M, Venturoli D. Pulmonary interstitial pressure in intact in situ lung: transition to interstitial edema. *J Appl Physiol* 74: 1171–1177, 1993.

298. Miteva DO, Rutkowski JM, Dixon JB, Kilarski W, Shields JD, Swartz MA. Transmural flow modulates cell and fluid transport functions of lymphatic endothelium. *Circ Res* 106: 920–1181, 2010.

299. Mobasheri A. Correlation between [Na^+], [glycosaminoglycan] and Na^+/K^+ pump density in the extracellular matrix of bovine articular cartilage. *Physiol Res* 47: 47–52, 1998.

300. Modi S, Stanton AW, Mortimer PS, Levick JR. Clinical assessment of human lymph flow using removal rate constants of interstitial macromolecules: a critical review of lymphoscintigraphy. *Lymphat Res Biol* 5: 183–202, 2007.

301. Modi S, Stanton AW, Svensson WE, Peters AM, Mortimer PS, Levick JR. Human lymphatic pumping measured in healthy and lymphoedematous arms by lymphatic congestion lymphoscintigraphy. *J Physiol* 583: 271–285, 2007.

302. Moriondo A, Mukenge S, Negrini D. Transmural pressure in rat initial subpleural lymphatics during spontaneous or mechanical ventilation. *Am J Physiol Heart Circ Physiol* 289: H263–H269, 2005.

303. Mueller MM, Fusenig NE. Friends or foes: bipolar effects of the tumour stroma in cancer. *Nat Rev Cancer* 4: 839–849, 2004.

304. Mullins RJ, Hudgens RW. Increased skin lymph protein clearance after a 6-h arterial bradykinin infusion. *Am J Physiol Heart Circ Physiol* 253: H1462–H1469, 1987.

305. Mumprecht V, Detmar M. Lymphangiogenesis and cancer metastasis. *J Cell Mol Med* 13: 1405–1416, 2009.

306. Munn DH, Mellor AL. The tumor-draining lymph node as an immune-privileged site. *Immunol Rev* 213: 146–158, 2006.

307. Murfee WL, Rappleye JW, Ceballos M, Schmid-Schönbein GW. Discontinuous expression of endothelial cell adhesion molecules along initial lymphatic vessels in mesentery: the primary valve structure. *Lymphat Res Biol* 5: 81–89, 2007.

308. Muthuchamy M, Zawieja D. Molecular regulation of lymphatic contractility. *Ann NY Acad Sci* 1131: 89–99, 2008.

309. Myllyharju J, Kivirikko KI. Collagens, modifying enzymes and their mutations in humans, flies and worms. *Trends Genet* 20: 33–43, 2004.

310. Nanjee MN, Cooke CJ, Olszewski WL, Miller NE. Lipid and apolipoprotein concentrations in prenodal leg lymph of fasted humans. Associations with plasma concentrations in normal subjects, lipoprotein lipase deficiency, and LCAT deficiency. *J Lipid Res* 41: 1317–1327, 2000.

311. Nanjee MN, Cooke CJ, Wong JS, Hamilton RL, Olszewski WL, Miller NE. Composition and ultrastructure of size subclasses of normal human peripheral lymph lipoproteins: quantification of cholesterol uptake by HDL in tissue fluids. *J Lipid Res* 42: 639–648, 2001.

312. Nedrebo T, Reed RK. Different serotypes of endotoxin (lipopolysaccharide) cause different increases in albumin extravasation in rats. *Shock* 18: 138–141, 2002.

313. Nedrebo T, Reed RK, Berg A. Effect of alpha-trinositol on interstitial fluid pressure, edema generation, and albumin extravasation after ischemia-reperfusion injury in rat hind limb. *Shock* 20: 149–153, 2003.

314. Nedrebo T, Reed RK, Jonsson R, Berg A, Wiig H. Differential cytokine response in interstitial fluid in skin and serum during experimental inflammation in rats. *J Physiol* 556: 193–202, 2004.

315. Negrini D, Del Fabbro M. Subatmospheric pressure in the rabbit pleural lymphatic network. *J Physiol* 520: 761–769, 1999.

316. Negrini D, Moriondo A, Mukenge S. Transmural pressure during cardiogenic oscillations in rodent diaphragmatic lymphatic vessels. *Lymphat Res Biol* 2: 69–81, 2004.

317. Negrini D, Passi A, Bertin K, Bosi F, Wiig H. Isolation of pulmonary interstitial fluid in rabbits by a modified wick technique. *Am J Physiol Lung Cell Mol Physiol* 280: L1057–L1065, 2001.

318. Negrini D, Passi A, de Luca G, Miserocchi G. Pulmonary interstitial pressure and proteoglycans during development of pulmonary edema. *Am J Physiol Heart Circ Physiol* 270: H2000–H2007, 1996.

319. Negrini D, Tenstad O, Passi A, Wiig H. Differential degradation of matrix proteoglycans and edema development in rabbit lung. *Am J Physiol Lung Cell Mol Physiol* 290: L470–L477, 2006.

320. Negrini D, Tenstad O, Wiig H. Interstitial exclusion of albumin in rabbit lung during development of pulmonary oedema. *J Physiol* 548: 907–917, 2003.

321. Negrini D, Tenstad O, Wiig H. Interstitial exclusion of albumin in rabbit lung measured with the continuous infusion method in combination with the wick technique. *Microcirculation* 10: 153–165, 2003.

322. Netti PA, Baxter LT, Boucher Y, Skalak R, Jain RK. Time-dependent behavior of interstitial fluid pressure in solid tumors: implications for drug delivery. *Cancer Res* 55: 5451–5458, 1995.

323. Netti PA, Berk DA, Swartz MA, Grodzinsky AJ, Jain RK. Role of extracellular matrix assembly in interstitial transport in solid tumors. *Cancer Res* 60: 2497–2503, 2000.

324. Ng CP, Helm CL, Swartz MA. Interstitial flow differentially stimulates blood and lymphatic endothelial cell morphogenesis in vitro. *Microvasc Res* 68: 258–264, 2004.

325. Ng CP, Hinz B, Swartz MA. Interstitial fluid flow induces myofibroblast differentiation and collagen alignment in vitro. *J Cell Sci* 118: 4731–4739, 2005.

326. Ng CP, Swartz MA. Fibroblast alignment under interstitial fluid flow using a novel 3-D tissue culture model. *Am J Physiol Heart Circ Physiol* 284: H1771–H1777, 2003.

327. Ng CP, Swartz MA. Mechanisms of interstitial flow-induced remodeling of fibroblast-collagen cultures. *Ann Biomed Eng* 34: 446–454, 2006.

328. Nicolaysen G, Nicolaysen A, Staub NC. A quantitative radioautographic comparison of albumin concentration in different dized lymph vessels in normal mouse lungs. *Microvasc Res* 10: 138–152, 1975.

329. Nicoll PA, Taylor AE. Lymph formation and flow. *Annu Rev Physiol* 39: 73–95, 1977.

330. Noddeland H, Hargens AR, Reed RK, Aukland K. Interstitial colloid osmotic and hydrostatic pressures in subcutaneous tissue of human thorax. *Microvasc Res* 24: 104–113, 1982.

331. Noddeland H, Riisnes SM, Fadnes HO. Interstitial fluid colloid osmotic and hydrostatic pressures in subcutaneous tissue of patients with nephrotic syndrome. *Scand J Clin Lab Invest* 42: 139–146, 1982.

332. O'Connor SW, Bale WF. Accessibility of circulating immunoglobulin G to the extravascular compartment of solid rat tumors. *Cancer Res* 44: 3719–3723, 1984.

333. Ogston AG. The spaces in a uniform random suspension of fibres. *Trans Faraday Soc* 54: 1754–1757, 1958.

334. Ogston AG, Phelps CF. The partition of solutes between buffer solutions and solutions containing hyaluronic acid. *Biochem J* 78: 827–833, 1961.

335. Ohtani O, Ohtani Y. Lymph circulation in the liver. *Anat Rec* 291: 643–652, 2008.

336. Ohtani O, Ohtani Y. Structure and function of rat lymph nodes. *Arch Histol Cytol* 71: 69–76, 2008.

337. Okiji T, Kawashima N, Kosaka T, Matsumoto A, Kobayashi C, Suda H. An immunohistochemical study of the distribution of immunocompetent cells, especially macrophages and Ia antigen-expressing cells of heterogeneous populations, in normal rat molar pulp. *J Dent Res* 71: 1196–1202, 1992.

338. Oldberg A, Kalamajski S, Salnikov AV, Stuhr L, Morgelin M, Reed RK, Heldin NE, Rubin K. Collagen-binding proteoglycan fibromodulin can determine stroma matrix structure and fluid balance in experimental carcinoma. *Proc Natl Acad Sci USA* 104: 13966–13971, 2007.

339. Olszewski W. Pathophysiological and clinical observations of obstructive lymphedema of the limbs. In: *Lymphedema*, edited by Clodius L. Stuttgart: Georg Thieme, 1977, p. 79–102.

340. Olszewski WL. Collection and physiological measurements of peripheral lymph and interstitial fluid in man. *Lymphology* 10: 137–145, 1977.

341. Olszewski WL. The lymphatic system in body homeostasis: physiological conditions. *Lymphat Res Biol* 1: 11–21, 2003.

342. Olszewski WL. Pathophysiological aspects of lymphedema of human limbs. I. Lymph protein composition. *Lymphat Res Biol* 1: 235–243, 2003.

343. Olszewski WL, Pazdur J, Kubasiewicz E, Zaleska M, Cooke CJ, Miller NE. Lymph draining from foot joints in rheumatoid arthritis provides insight into local cytokine and chemokine production and transport to lymph nodes. *Arthritis Rheum* 44: 541–549, 2001.

344. Ono N, Mizuno R, Ohhashi T. Effective permeability of hydrophilic substances through walls of lymph vessels: roles of endothelial barrier. *Am J Physiol Heart Circ Physiol* 289: H1676–H1682, 2005.

345. Orimo A, Gupta PB, Sgroi DC, Arenzana-Seisdedos F, Delaunay T, Naeem R, Carey VJ, Richardson AL, Weinberg RA. Stromal fibroblasts present in invasive human breast carcinomas promote tumor growth and angiogenesis through elevated SDF-1/CXCL12 secretion. *Cell* 121: 335–348, 2005.

346. Ott CE, Cuche JL, Knox FG. Measurement of renal interstitial fluid pressure with polyethylene matrix capsules. *J Appl Physiol* 38: 937–941, 1975.

347. Oxlund H, Manschot J, Viidik A. The role of elastin in the mechanical properties of skin. *J Biomech* 21: 213–218, 1988.

348. Ozerdem U. Measuring interstitial fluid pressure with fiberoptic pressure transducers. *Microvasc Res* 77: 226–229, 2009.

349. Ozerdem U, Hargens AR. A simple method for measuring interstitial fluid pressure in cancer tissues. *Microvasc Res* 70: 116–120, 2005.

350. Padera TP, Kadambi A, di Tomaso E, Carreira CM, Brown EB, Boucher Y, Choi NC, Mathisen D, Wain J, Mark EJ, Munn LL, Jain RK. Lymphatic metastasis in the absence of functional intratumor lymphatics. *Science* 296: 1883–1886, 2002.

351. Padera TP, Stoll BR, Tooredman JB, Capen D, di Tomaso E, Jain RK. Pathology: cancer cells compress intratumour vessels. *Nature* 427: 695, 2004.

352. Parameswaran S, Barber BJ, Babbitt RA, Dutta S. Age-related changes in albumin-excluded volume fraction. *Microvasc Res* 50: 373–380, 1995.

353. Parker JC, Falgout HJ, Grimbert FA, Taylor AE. The effect of increased vascular pressure on albumin-excluded volume and lymph flow in the dog lung. *Circ Res* 47: 866–875, 1980.

354. Parker JC, Falgout HJ, Parker RE, Granger DN, Taylor AE. The effect of fluid volume loading on exclusion of interstitial albumin and lymph flow in the dog lung. *Circ Res* 45: 440–450, 1979.

355. Parker JC, Gilchrist S, Cartledge JT. Plasma-lymph exchange and interstitial distribution volumes of charged macromolecules in the lung. *J Appl Physiol* 59: 1128–1136, 1985.

356. Paszek MJ, Zahir N, Johnson KR, Lakins JN, Rozenberg GI, Gefen A, Reinhart-King CA, Margulies SS, Dembo M, Boettiger D, Hammer DA, Weaver VM. Tensional homeostasis and the malignant phenotype. *Cancer Cell* 8: 241–254, 2005.

357. Patlak CS, Goldstein DA, Hoffman JF. The flow of solute and solvent across a two-membrane system. *J Theor Biol* 5: 426–442, 1963.

358. Pedersen JA, Boschetti F, Swartz MA. Effects of extracellular fiber architecture on cell membrane shear stress in a 3D fibrous matrix. *J Biomech* 40: 1484–1492, 2007.

359. Pedersen JA, Lichter S, Swartz MA. Cells in 3D matrices under interstitial flow: effects of pericellular matrix alignment on cell shear stress and drag forces. *J Biomech* 43: 900–905, 2010.

360. Petricoin EF, Belluco C, Araujo RP, Liotta LA. The blood peptidome: a higher dimension of information content for cancer biomarker discovery. *Nat Rev Cancer* 6: 961–967, 2006.

361. Pietras K, Ostman A, Sjoquist M, Buchdunger E, Reed RK, Heldin CH, Rubin K. Inhibition of platelet-derived growth factor receptors reduces interstitial hypertension and increases transcapillary transport in tumors. *Cancer Res* 61: 2929–2934, 2001.

362. Pietras K, Rubin K, Sjoblom T, Buchdunger E, Sjoquist M, Heldin CH, Ostman A. Inhibition of PDGF receptor signaling in tumor stroma enhances antitumor effect of chemotherapy. *Cancer Res* 62: 5476–5484, 2002.

363. Pietras K, Stumm M, Hubert M, Buchdunger E, Rubin K, Heldin CH, McSheehy P, Wartmann M, Ostman A. STI571 enhances the therapeutic index of epothilone B by a tumor-selective increase of drug uptake. *Clin Cancer Res* 9: 3779–3787, 2003.

364. Pitt Ford TR, Sachs JR, Grotberg JB, Glucksberg MR. Perialveolar interstitial resistance and compliance in isolated rat lung. *J Appl Physiol* 70: 2750–2756, 1991.

365. Pluen A, Boucher Y, Ramanujan S, McKee TD, Gohongi T, di Tomaso E, Brown EB, Izumi Y, Campbell RB, Berk DA, Jain RK. Role of tumor-host interactions in interstitial diffusion of macromolecules: cranial vs. subcutaneous tumors. *Proc Natl Acad Sci USA* 98: 4628–4633, 2001.

366. Podgrabinska S, Kamalu O, Mayer L, Shimaoka M, Snoeck H, Randolph GJ, Skobe M. Inflamed lymphatic endothelium suppresses dendritic cell maturation and function via Mac-1/ICAM-1-dependent mechanism. *J Immunol* 183: 1767–1779, 2009.

367. Polacheck WJ, Charest JL, Kamm RD. Interstitial flow influences direction of tumor cell migration through competing mechanisms. *Proc Natl Acad Sci USA* 108: 11115–11120, 2011.

368. Poli A, Scott D, Bertin K, Miserocchi G, Mason RM, Levick JR. Influence of actin cytoskeleton on intra-articular and interstitial fluid pressures in synovial joints. *Microvasc Res* 62: 293–305, 2001.

369. Proulx ST, Luciani P, Derzsi S, Rinderknecht M, Mumprecht V, Leroux JC, Detmar M. Quantitative imaging of lymphatic function with liposomal indocyanine green. *Cancer Res* 70: 7053–7062, 2010.

370. Provenzano PP, Eliceiri KW, Campbell JM, Inman DR, White JG, Keely PJ. Collagen reorganization at the tumor-stromal interface facilitates local invasion. *BMC Med* 4: 38, 2006.

371. Provenzano PP, Inman DR, Eliceiri KW, Knittel JG, Yan L, Rueden CT, White JG, Keely PJ. Collagen density promotes mammary tumor initiation and progression. *BMC Med* 6: 11, 2008.

372. Putnam FW. Alpha, beta, gamma, omega–The roster of the plasma proteins. In: *The Plasma Proteins Structure, Function, and Genetic Control*, edited by Putman FW. New York: Academic, 1975, p. 52–108.

373. Quick CM, Venugopal AM, Gashev AA, Zawieja DC, Stewart RH. Intrinsic pump-conduit behavior of lymphangions. *Am J Physiol Regul Integr Comp Physiol* 292: R1510–R1518, 2007.

374. Raman R, Sasisekharan V, Sasisekharan R. Structural insights into biological roles of protein-glycosaminoglycan interactions. *Chem Biol* 12: 267–277, 2005.

375. Randolph GJ, Angeli V, Swartz MA. Dendritic-cell trafficking to lymph nodes through lymphatic vessels. *Nat Rev Immunol* 5: 617–628, 2005.

376. Reddy NP. Lymph circulation: physiology, pharmacology, and biomechanics. *Crit Rev Biomed Eng* 14: 45–91, 1986.

377. Reed RK. An implantable colloid osmometer. Measurements in subcutis and skeletal muscle of rats. *Microvasc Res* 18: 83–94, 1979.

378. Reed RK, Bowen BD, Bert JL. Microvascular exchange and interstitial volume regulation in the rat: implications of the model. *Am J Physiol Heart Circ Physiol* 257: H2081–H2091, 1989.

379. Reed RK, Lepsoe S, Wiig H. Interstitial exclusion of albumin in rat dermis and subcutis in over- and dehydration. *Am J Physiol Heart Circ Physiol* 257: H1819–H1827, 1989.

380. Reed RK, Lilja K, Laurent TC. Hyaluronan in the rat with special reference to the skin. *Acta Physiol Scand* 134: 405–411, 1988.

381. Reed RK, Rubin K. Transcapillary exchange: role and importance of the interstitial fluid pressure and the extracellular matrix. *Cardiovasc Res* 87: 211–217, 2010.

382. Reed RK, Rubin K, Wiig H, Rodt SA. Blockade of beta 1-integrins in skin causes edema through lowering of interstitial fluid pressure. *Circ Res* 71: 978–983, 1992.

383. Reichl D. Extravascular circulation of lipoproteins: their role in reverse transport of cholesterol. *Atherosclerosis* 105: 117–129, 1994.

384. Reigle KL, Di Lullo G, Turner KR, Last JA, Chervoneva I, Birk DE, Funderburgh JL, Elrod E, Germann MW, Surber C, Sanderson RD, San Antonio JD. Non-enzymatic glycation of type I collagen diminishes collagen-proteoglycan binding and weakens cell adhesion. *J Cell Biochem* 104: 1684–1698, 2008.

385. Reitsma S, Slaaf DW, Vink H, van Zandvoort MA, oude Egbrink MG. The endothelial glycocalyx: composition, functions, and visualization. *Pflügers Arch* 454: 345–359, 2007.

386. Renkin EM. Lymph as a measure of the compositon of interstitial fluid. In: *Pulmonary Edema*, edited by Fishman AP, Renkin EM. Bethesda, MD: Am. Physiol. Soc., 1979, p. 145–159.

387. Rippe B, Haraldsson B. Transport of macromolecules across microvascular walls: the two-pore theory. *Physiol Rev* 74: 163–219, 1994.

388. Rockson SG. Lymphedema. *Am J Med* 110: 288–295, 2001.

389. Rodt SA, Ahlen K, Berg A, Rubin K, Reed RK. A novel physiological function for platelet-derived growth factor-BB in rat dermis. *J Physiol* 495: 193–200, 1996.

390. Ronnov-Jessen L, Bissell MJ. Breast cancer by proxy: can the microenvironment be both the cause and consequence? *Trends Mol Med* 15: 5–13, 2009.

391. Ronnov-Jessen L, Petersen OW, Bissell MJ. Cellular changes involved in conversion of normal to malignant breast: importance of the stromal reaction. *Physiol Rev* 76: 69–125, 1996.

392. Roozendaal R, Mebius RE, Kraal G. The conduit system of the lymph node. *Int Immunol* 20: 1483–1487, 2008.

393. Roozendaal R, Mempel TR, Pitcher LA, Gonzalez SF, Verschoor A, Mebius RE, von Andrian UH, Carroll MC. Conduits mediate transport of low-molecular-weight antigen to lymph node follicles. *Immunity* 30: 264–276, 2009.

394. Rosengren BI, Rippe B, Tenstad O, Wiig H. Acute peritoneal dialysis in rats results in a marked reduction of interstitial colloid osmotic pressure. *J Am Soc Nephrol* 15: 3111–3116, 2004.

395. Rubin K, Sjoquist M, Gustafsson AM, Isaksson B, Salvessen G, Reed RK. Lowering of tumoral interstitial fluid pressure by prostaglandin E_1 is paralleled by an increased uptake of ^{51}Cr-EDTA. *Int J Cancer* 86: 636–643, 2000.

396. Ruddell A, Harrell MI, Furuya M. Sentinel lymph node lymphangiogenesis and increased lymph flow in murine tumor metastasis. *Clin Exp Met* 26: 883–884, 2009.

397. Ruddell A, Harrell MI, Minoshima S, Maravilla KR, Iritani B, White SW, Partridge SC. Dynamic contrast-enhanced magnetic resonance imaging of tumor-induced lymph flow. *Neoplasia* 10: 706-883–U704, 2008.

398. Rutili G, Arfors KE. Collections of interstitial fluid: a comparison between wick and micropuncture techniques. *Microvasc Res* 15: 107–109, 1978.

399. Rutili G, Arfors KE. Protein concentration in interstitial and lymphatic fluids from the subcutaneous tissue. *Acta Physiol Scand* 99: 1–8, 1977.

400. Rutkowski JM, Boardman KC, Swartz MA. Characterization of lymphangiogenesis in a model of adult skin regeneration. *Am J Physiol Heart Circ Physiol* 291: H1402–H1410, 2006.

401. Rutkowski JM, Markhus CE, Gyenge CC, Alitalo K, Wiig H, Swartz MA. Dermal collagen and lipid deposition correlate with tissue swelling and hydraulic conductivity in murine primary lymphedema. *Am J Pathol* 176: 1122–1129, 2010.

402. Rutkowski JM, Moya M, Johannes J, Goldman J, Swartz MA. Secondary lymphedema in the mouse tail: lymphatic hyperplasia, VEGF-C upregulation, and the protective role of MMP-9. *Microvasc Res* 72: 161–171, 2006.

403. Ryan TJ. Structure and function of lymphatics. *J Invest Dermatol* 93: 18S–24S, 1989.

404. Sakai LY, Keene DR, Morris NP, Burgeson RE. Type VII collagen is a major structural component of anchoring fibrils. *J Cell Biol* 103: 1577–1586, 1986.

405. Salnikov AV, Heldin NE, Stuhr LB, Wiig H, Gerber H, Reed RK, Rubin K. Inhibition of carcinoma cell-derived VEGF reduces inflammatory characteristics in xenograft carcinoma. *Int J Cancer* 119: 2795–2802, 2006.

406. Salnikov AV, Iversen VV, Koisti M, Sundberg C, Johansson L, Stuhr LB, Sjoquist M, Ahlstrom H, Reed RK, Rubin K. Lowering of tumor interstitial fluid pressure specifically augments efficacy of chemotherapy. *FASEB J* 17: 1756–1758, 2003.

407. Sanders JE, Goldstein BS. Collagen fibril diameters increase and fibril densities decrease in skin subjected to repetitive compressive and shear stresses. *J Biomech* 34: 1581–1587, 2001.

408. Sasisekharan R, Shriver Z, Venkataraman G, Narayanasami U. Roles of heparan-sulphate glycosaminoglycans in cancer. *Nat Rev Cancer* 2: 521–528, 2002.

409. Sawa Y, Tsuruga E, Iwasawa K, Ishikawa H, Yoshida S. Leukocyte adhesion molecule and chemokine production through lipoteichoic acid recognition by toll-like receptor 2 in cultured human lymphatic endothelium. *Cell Tissue Res* 333: 237–252, 2008.

410. Scallan J, Huxley VH, Korthuis RJ. Capillary fluid exchange: regulation, functions, and pathology. In: *Colloquium Lectures on Integrated Systems Physiology-From Molecules to Function*, edited by Granger DN, Granger JP. New Jersey: Morgan & Claypool Life Sciences, 2010.

411. Scallan JP, Huxley VH. In vivo determination of collecting lymphatic vessel permeability to albumin: a role for lymphatics in exchange. *J Physiol* 588: 243–254, 2010.

412. Schafflhuber M, Volpi N, Dahlmann A, Hilgers KF, Maccari F, Dietsch P, Wagner H, Luft FC, Eckardt KU, Titze J. Mobilization of osmotically inactive Na^+ by growth and by dietary salt restriction in rats. *Am J Physiol Renal Physiol* 292: F1490–F1500, 2007.

413. Scheinecker C, McHugh R, Shevach EM, Germain RN. Constitutive presentation of a natural tissue autoantigen exclusively by dendritic cells in the draining lymph node. *J Exp Med* 196: 1079–1090, 2002.

414. Schmid-Schönbein GW. Microlymphatics and lymph flow. *Physiol Rev* 70: 987–1028, 1990.

415. Schneiderheinze JM, Hogan BL. Selective in vivo and in vitro sampling of proteins using miniature ultrafiltration sampling probes. *Anal Chem* 68: 3758–3762, 1996.

416. Scholander PF, Hargens AR, Miller SL. Negative pressure in the interstitial fluid of animals. Fluid tensions are spectacular in plants; in animals they are elusively small, but just as vital. *Science* 161: 321–328, 1968.

417. Schoppmann SF, Birner P, Stockl J, Kalt R, Ullrich R, Caucig C, Kriehuber E, Nagy K, Alitalo K, Kerjaschki D. Tumor-associated macrophages express lymphatic endothelial growth factors and are related to peritumoral lymphangiogenesis. *Am J Pathol* 161: 947–956, 2002.

418. Schraufnagel DE, Agaram NP, Faruqui A, Jain S, Jain L, Ridge KM, Sznajder JI. Pulmonary lymphatics and edema accumulation after brief lung injury. *Am J Physiol Lung Cell Mol Physiol* 284: L891–L897, 2003.

419. Scofield DE, McClung HL, McClung JP, Kraemer WJ, Rarick KR, Pierce JR, Cloutier GJ, Fielding RA, Matheny RW Jr, Young AJ, Nindl BC. A novel, noninvasive transdermal fluid sampling methodology: IGF-I measurement following exercise. *Am J Physiol Regul Integr Comp Physiol* 300: R1326–R1332, 2011.

420. Semaeva E, Tenstad O, Bletsa A, Gjerde EA, Wiig H. Isolation of rat trachea interstitial fluid and demonstration of local cytokine production in lipopolysaccharide-induced systemic inflammation. *J Appl Physiol* 104: 809–820, 2008.

421. Semaeva E, Tenstad O, Skavland J, Enger M, Iversen PO, Gjertsen BT, Wiig H. Access to the spleen microenvironment through lymph shows local cytokine production, increased cell flux, and altered signaling of immune cells during lipopolysaccharide-induced acute inflammation. *J Immunol* 184: 4547–4556, 2010.

422. Senger DR, Galli SJ, Dvorak AM, Perruzzi CA, Harvey VS, Dvorak HF. Tumor cells secrete a vascular permeability factor that promotes accumulation of ascites fluid. *Science* 219: 983–985, 1983.

423. Shi ZD, Ji XY, Berardi DE, Qazi H, Tarbell JM. Interstitial flow induces MMP-1 expression and vascular SMC migration in collagen I gels via an ERK1/2-dependent and c-Jun-mediated mechanism. *Am J Physiol Heart Circ Physiol* 298: H127–H135, 2010.

424. Shi ZD, Wang H, Tarbell JM. Heparan sulfate proteoglycans mediate interstitial flow mechanotransduction regulating MMP-13 expression and cell motility via FAK-ERK in 3D collagen. *PLoS One* 6: e15956, 2011.

425. Shieh A, Rozansky H, Hinz B, Swartz MA. Tumor cell invasion is promoted by interstitial flow-induced matrix priming by stromal fibroblasts. *Cancer Res* 71: 790–800, 2011.

426. Shields JD, Emmett MS, Dunn DB, Joory KD, Sage LM, Rigby H, Mortimer PS, Orlando A, Levick JR, Bates DO. Chemokine-mediated migration of melanoma cells towards lymphatics–a mechanism contributing to metastasis. *Oncogene* 26: 2997–3005, 2007.

427. Shields JD, Fleury ME, Yong C, Tomei AA, Randolph GJ, Swartz MA. Autologous chemotaxis as a mechanism of tumor cell homing to lymphatics via interstitial flow and autocrine CCR7 signaling. *Cancer Cell* 11: 526–538, 2007.

428. Shimizu S, Tanaka H, Sakaki S, Yukioka T, Matsuda H, Shimazaki S. Burn depth affects dermal interstitial fluid pressure, free radical production, and serum histamine levels in rats. *J Trauma* 52: 683–687, 2002.

429. Shoulders MD, Raines RT. Collagen structure and stability. *Annu Rev Biochem* 78: 929–958, 2009.

430. Shrestha B, Hashiguchi T, Ito T, Miura N, Takenouchi K, Oyama Y, Kawahara K, Tancharoen S, Ki IY, Arimura N, Yoshinaga N, Noma S, Shrestha C, Nitanda T, Kitajima S, Arimura K, Sato M, Sakamoto T, Maruyama I. B cell-derived vascular endothelial growth factor A promotes lymphangiogenesis and high endothelial venule expansion in lymph nodes. *J Immunol* 184: 4819–4826, 2010.

431. Simpson RJ, Bernhard OK, Greening DW, Moritz RL. Proteomics-driven cancer biomarker discovery: looking to the future. *Curr Opin Chem Biol* 12: 72–77, 2008.

432. Sixt M, Kanazawa N, Selg M, Samson T, Roos G, Reinhardt DP, Pabst R, Lutz MB, Sorokin L. The conduit system transports soluble antigens from the afferent lymph to resident dendritic cells in the T cell area of the lymph node. *Immunity* 22: 19–29, 2005.

433. Skobe M, Hamberg LM, Hawighorst T, Schirner M, Wolf GL, Alitalo K, Detmar M. Concurrent induction of lymphangiogenesis, angiogenesis, and macrophage recruitment by vascular endothelial growth factor-C in melanoma. *Am J Pathol* 159: 893–903, 2001.

434. Smaje L, Zweifach BW, Intaglietta M. Micropressures and capillary filtration coefficients in single vessels of the cremaster muscle of the rat. *Microvasc Res* 2: 96–110, 1970.

435. Staberg B, Groth S, Rossing N. Passage of albumin from plasma to suction skin blisters. *Clin Physiol* 3: 375–380, 1983.

436. Starling EH. On the absorption of fluids from the connective tissue spaces. *J Physiol* 19: 312–326, 1896.

437. Stenken JA, Church MK, Gill CA, Clough GF. How minimally invasive is microdialysis sampling? A cautionary note for cytokine collection in human skin and other clinical studies. *AAPS J* 12: 73–78, 2010.

438. Stewart RH, Rohn DA, Mehlhorn U, Davis KL, Allen SJ, Laine GA. Regulation of microvascular filtration in the myocardium by interstitial fluid pressure. *Am J Physiol Regul Integr Comp Physiol* 271: R1465–R1469, 1996.

439. Stohrer M, Boucher Y, Stangassinger M, Jain RK. Oncotic pressure in solid tumors is elevated. *Cancer Res* 60: 4251–4255, 2000.

440. Stone MD, Odland RM, McGowan T, Onsongo G, Tang C, Rhodus NL, Jagtap P, Bandhakavi S, Griffin TJ. Novel in situ collection of tumor interstitial fluid from a head and neck squamous carcinoma reveals a unique proteome with diagnostic potential. *Clin Proteomics* 6: 75–82, 2010.

441. Stromberg DD, Wiederhielm CA. Interstitial fluid oncotic pressures in rabbit subcutaneous tissue. *Am J Physiol* 231: 888–891, 1976.

442. Stuht S, Gwinner W, Franz I, Schwarz A, Jonigk D, Kreipe H, Kerjaschki D, Haller H, Mengel M. Lymphatic neoangiogenesis in human renal allografts: results from sequential protocol biopsies. *Am J Transplant* 7: 377–384, 2007.

443. Sun W, Ma J, Wu S, Yang D, Yan Y, Liu K, Wang J, Sun L, Chen N, Wei H, Zhu Y, Xing B, Zhao X, Qian X, Jiang Y, He F. Characterization of the liver tissue interstitial fluid (TIF) proteome indicates potential for application in liver disease biomarker discovery. *J Proteome Res* 9: 1020–1031, 2010.

444. Sund M, Kalluri R. Tumor stroma derived biomarkers in cancer. *Cancer Metastasis Rev* 28: 177–183, 2009.

445. Svendsen OS, Barczyk MM, Popova SN, Liden A, Gullberg D, Wiig H. The alpha1beta1 integrin has a mechanistic role in control of interstitial fluid pressure and edema formation in inflammation. *Arterioscler Thromb Vasc Biol* 29: 1864–1870, 2009.

446. Svoboda EL, Howley TP, Deporter DA. Collagen fibril diameter and its relation to collagen turnover in three soft connective tissues in the rat. *Connect Tissue Res* 12: 43–48, 1983.

447. Swabb EA, Wei J, Gullino PM. Diffusion and convection in normal and neoplastic tissues. *Cancer Res* 34: 2814–2822, 1974.

448. Swartz MA. The physiology of the lymphatic system. *Adv Drug Deliv Rev* 50: 3–20, 2001.

449. Swartz MA, Berk DA, Jain RK. Transport in lymphatic capillaries. I. Macroscopic measurements using residence time distribution theory. *Am J Physiol Heart Circ Physiol* 270: H324–H329, 1996.

450. Swartz MA, Boardman KC Jr. The role of interstitial stress in lymphatic function and lymphangiogenesis. *Ann NY Acad Sci* 979: 197–210, 2002.

451. Swartz MA, Fleury ME. Interstitial flow and its effects in soft tissues. *Annu Rev Biomed Eng* 9: 229–256, 2007.

452. Swartz MA, Kaipainen A, Netti PA, Brekken C, Boucher Y, Grodzinsky AJ, Jain RK. Mechanics of interstitial-lymphatic fluid transport: theoretical foundation and experimental validation. *J Biomech* 32: 1297–1307, 1999.

453. Sylven B, Bois I. Protein content and enzymatic assays of interstitital fluid from some normal tissues and transplanted mouse tumors. *Cancer Res* 20: 831–836, 1960.

454. Sylven B, Bois Svensson I. On the chemical pathology of interstitial fluid. i. proteolytic activities in transplanted mouse tumors. *Cancer Res* 25: 458–468, 1965.

455. Tada S, Tarbell JM. Interstitial flow through the internal elastic lamina affects shear stress on arterial smooth muscle cells. *Am J Physiol Heart Circ Physiol* H1589–H1597, 2000.

456. Tailor TD, Hanna G, Yarmolenko PS, Dreher MR, Betof AS, Nixon AB, Spasojevic I, Dewhirst MW. Effect of pazopanib on tumor microenvironment and liposome delivery. *Mol Cancer Ther* 9: 1798–1808, 2010.

457. Takahashi T, Shibata M, Kamiya A. Mechanism of macromolecule concentration in collecting lymphatics in rat mesentery. *Microvasc Res* 54: 193–205, 1997.

458. Takeuchi J, Sobue M, Sato E, Shamoto M, Miura K. Variation in glycosaminoglycan components of breast tumors. *Cancer Res* 36: 2133–2139, 1976.

459. Tammela T, Alitalo K. Lymphangiogenesis: molecular mechanisms and future promise. *Cell* 140: 460–476, 2010.

460. Taylor A, Granger D. Exchange of macromolecular substances across the capillary wall. In: *Handbook of Physiology. The Cardiovascular System. Microcirculation*. Bethesda, MD: Am. Physiol. Soc., 1984, sect. 2, vol. IV, pt. 1, chapt. 11, p. 467–520.

461. Taylor AE, Gibson WH, Granger HJ, Guyton AC. The interaction between intracapillary and tissue forces in the overall regulation of interstitial fluid volume. *Lymphology* 6: 192–208, 1973.

462. Taylor AE, Parker JC. Pulmonary interstitial spaces and lymphatics. In: *Handbook of Physiology. The Respiratory System. Circulatory and Nonrespiratory Functions*. Bethesda, MD: Am. Physiol. Soc., 1985, sect. 3, vol. 1, p. 167–230.

463. Taylor GW, Kinmonth JB, Dangerfield WG. Protein content of oedema fluid in lymphoedema. *Br Med J* 1: 1159–1160, 1958.

464. Tengblad A, Laurent UB, Lilja K, Cahill RN, Engstrom-Laurent A, Fraser JR, Hansson HE, Laurent TC. Concentration and relative molecular mass of hyaluronate in lymph and blood. *Biochem J* 236: 521–525, 1986.

465. Thaunat O, Kerjaschki D, Nicoletti A. Is defective lymphatic drainage a trigger for lymphoid neogenesis? *Trends Immunol* 27: 441–445, 2006.

466. Timar J, Lapis K, Dudas J, Sebestyen A, Kopper L, Kovalszky I. Proteoglycans and tumor progression: Janus-faced molecules with contradictory functions in cancer. *Semin Cancer Biol* 12: 173–186, 2002.

467. Tisdall MM, Smith M. Cerebral microdialysis: research technique or clinical tool. *Br J Anaesth* 97: 18–25, 2006.

468. Titze J, Shakibaei M, Schafflhuber M, Schulze-Tanzil G, Porst M, Schwind KH, Dietsch P, Hilgers KF. Glycosaminoglycan polymerization may enable osmotically inactive Na^+ storage in the skin. *Am J Physiol Heart Circ Physiol* 287: H203–H208, 2004.

469. Tlsty TD, Coussens LM. Tumor stroma and regulation of cancer development. *Annu Rev Pathol* 1: 119–150, 2006.

470. Tomasek JJ, Gabbiani G, Hinz B, Chaponnier C, Brown RA. Myofibroblasts and mechano-regulation of connective tissue remodelling. *Nat Rev Mol Cell Biol* 3: 349–363, 2002.

471. Tomei AA, Siegert S, Britschgi MR, Luther SA, Swartz MA. Fluid flow regulates stromal cell organization and CCL21 expression in a tissue-engineered lymph node microenvironment. *J Immunol* 183: 4273–4283, 2009.

472. Tong RT, Boucher Y, Kozin SV, Winkler F, Hicklin DJ, Jain RK. Vascular normalization by vascular endothelial growth factor receptor 2 blockade induces a pressure gradient across the vasculature and improves drug penetration in tumors. *Cancer Res* 64: 3731–3736, 2004.

473. Toole BP. Hyaluronan promotes the malignant phenotype. *Glycobiology* 12: 37R–42R, 2002.

474. Toole BP. Hyaluronan: from extracellular glue to pericellular cue. *Nat Rev Cancer* 4: 528–539, 2004.

475. Townsley MI, Snell KS, Ivey CL, Culberson DE, Liu DC, Reed RK, Mathieu-Costello O. Remodeling of lung interstitium but not resistance vessels in canine pacing-induced heart failure. *J Appl Physiol* 87: 1823–1830, 1999.

476. Trzewik J, Mallipattu SK, Artmann GM, Delano FA, Schmid-Schönbein GW. Evidence for a second valve system in lymphatics: endothelial microvalves. *FASEB J* 15: 1711–1717, 2001.

477. Tsunemoto H, Ikomi F, Ohhashi T. Flow-mediated release of nitric oxide from lymphatic endothelial cells of pressurized canine thoracic duct. *Jpn J Physiol* 53: 157–163, 2003.

478. Vaupel P, Mayer A. Hypoxia in cancer: significance and impact on clinical outcome. *Cancer Metastasis Rev* 26: 225–239, 2007.

479. Veenstra TD. Global and targeted quantitative proteomics for biomarker discovery. *J Chromatogr B Analyt Technol Biomed Life Sci* 847: 3–11, 2007.

480. Vermeer BJ, Reman FC, van Gent CM. The determination of lipids and proteins in suction blister fluid. *J Invest Dermatol* 73: 303–305, 1979.

481. Volden G, Thorsrud AK, Bjornson I, Jellum E. Biochemical composition of suction blister fluid determined by high resolution multicomponent analysis (capillary gas chromatography–mass spectrometry and two-dimensional electrophoresis). *J Invest Dermatol* 75: 421–424, 1980.

482. Von der Weid PY, Muthuchamy M. Regulatory mechanisms in lymphatic vessel contraction under normal and inflammatory conditions. *Pathophysiology* 17: 263–276, 2010.

483. Von der Weid PY, Rehal S, Ferraz JGP. Role of the lymphatic system in the pathogenesis of Crohn's disease. *Curr Opin Gastroenterol* 27: 335–341, 2011.

484. Vreim CR, Snashall PD, Demling RH, Staub NC. Lung lymph and free interstitial fluid protein composition in sheep with edema. *Am J Physiol* 230: 1650–1653, 1976.

485. Wachtel E, Maroudas A. The effects of pH and ionic strength on intrafibrillar hydration in articular cartilage. *Biochim Biophys Acta* 1381: 37–48, 1998.

486. Wang DM, Tarbell JM. Modeling interstitial flow in an artery wall allows estimation of wall shear stress on smooth muscle cells. *J Biomech Eng* 117: 1995.

487. Wang S, Tarbell JM. Effect of fluid flow on smooth muscle cells in a 3-dimensional collagen gel model. *Arterioscler Thromb Vasc Biol* 20: 2220–2225, 2000.

488. Wang W, Gou L, Xie G, Tong A, He F, Lu Z, Yao Y, Liu K, Li J, Tang M, Chen L, Yang J, Hu H, Wei YQ. Proteomic analysis of interstitial fluid in bone marrow identified that peroxiredoxin 2 regulates H_2O_2 level of bone marrow during aging. *J Proteome Res* 9: 3812–3819, 2010.

489. Wick N, Haluza D, Gurnhofer E, Raab I, Kasimir MT, Prinz M, Steiner CW, Reinisch C, Howorka A, Giovanoli P, Buchsbaum S, Krieger S, Tschachler E, Petzelbauer P, Kerjaschki D. Lymphatic precollectors contain a novel, specialized subpopulation of podoplanin low, CCL27-expressing lymphatic endothelial cells. *Am J Pathol* 173: 1202–1209, 2008.

490. Widdicombe J. The airway vasculature. *Exp Physiol* 78: 433–452, 1993.

491. Wiederhielm CA, Woodbury JW, Kirk S, Rushmer RF. Pulsatile pressures in the microcirculation of frog's mesentery. *Am J Physiol* 207: 173–176, 1964.

492. Wiig H. Cornea fluid dynamics. I. Measurement of hydrostatic and colloid osmotic pressure in rabbits. *Exp Eye Res* 49: 1015–1030, 1989.

493. Wiig H. Evaluation of methodologies for measurement of interstitial fluid pressure (Pi): physiological implications of recent Pi data. *Crit Rev Biomed Eng* 18: 27–54, 1990.

494. Wiig H, Aukland K, Tenstad O. Isolation of interstitial fluid from rat mammary tumors by a centrifugation method. *Am J Physiol Heart Circ Physiol* 284: H416–H424, 2003.

495. Wiig H, Berggreen E, Borge BA, Iversen PO. Demonstration of altered signaling responses in bone marrow extracellular fluid during increased hematopoiesis in rats using a centrifugation method. *Am J Physiol Heart Circ Physiol* 286: H2028–H2034, 2004.

496. Wiig H, DeCarlo M, Sibley L, Renkin EM. Interstitial exclusion of albumin in rat tissues measured by a continuous infusion method. *Am J Physiol Heart Circ Physiol* 263: H1222–H1233, 1992.

497. Wiig H, Gyenge C, Iversen PO, Gullberg D, Tenstad O. The role of the extracellular matrix in tissue distribution of macromolecules in normal and pathological tissues: potential therapeutic consequences. *Microcirculation* 15: 283–296, 2008.

498. Wiig H, Gyenge CC, Tenstad O. The interstitial distribution of macromolecules in rat tumours is influenced by the negatively charged matrix components. *J Physiol* 567: 557–567, 2005.

499. Wiig H, Heir S, Aukland K. Colloid osmotic pressure of interstitial fluid in rat subcutis and skeletal muscle: comparison of various wick sampling techniques. *Acta Physiol Scand* 133: 167–175, 1988.

500. Wiig H, Kaysen GA, al-Bander HA, De Carlo M, Sibley L, Renkin EM. Interstitial exclusion of IgG in rat tissues estimated by continuous infusion. *Am J Physiol Heart Circ Physiol* 266: H212–H219, 1994.

501. Wiig H, Keskin D, Kalluri R. Interaction between the extracellular matrix and lymphatics: consequences for lymphangiogenesis and lymphatic function. *Matrix Biol* 2010.

502. Wiig H, Kolmannskog O, Tenstad O, Bert JL. Effect of charge on interstitial distribution of albumin in rat dermis in vitro. *J Physiol* 550: 505–514, 2003.

503. Wiig H, Lund T. Relationship between interstitial fluid volume and pressure (compliance) in hypothyroid rats. *Am J Physiol Heart Circ Physiol* 281: H1085–H1092, 2001.

504. Wiig H, Reed RK. Compliance of the interstitial space in rats. II. Studies on skin. *Acta Physiol Scand* 113: 307–315, 1981.

505. Wiig H, Reed RK. Rat brain interstitial fluid pressure measured with micropipettes. *Am J Physiol Heart Circ Physiol* 244: H239–H246, 1983.

506. Wiig H, Reed RK. Volume-pressure relationship (compliance) of interstitium in dog skin and muscle. *Am J Physiol Heart Circ Physiol* 253: H291–H298, 1987.

507. Wiig H, Reed RK, Aukland K. Measurement of interstitial fluid pressure in dogs: evaluation of methods. *Am J Physiol Heart Circ Physiol* 253: H283–H290, 1987.

508. Wiig H, Reed RK, Aukland K. Micropuncture measurement of interstitial fluid pressure in rat subcutis and skeletal muscle: comparison to wick-in-needle technique. *Microvasc Res* 21: 308–319, 1981.

509. Wiig H, Reed RK, Tenstad O. Interstitial fluid pressure, composition of interstitium, and interstitial exclusion of albumin in hypothyroid rats. *Am J Physiol Heart Circ Physiol* 278: H1627–H1639, 2000.

510. Wiig H, Rubin K, Reed RK. New and active role of the interstitium in control of interstitial fluid pressure: potential therapeutic consequences. *Acta Anaesthesiol Scand* 47: 111–121, 2003.

511. Wiig H, Sibley L, DeCarlo M, Renkin EM. Sampling interstitial fluid from rat skeletal muscles by intermuscular wicks. *Am J Physiol Heart Circ Physiol* 261: H155–H165, 1991.

512. Wiig H, Tenstad O. Interstitial exclusion of positively and negatively charged IgG in rat skin and muscle. *Am J Physiol Heart Circ Physiol* 280: H1505–H1512, 2001.

513. Wiig H, Tenstad O, Bert JL. Effect of hydration on interstitial distribution of charged albumin in rat dermis in vitro. *J Physiol* 569: 631–641, 2005.

514. Wiig H, Tenstad O, Iversen PO, Kalluri R, Bjerkvig R. Interstitial fluid: the overlooked component of the tumor microenvironment? *Fibrogenesis Tissue Repair* 3: 12, 2010.

515. Wiig H, Tveit E, Hultborn R, Reed RK, Weiss L. Interstitial fluid pressure in DMBA-induced rat mammary tumours. *Scand J Clin Lab Invest* 42: 159–164, 1982.

516. Willett CG, Boucher Y, di Tomaso E, Duda DG, Munn LL, Tong RT, Chung DC, Sahani DV, Kalva SP, Kozin SV, Mino M, Cohen KS, Scadden DT, Hartford AC, Fischman AJ, Clark JW, Ryan DP, Zhu AX, Blaszkowsky LS, Chen HX, Shellito PC, Lauwers GY, Jain RK. Direct evidence that the VEGF-specific antibody bevacizumab has antivascular effects in human rectal cancer. *Nat Med* 10: 145–147, 2004.

517. Wipff PJ, Hinz B. Integrins and the activation of latent transforming growth factor beta1: an intimate relationship. *Eur J Cell Biol* 87: 601–615, 2008.

518. Wipff PJ, Rifkin DB, Meister JJ, Hinz B. Myofibroblast contraction activates latent TGF-beta1 from the extracellular matrix. *J Cell Biol* 179: 1311–1323, 2007.

519. Woie K, Koller ME, Heyeraas KJ, Reed RK. Neurogenic inflammation in rat trachea is accompanied by increased negativity of interstitial fluid pressure. *Circ Res* 73: 839–845, 1993.

520. Woie K, Reed RK. The relationship between interstitial fluid pressure and volume in rat trachea. *Acta Physiol Scand* 156: 69–74, 1996.

521. Xie SL, Reed RK, Bowen BD, Bert JL. A model of human microvascular exchange. *Microvasc Res* 49: 141–162, 1995.

522. Xing LP, Ji RC. Lymphangiogenesis, myeloid cells and inflammation. *Exp Rev Clin Immunol* 4: 599–613, 2008.

523. Xu BJ, Yan W, Jovanovic B, Shaw AK, An QA, Eng J, Chytil A, Link AJ, Moses HL. Microdialysis combined with proteomics for protein identification in breast tumor microenvironment in vivo. *Cancer Microenviron* 4: 61–71, 2010.

524. Yang Y, MacLeod V, Dai Y, Khotskaya-Sample Y, Shriver Z, Venkataraman G, Sasisekharan R, Naggi A, Torri G, Casu B, Vlodavsky I, Suva LJ, Epstein J, Yaccoby S, Shaughnessy JD Jr, Barlogie B, Sanderson RD. The syndecan-1 heparan sulfate proteoglycan is a viable target for myeloma therapy. *Blood* 110: 2041–2048, 2007.

525. Yeo TK, Brown L, Dvorak HF. Alterations in proteoglycan synthesis common to healing wounds and tumors. *Am J Pathol* 138: 1437–1450, 1991.

526. Yin N, Zhang N, Xu JN, Shi QX, Ding YZ, Bromberg JS. Targeting lymphangiogenesis after islet transplantation prolongs islet allograft survival. *Transplantation* 92: 25–30, 2011.

527. Yoffey JM, Courtice FC. *Lymphatics, Lymph and the Lymphomyeloid Complex*. London: Academic, 1970.

528. Young JS, Lumsden CE, Stalker AL. The significance of the tissue pressure of normal testicular and of neoplastic (Brown-Pearce carcinoma) tissue in the rabbit. *J Pathol Bacteriol* 62: 313–333, 1950.

529. Yu HM, Mouw JK, Weaver VM. Forcing form and function: biomechanical regulation of tumor evolution. *Trends Cell Biol* 21: 47–56, 2011.

530. Zakaria ER, Lofthouse J, Flessner MF. In vivo effects of hydrostatic pressure on interstitium of abdominal wall muscle. *Am J Physiol Heart Circ Physiol* 276: H517–H529, 1999.

531. Zakaria ER, Lofthouse J, Flessner MF. In vivo hydraulic conductivity of muscle: effects of hydrostatic pressure. *Am J Physiol Heart Circ Physiol* 273: H2774–H2782, 1997.

532. Zawieja DC, Barber BJ. Lymph protein concentration in initial and collecting lymphatics of the rat. *Am J Physiol Gastrointest Liver Physiol* 252: G602–G606, 1987.

533. Zhang WB, Aukland K, Lund T, Wiig H. Distribution of interstitial fluid pressure and fluid volumes in hind-limb skin of rats: relation to meridians? *Clin Physiol* 20: 242–249, 2000.

534. Zhong H, Han B, Tourkova IL, Lokshin A, Rosenbloom A, Shurin MR, Shurin GV. Low-dose paclitaxel prior to intratumoral dendritic cell vaccine modulates intratumoral cytokine network and lung cancer growth. *Clin Cancer Res* 13: 5455–5462, 2007.

535. Zhou Q, Gallo JM. In vivo microdialysis for PK and PD studies of anticancer drugs. *AAPS J* 7: E659–667, 2005.

536. Zhou Q, Guo R, Wood R, Boyce BF, Liang Q, Wang YJ, Schwarz EM, Xing L. Vascular endothelial growth factor C attenuates joint damage in chronic inflammatory arthritis by accelerating local lymphatic drainage in mice. *Arthritis Rheum* 63: 2318–2328, 2011.

537. Zweiman B, Kaplan AP, Tong L, Moskovitz AR. Cytokine levels and inflammatory responses in developing late-phase allergic reactions in the skin. *J Allergy Clin Immunol* 100: 104–109, 1997.